

https://dspace.org/

The desulfurization of petroleum compounds using a polymer-supported imidation agent

Matoro, Tshilidzi Benedicta

2016

http://hdl.handle.net/10539/21103

Matoro, Tshilidzi Benedicta (2016) The desulfurization of petroleum compounds using a polymer-supported imidation agent, University of Witwatersrand, Johannesburg, <http://wiredspace.wits.ac.za/handle/10539/21103>

Downloaded from a DSpace repository. https://dspace.org/



THE DESULFURIZATION OF PETROLEUM COMPOUNDS USING A POLYMER – SUPPORTED IMIDATION AGENT

Tshilidzi Benedicta Matoro

A dissertation submitted to the Faculty of Engineering and the Built Environment, University of the Witwatersrand, Johannesburg, in fulfilment of the requirements for the degree of Master of Science in Engineering.

Johannesburg, April 2016

Declaration

I declare that this dissertation is my own unaided work. It is being submitted to the Degree of Master of Science to the University of the Witwatersrand, Johannesburg. It has not been submitted before for any degree or examination to any other University.

.....

(Signature of Candidate)

..... day of ..... year .....

day month year

Abstract

The sulfur removal methods from petroleum products have become an important research topic. Sulfur poisons the catalysts found in vehicles engines and it is also a major air pollutant (Nehlsen, 2005). Recent sulfur specifications require refineries to produce ultra-clean products (Ma *et al*., 2002). This work aims at exploring a batch adsorptive desulfurization technique using a polymer-supported imidation agent (PI) as an adsorbent. The test was carried out at atmospheric pressure and on two commercial diesel fuels with sulfur contents of 5200 (Case 1) and 670 (Case 2) mg/kg which resembles the feed and outlet streams from the hydrodesulfurization (HDS) reactor respectively. The adsorbent was synthesized according to the procedure described by Shiraishi *et al*. (2003), BET, FTIR, SEM equipped with EDS and TGA were used for charaterization of the adsorbent.

The PI was successfully synthesized and its surface area was 0.5333 m^2/g which was incredibly lower than that of the PI synthesized by Fadhel (2010). Hence carbon nanotubes (CNTs) were added to the solution with the aim of improving the sulfur removal efficiency of PI. The obtained results indicated that PI with CNTs yield better results than PI without CNTs. In overall, the lowest sulfur content of 3462 mg/kg (33% removal efficiency) and 26 mg/kg (96% removal efficiency) for Case 1 and Case 2 respectively were obtained. Furthermore, the adsorbents were most effective at lower mixing rates (150 – 400 rpm), longer contact time (30 – 40 hours), practically high adsorbent amount (1 g) and moderate lower temperatures (25 – 50 ºC).

The Freundlich adsorption isotherm model was the best fit to the experimental data in both Case 1 and Case 2. The kinetic model that best fitted well the experimental data is the pseudo-second-order model for both Case 1 and Case 2. The kinetic rate constant for Case 2 (4.079×10^{-3} g/mg.min) was greater than that for Case 1 (6.75×10^{-5} g/mg.min) thus indicating that fuel with low sulfur content has a higher sorption uptake than fuel with high sulfur content.

Based on the results obtained in this study, it is suggested that the adsorption of sulfur at high sulfur content fuel is not capable to be used as a complimentary method to the HDS process. On the other hand, at low sulfur content fuel, there is an opportunity for combining this method with the traditional HDS method to achieve ultra-clean fuel.

Dedication

In loving memory of my mother

Shonisani Gladys Matoro

(1958 – 2015)

May her soul rest in peace

Acknowledgements

First and foremost, my gratitude goes to God who gives me the strength and wisdom to do my research. My gratitude goes to my supervisors, Dr Jean Mulopo and Dr Diakanua Nkazi for their guidance and supervision throughout this work. I greatly acknowledge the support I received from the staff members at the school of Chemical and Metallurgical Engineering, University of the Witwatersrand and the school for providing the research facilities. My appreciation goes to the staff members from the School of Chemistry, University of the Witwatersrand for providing the vacuum oven, assistance with characterization techniques and assistance with the sulfur analysis of diesel samples. My gratitude goes to the University of Stellenbosch for the assistance with sulfur analysis of diesel fuel. My gratitude goes to the National Research Foundation (NRF) and Environmental Resources Management (ERM) for providing with funding. My gratitude goes to my family and friends for their continuous moral support.

Publications

1. Tshilidzi Benedicta Matoro, Jean Mulopo, Diakanua Nkazi: (514b) Evaluation of the desulfurization of commercial diesel fuel using a polymer-supported imidation agent with carbon nanotubes as catalyst. 2015 AICHE Annual Meeting (ISBN: 978-0-8169-1094-6) (presented on 11/11/2015, published as a conference proceeding)
2. Matoro, T.B., Mulopo, J., Nkazi, D: Assessment of Adsorptive Desulfurization of FCC Vacuum Gasoil and Light Cycle Oil using a Nanocatalyzed Polymer-Supported Imidation Agent (finished, to be submitted in April 2016)

Contents

Declaration i

Abstract ii

Dedication iii

Acknowledgements iv

Publications v

List of figures x

List of Tables xii

List of symbols xiii

List of abbreviations xiv

Chapter 1 Introduction 1

1.1 General 1

1.2 Justification 2

1.3 Problem statement 3

1.4 Hypothesis 4

1.5 Research aim and objectives 4

Chapter 2 Literature 5

2.1 Introduction 5

2.2 Crude oil 5

2.1.1 Crude oil categorization 6

2.1.2 Crude oil composition 7

2.3 Overview of oil refinery 8

2.2.1 Separation process 9

2.2.2 Conversion process 9

2.2.3 Formulation and blending process 10

2.2.4 Petroleum products 10

2.2.5 An example of an oil refinery 11

2.4 Sulfur compounds 13

2.5 Desulfurization process 13

2.5.1 Traditional process 13
2.5.2 Challenges that the traditional process is facing 15
2.5.3 Proposed solution to the challenges 16
2.6 Factors that are driving attention to ultra-deep desulfurization 17
2.6.1 Quality of crude oil 17
2.6.2 Environmental concern 17
2.6.3 Cost for upgrading HDS process 18
2.6.4 The use of fuel cells 18
2.7 Classifications of the desulfurization processes 18
2.8 Catalysis based technology 19
2.8.1 Advanced HDS catalysts 20
2.8.2 Advanced HDS reactor 21
2.9 Non-HDS based technology 22
2.9.1 Oxidative desulfurization (ODS) 22
2.9.2 Extractive desulfurization 24
2.9.3 Desulfurization via conversion and extraction 26
2.9.4 Biodesulfurization (biocatalytic desulfurization) 26
2.9.5 Desulfurization by precipitation 28
2.10 Desulfurization by adsorption (ADS) 29
2.10.1 Introduction 29
2.10.2 Adsorptive desulfurization 29
2.10.3 Reactive adsorption desulfurization 31
2.10.4 Challenges that adsorption process is facing 31
2.10.5 ADS adsorbents 32
2.10.6 Factors affecting the adsorption process 38
2.11 Adsorption kinetics and adsorption isotherms 39
2.11.1 Adsorption capacity 39
2.11.2 Adsorption kinetics 40
2.11.3 Equilibrium adsorption 41
2.11.4 Activation energy 43
2.11.5 Thermodynamic parameters 44

2.12 Background on PI 44
2.12.1 Introduction 44
2.12.2 Applications of macroporous chlorosulfonated resins 45
2.12.3 Preparation method of the chlorosulfonated resins 46
2.12.4 Factors affecting the chlorosulfonation reaction 48
Chapter 3 Experimental work 50
3.1 Introduction 50
3.2 Materials 50
3.3 Experimental procedure 51
3.3.1 Synthesis of sodium N-chloro-polystyrene sulfonamide (PI) 51
3.3.2 Characterization techniques 54
3.3.3 Desulfurization process 56
3.3.4 Sulfur analysis method 59
Chapter 4 Results and discussion 61
4.1 Adsorbent characterization results 61
4.1.1 BET results 61
4.1.2 FTIR results 62
4.1.3 SEM and EDS results 65
4.1.4 TGA analysis 69
4.2 Comparison of the desulfurization activity of different PI 70
4.3 Results for the HDS reactor inlet stream (Case 1) 72
4.3.1 Effect of contact time 72
4.3.2 Effect of adsorbent amount 73
4.3.3 Effect of mixing speed 74
4.3.4 Effect of temperature 75
4.3.5 Optimum operating conditions 77
4.3.6 Adsorption isotherms 78
4.3.7 Kinetic study 80
4.3.8 Characterization of spent adsorbent 83
4.4 Results for the HDS reactor outlet stream (Case 2) 85
4.4.1 Effect of contact time 85

4.4.2 Effect of adsorbent amount 86
4.4.3 Effect of mixing speed 88
4.4.4 Effect of temperature 89
4.4.5 Optimum operating conditions 91
4.4.6 Adsorption isotherm 92
4.4.7 Adsorption kinetics 94
4.4.8 Activation parameters 97
4.4.9 Thermodynamic parameters 98
4.4.10 Characterization of spent adsorbent 99
4.4.11 Advantages offered by CNTs 101
Chapter 5 Conclusions and recommendations 102
Recommendations 104
Chapter 6 References 105
Appendix A: Sulfur analysis data for Case 1 118
Appendix B: Sulfur analysis data for Case 2 120
Appendix C: Adsorption isotherm data 123
Appendix D: Adsorption kinetics data 125
Appendix E: Activation and thermodynamic parameters 128

List of figures

Figure 2.1: Energy consumption from various sources in South Africa 6
Figure 2.2: Simplified flowchart of crude processing at BP Kwinana Refinery, from crude distillation units to the resulting products output 11
Figure 2.3: A simplified HDS process 14
Figure 2.4: General process flow diagram for extractive desulfurization process 24
Figure 2.5: A simplified process flow diagram for adsorption process 30
Figure 2.6: Reaction mechanism for reactive adsorption 31
Figure 2.7: The difference between chloramine T and PI 37
Figure 3.1: Pictures taken in the laboratory during the synthesis of polystyrene sulfonyl chloride 53
Figure 3.2: The synthesized PI 54
Figure 3.3: Experimental set-up for batch adsorption process of sulfur from diesel using PI 56
Figure 4.1: FTIR spectra of polystyrene sulfonyl chloride (P-SO_2Cl) 63
Figure 4.2: FTIR spectra of polystyrene sulfonamide 64
Figure 4.3: FTIR spectra of sodium N-chloro polystyrene sulfonamide 65
Figure 4.4: SEM images for polystyrene sulfonyl chloride (a), polystyrene sulfonamide (b) and sodium N-chloro polystyrene sulfonamide (c, d) 66
Figure 4.5: EDS spectrum (a), EDS image (b), polymer structure where P represents polystyrene (c) and EDS elemental composition (d) for polystyrene sulfonyl chloride 67
Figure 4.6: EDS spectrum (a), EDS image (b), polymer structure where P represents polystyrene (c) and EDS elemental composition (d) for polystyrene sulfonamide 68
Figure 4.7: EDS spectrum (a), EDS image (b), polymer structure where P represents polystyrene (c) and EDS elemental composition (d) for sodium N-chloro polystyrene sulfonamide 69
Figure 4.8: TGA analysis curve for PI_3 69
Figure 4.9: The sulfur content of treated diesel fuel with initial concentration (C_o) of 5200 mg/kg using different PI 70
Figure 4.10: The sulfur content of treated diesel fuel with Co of 670.7 mg/kg using different PI71
Figure 4.11: The effect of contact time on the sulfur removal efficiency at 1 g, 50 ° C, 625 rpm and C_o of 5200 mg/kg 72
Figure 4.12: Effect of mixing speed on sulfur removal efficiency at 50 ºC, 0.3 g, 30 hours and C_o of 5200 mg/kg 75
Figure 4.13: The effect of temperature on sulfur removal efficiency at 0.3 g, 625 rpm, 30 hours and C_o of 5200 m/kg 76
Figure 4.14: Langmuir isotherm for sulfur adsorption at C_0 of 5200 mg/kg 79
Figure 4.15: Freundlich isotherm for sulfur adsorption at C_0 of 5200 mg/kg 79
Figure 4.16: Pseudo-first-order kinetic graph for sulfur adsorption at C_0 of 5200 mg/kg 81
Figure 4.17: Pseudo-second-order kinetic model for sulfur adsorption at C0 of 5200 mg/kg 82
Figure 4.18: FTIR spectra of spent PI used to treat HDS reactor inlet stream with C_o of 5200 mg/kg 83

Figure 4.19: SEM images for unused PI a (i), used PI b (i) and used PI with CNTs c (i) alongside with their corresponding EDS spectra (ii) at Case 1 84
Figure 4.20: The effect of doubling stirring rate on the sulfur removal efficiency at 1 g, 50 ºC and C_o of 670.6 mg/kg..... 86
Figure 4.21: The effect of adsorbent amount on sulfur removal efficiency at 50 ºC, 625 rpm, 30 hrs and C_o 670.6 mg/kg 87
Figure 4.22: Effect of mixing speedon sulfur removal efficiency at 50 ºC, 0.3 g, 30 hours and C_o of 670.6 mg/kg..... 88
Figure 4.23: Effect of temperature as a function of time on sulfur removal efficiency at 0.3 g PI, 625 rpm, 30 hours and C_o of 607.6 m/kg..... 89
Figure 4.24: Effect of temperature as a function of time on sulfur removal efficiency at 0.3 g PI with CNTs, 625 rpm, 30 hours and C_o of 607.6 m/kg..... 90
Figure 4.25: Effect of temperature on sulfur removal efficiency at 0.3 g, 625 rpm, 30 hours and C_o of 670.6 m/kg..... 91
Figure 4.26: Langmuir isotherm for sulfur adsorption at C_o of 670.6 mg/kg..... 93
Figure 4.27: Freundlich isotherm for sulfur adsorption at C_o of 670.6 mg/kg 94
Figure 4.28: An Arrhenius plot for sulfur adsorption on PI with and without CNTs..... 97
Figure 4.29: Van't Hoff plot..... 98
Figure 4.30: FTIR spectra of spent PI used to treat HDS reactor outlet stream with C_o of 670.7 mg/kg..... 99
Figure 4.31: SEM images for unused PI a (i), used PI b (i) and used PI with CNTs c (i) alongside with their corresponding EDS spectra (ii) at Case 2 100

List of Tables

Table 2.1: Elemental composition in whole series of crude oils 7
Table 2.2: Commonly used cut points for petroleum fractions 8
Table 2.3: Boiling point of various sulfur compounds 16
Table 2.4: r-values and their relative isotherm type 42
Table 3.1: Properties of diesel fuel tested in this study 50
Table 3.2: A list of chemicals used during the synthesis of PI and their purity 51
Table 3.3: Settings for microwave digester 60
Table 4.1: Structural properties of the synthesized PI 61
Table 4.2: Sulfur removal efficiency (η) of different synthesized PI 71
Table 4.3: Effect of adsorbent amount on sulfur removal efficiency at 50 ºC, 625 rpm, 30 hrs and C_o of 5200 mg/kg 73
Table 4.4: The optimum operating condition for sulfur adsorption process at C_o of 5200 mg/kg 77
Table 4.5: Langmuir and Freundlich isotherm constants and correlation coefficients for sulfur adsorption at C_0 of 5200 mg/kg 80
Table 4.6: Pseudo-first-order and pseudo-second-order constants and correlation coefficients for sulfur adsorption at C0 of 5200 mg/kg 82
Table 4.7: The optimum operating condition for sulfur adsorption process at C_o of 670.6 mg/kg 92
Table 4.8: Langmuir and Freundlich isotherm constants and correlation coefficients for sulfur adsorption at C_o of 5200 mg/kg 94
Table 4.9: Pseudo-first-order constants and correlation coefficients for sulfur adsorption at Co of 607.6 mg/kg 96
Table 4.10: Pseudo-second-order constants and correlation coefficients for sulfur adsorption at Co of 607.6 mg/kg 96
Table 4.11: Thermodynamic parameters 99

List of symbols

Symbols	Definitions	Units
q_t	Amount of sulfur adsorbed per gram of an adsorbent	mg/g
C_o	Initial concentration	mg/l
C_t	Concentration at time t	mg/l
V	Volume of solution	l
W	Weight of an adsorbent	g
q_e	Equilibrium amount of sulfur adsorbed per gram of an adsorbent	mg/g
C_e	Equilibrium concentration	mg/l
k_1	Rate constant for pseudo first-order adsorption	min
k_2	Rate constant for pseudo second-order adsorption	g/mg.min
h_i	Initial sulfur adsorption rate	mg/g PI min
A	Pre-exponential factor	
E_a	Activation energy	KJ/mol
R	Gas constant	8.314 J/mol.K
k	Either pseudo first- or second- order rate constants depending on R^2	
T	Temperature	°C
Q	Maximum amount of adsorbate per unit weigh adsorbent to form a complete coverage on the surface bound	
b	Langmuir constant related to the affinity of binding sites	l/mg
r	Separation factor	
Q_f	An indicator of the adsorption capacity	mg/g
1/n	Adsorption intensity	l/mg
P/P_0	Relative equilibrium pressure	

List of abbreviations

Abbreviations	Definitions
HDS	Hydrodesulfurization
Chloramine T	Sodium N-Chloro-p-toluene sulfonamide
PI	Sodium N-chloro-polystyrene sulfonamide
ppm	Parts per million
CNTs	Carbon nanotubes
HDM	Hydrodemetallation
HDN	Hydrodenitrogenization
CDU	Crude Distillation Unit
LPG	Light Petroleum Gas
PPU	Propane Production Unit
RCU	Residue Cracking Unit
CPU	Catalytic Polymerization Unit
VDU	Vacuum Distillation Unit
BT	Benzothiophene
DBT	Dibenzothiophene
4-DBT	4-methyl dibenzothiphene
4,6-DMDBT	4,6-dimethyl dibenzothiphene
STARS	Super Type II Active Reaction Sites
NEBULA	New Bulk Activity
TBHP	t-butyl hydroperoxide
DMF	Dimethylformamide
ODS	Oxidative desulfurization
BDS	Biodesulfurization
TNF	2, 4, 5, 7-tetranitro-9-fluorene
ADS	Desulfurization by adsorption
LPIE	Liquid phase ion exchange

Abbreviations	Definitions
VPIE	Vapor phase ion exchange
SPIE	Solid phase ion exchange
PASH	Poly-aromatic sulfur heteroatoms
PAH	Poly-aromatic hydrocarbon
MCP	Microporous Coordination Polymers
MIPs	Molecular Imprinted Polymers
ST	Styrene
DVB	Divinylbenzene
ATRP	Atom transfer radical graft polymerization
DCE	1, 2-dichloroethane
THF	Tetrahydrofuran

Chapter 1 Introduction

1.1 General

Due to the public concern of sulfur compounds on the environment, there is an increase in the number and stringency of legislative actions on sulfur specifications, particularly for transportation fuel (Ma *et al*., 2002). As a result, petroleum refining industries are largely affected since they are perceived as one of the largest air polluters both directly and indirectly (Nehlsen, 2005). The most recent sulfur specification in diesel fuel adopted by many countries is 50ppm while the Euro 5 specification has adopted a sulfur specification of 10ppm (Sarda *et al*., 2012). In South Africa, the government is planning to reduce the sulfur content in diesel fuel from a current value of 50ppm to 10ppm by year 2017 (Kotze, 2012). Due to this pressure from legislative actions, refining operators are expected to produce cleaner products in an environmentally friendly manner.

To date, there are different ways that are used to reduce the sulfur oxide pollutants. Jawad (2007) cited in Fadhel (2010) mentioned three approaches, wherein the first one involves using fuel with natural low sulfur content, the second approach involves the desulfurization of fuel and the third approach involves removing sulfur from stack gases in large combustion operations such as power station. Of all these approaches, the desulfurization of fuels is the widely used (Ma *et al*., 2002). However, this desulfurization process has become very challenging because of the abundance of heavy sulfur content crude oil reserves (Nehlsen, 2005).

Different methods have been proposed in the last decades for the removal of sulfur compounds from petroleum streams i.e. the catalytic hydrodesulfurization (HDS) method. The HDS reactor is usually operated at a temperature range of 300 to 400 ºC and a pressure range of 35 to 270 bar (Nehlsen, 2005). The mostly used catalyst is the sulfide Co-Mo/Al_2O_3 or Ni-Mo/Al_2O_3 catalysts (Hernández-Maldonado *et al*., 2005). Unfortunately, the traditional process has difficulties in further lowering the sulfur levels due to the HDS catalysts' low reactivity to refractory sulfur compounds. In order to achieve low sulfur levels in transportation fuel, the proposed solution

was to increase the reactor size and thus the hydrogen consumption (Ma *et al*., 1994; Velu *et al*., 2003).

The problem with this proposed solution as stipulated by other researchers is that under these conditions, the olefins and aromatics contained in the fuel are saturated resulting in the reduction of the octane number (Velu *et al*., 2002). In addition, increasing the reactor size of high temperature and pressure operation might lead to high operating costs (Gong *et al*., 2009; Bu *et al*., 2011; Ma *et al*., 2002). Due to these issues, researchers saw a huge need to further investigate other complementary processes and/or to improve the current process (Yang *et al*., 2003). Much effort has been dedicated to exploring other desulfurization processes such as oxidation, extraction, precipitation, biodesulfurization and adsorption (Babich and Moulijn, 2003). Among these techniques, adsorption has received enormous interest as a promising technique. This is due to, among other factors, its low operating temperatures and pressures, the capability of adsorbents in removing refractory sulfur compounds and their adjustable pore structure and surface functional groups (Velu *et al*., 2002; Shen *et al*., 2007).

The reaction of sulfur compounds in fuel with imidation agents i.e. chloramines T (sodium N-chloro-p-toluene sulfonamide) and PI (sodium N-chloro-polystyrene sulfonamide) had been reported (Shiraishi *et al*., 2003; Fadhel, 2010). According to the best of our knowledge, only few publications have focused on the use of these imidation agents in the petroleum desulfurization process. The findings from a study by Shiraishi *et al*. (2003) and Fadhel (2010) revealed that for low sulfur content fuels, PI performs very well since a sulfur content of 50ppm was achieved. Contrary, for high sulfur content fuels, PI is incapable of achieving deep desulfurization levels.

There is still an opportunity to improve the adsorption capacity of PI at both low and high sulfur content fuel. This study aims at establishing whether the adsorption process can be applied before and (or) after the HDS process in order to achieve clean fuel with 10ppm sulfur content.

1.2 Justification

Naturally, crude oil is composed mainly of straight chain hydrocarbons, the aromatics and heteroatom containing molecules (Fadhel, 2010). Among the heteroatoms, sulfur species are of

particular interest because of their environmental impact. This is because during the combustion process of fuels in vehicle engines, a major air pollutant and a source of acid rain, i.e. SO_x is released to the atmosphere (Babich and Moulijn, 2003). It is also known that the diesel engines do not emit only SO_x, but also the particulate matters which have been shown to have a potential of causing respiratory ailments and cancer (Fadhel, 2010). Sulfur impurities are not only problematic to the environment, but also in the oil refineries and vehicle engines. In oil refineries, sulfur poisons the catalyst used in pipeline, pumping and refining equipment, and in vehicle engines it leads to early failure of combustion engines and the poisoning of the catalytic converters (Huang *et al*., 2006).

Due to these negative effects of the sulfur species, there is a huge interest in the use of clean energy sources such as solar energy. However, it is believed in the scientific community that the implementation of these clean technologies will take many years in order to meet the current energy demand (Nehlsen, 2005). Therefore, it has been postulated that crude oil will continue to dominate as a source of energy and hence the increase in the legislations on sulfur specifications. As a result, a continuous search on alternative techniques that will produce clean petroleum products is ongoing. Among these techniques, adsorption is one of the most promising complimentary methods to the HDS process. This study is relevant to South African refineries since sulfur specification of 10ppm is yet to be implemented.

1.3 Problem statement

To date, there are different ways that are used to reduce the sulfur oxide pollutants wherein the desulfurization of fuels is the widely used approach (Ma *et al*., 2002). However, this desulfurization process has become very challenging because of the abundance of heavy sulfur content crude oil reserves (Nehlsen, 2005). Furthermore, strict sulfur specifications have put a lot of pressure on refineries so that they can produce clean petroleum products. Due to this, most refineries are considering upgrading their sulfur treatment process which involves high costs while some are considering to eliminate the production of the high-sulfur content fuel (Takahashi *et al*., 2002). There is ongoing research on the investigation of other alternative processes though most of them are not yet proven to be commercially viable. Therefore, most of the research is

focusing on the application of alternative desulfurization techniques in series with the traditional HDS process. This is crucial since ultra-clean petroleum products are desired.

1.4 Hypothesis

The batch adsorptive desulfurization method using the synthesized PI as an adsorbent is capable of lowering the sulfur content in diesel fuel. Furthermore, the use of PI with carbon nanotubes (CNTs) gives better adsorption capacity than PI without CNTs. The adsorption parameters such as temperature, adsorbent amount, mixing speed and contact time affect the adsorption process.

1.5 Research aim and objectives

The current study is aimed to improve an adsorbent's sulfur removal capacity in diesel fuel and to evaluate its applicability in achieving ultra-low sulfur specifications after the HDS process.

Thus the objectives of this study are:

- Synthesizing and characterizing an imidation agent supported on a polymer (PI).
- Studying the adsorption capacity of the synthesized PI with and without CNTs.
- Comparing the performance of PI with and without CNTs.
- Studying the effects of the main parameters on the adsorption process (temperature, mixing speed, contact time and amount of an adsorbent).
- Determining the optimum operating conditions for PI with and without CNTs.
- Studying the adsorption isotherms and adsorption kinetics under various experimental conditions.

Chapter 2 Literature

2.1 Introduction

In this chapter, the literature applicable to this work was discussed. Crude oil which is the feed material to the oil refinery was discussed and also a basic introduction of its refining process. Sulfur compounds, their effects on the environment as well as the refinery were discussed in order to indicate why the sulfur removal processes are a necessity. This then lead to a discussion of different desulfurization methods together with their limitations. Then it was highlighted why adsorption process is becoming popular in sulfur removal techniques. Different adsorbents were discussed and the emphasis was placed on polymers. Furthermore, literature on adsorption isotherms and kinetics was discussed in order to understand the extent and rate of adsorption.

2.2 Crude oil

Crude oil is formed when the remains of dead organic creatures buried under the earth for millions of years underwent high temperature and pressure inside the earth crust (Speight & Ozum, 2001). The global major source of energy is derived from fossil fuels such as crude oil, natural gas and coal as compared to renewable energy (Speight & Ozum, 2001). For example, in South Africa coal is the major source of energy (as shown in Figure 2.1) since the country has limited proved reserves of oil and natural gas. The figure also show that the total renewable energy accounts for less than five percent which is very low compared to fossil fuels (crude oil and coal).

In South Africa, it has been reported that the energy demand has increased rapidly and as a result the government is seeking ways of increasing the use of renewable energy to meet the current demand (Oxford Business Group, 2012). This is because renewable energy sources are environmentally friendly and hence they are becoming popular as alternative energy sources. This has resulted in many uncertainties in the future of fossil fuels. Despite the uncertainties, it is postulated that the use of fossil fuel as an energy source will continue in 50 years to come due to some uncertainties in the future of other renewable energy sources (Speight & Ozum, 2001).

Furthermore, it is also believed that the implementation of renewable energy will take many years to meet the current energy demand (Nehlsen, 2005). As a result crude oil will continue to be dominating as a source of energy.

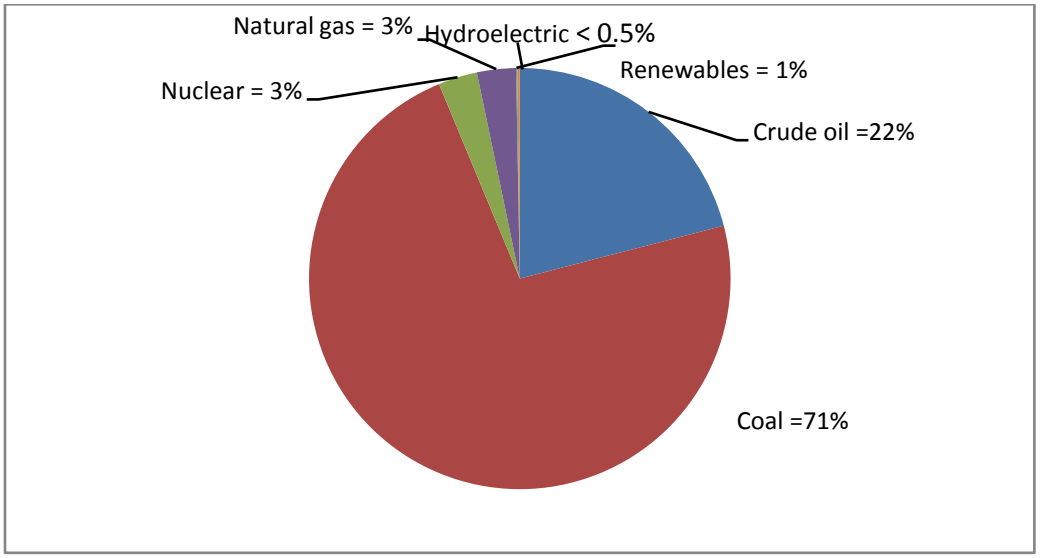

Figure 2.1: Energy consumption from various sources in South Africa, adapted from Oxford Business Group (2012)

2.1.1 Crude oil categorization

Crude oil can be classified in various ways based on its chemical and physical properties. The mostly adopted classifications are based on its physical properties such as the specific density, sulfur content, viscosity and capillarity (Buryakovsky *et al*., 2005; Al-Sahlawi, 1992). Amongst these properties, specific gravity and the sulfur content are of greatest concern to the refineries since they determine the value of the crude oil (Al-Sahlawi, 1992). Thus in this study, crude oil is classified based on the specific gravity and the sulfur content.

The specific gravity of crude oil is given in terms of the API gravity which is the relative measure of the weight of petroleum liquid to the weight of water at ~16 °C (Al-Sahlawi, 1992). According to the rule of thumb, crude oil with an API gravity of less than 30 is regarded as the heavy crude oil while the one with an API gravity of greater than 30 is regarded as the light crude oil (AFPM, n.d.). Furthermore, the sulfur content in crude oil is expressed as a percentage

of sulfur by weight. Crude oil with a sulfur content between 1 and 5wt% is regarded as sour crude oil while the one with less than 1wt% is regarded as the sweet crude oil (Fahim *et al*., 2009). Additionally, sulfur compounds are known to be mainly concentrated in the heavy crude oil (Fadhel, 2010). Therefore, based on these descriptions, crude oil can be either heavy sour or light sweet.

2.1.2 Crude oil composition

Crude oil is composed mainly of straight chain hydrocarbons, the aromatics and heteroatom containing molecules (Fadhel, 2010). The heteroatoms contain other atoms besides carbon and hydrogen such as nitrogen, oxygen, sulfur and metals particularly Nickel and Vanadium (Speight & Ozum, 2001). The elemental composition in crude oils varies depending on, among other factors, the location and the age of the crude oil. The general composition range for each element present in crude oil is shown in Table 2.1 wherein nitrogen, oxygen, sulfur and the metals are the heteroatoms.

Table 2.1: Elemental composition in whole series of crude oils, adapted from Speight & Ozum (2001)

Elements	Narrow limits of composition (%)
Carbon	83.0 – 87.0
Hydrogen	10.0 – 14.0
Nitrogen	0.1 – 2.0
Oxygen	0.05 – 1.5
Sulfur	0.05 – 6.0
Metals (Ni and V)	< 1000 ppm

There are more than 2000 heteroatom species in crude oil which account for about 10 wt% wherein about 1 wt% is organic sulfur compounds (Fadhel, 2010). Among the heteroatoms, nitrogen poisons the HDS catalysts and has a potential for producing nitrogen oxides (NO_x) which is a precursor to acid rain (Speight & Ozum, 2001). Other heteroatom species are poisonous and cause problems during handling, damage the catalysts and lead to coke deposition (Fadhel, 2010). In addition, sulfur has received enormous attention due to its pronounced effects on the refinery and the environment. These heteroatoms are considered impurities and thus refineries use the hydrodemetallation (HDM) unit, hydrodenitrogenization (HDN) unit and

hydrodesulfurization (HDS) unit to remove them. Crude oil in its raw form has minimal value and therefore oil refining process is a necessity for converting it into usable forms such as liquid fuels.

2.3 Overview of oil refinery

The refining process of crude oil is made up of a series of complicated chemical processes that separates petroleum products into a variety of useful products, each meeting certain compositional criteria as specified by the refineries (Nehlsen, 2005). Before the refining process, crude oil is firstly taken to the desalting unit wherein salt and other impurities are removed. There are different processes that can be used in crude oil refining and the process selection is determined by the quantity and quality of end products required and the nature of crude oil available (Speight, 2011). The economic factors such as crude oil costs, product values, transportation and the availability of utilities also affect the process selection of refineries (Kraus, 2011).

The first step in oil refining involves the heating of crude oil into different compounds known as the petroleum fractions. These fractions boil between two temperatures known as the cut points (Nehlsen, 2005). Table 2.2 below shows the commonly used cut points for petroleum fractions. Petroleum fractions that have a low cut point are light gases (e.g. butanes) and they are removed at the top of the column while those with a high cut point are removed at the bottom of a column (e.g. residues) (Leffler, 2008).

Table 2.2: Commonly used cut points for petroleum fractions, adapted from Leffler (2008)

Temperatures (°F)	Petroleum fraction
< 90	Butanes and lighter
90 – 220	Gasoline or Petrol
220 – 315	Naphtha
315 – 450	Kerosene or jet fuel
450 – 800	Gas oil
800 and higher	Residue

The refining process differs from one company to the other but the three basic processes are separation, conversion, and formulating and blending (Kraus, 2011).

2.2.1 Separation process

This is the first stage and it involves the separation of crude oil into different fractions by fractionation in the atmospheric and vacuum distillation towers. Crude oil is firstly heated into a gas. The heated gases are passed into the bottom of the distillation column and they cool as they move up the height of the column and hence condense into a liquid or fractions (AFPM, n.d.). Then the fractions are removed from the column at specific heights; heavy residuals are removed at the bottom, raw diesel fuels in the mid-sections and raw petrol at the top of the column (Leffler, 2008). Depending on the market demand of certain products, the raw fractions are taken to the conversion process to make the finished products.

2.2.2 Conversion process

Conversion process converts separation products into more valuable products based on the market demand. Fuels such as petrol, diesel, and jet fuel are the most valuable petroleum products due to their use in transportation and fuel cell applications and as a result most of these processes focus on them (Ma *et al*., 2005). The conversion process is done by changing the size and structure of hydrocarbons through the following processes or reactions:

- **Decomposition process**

Decomposition involves the breaking of heavy fractions (i.e. residues) that are formed in the crude and vacuum distillation columns into lighter products. The heavier molecules are broken down with the use of catalysts, usually solid zeolites, into the naphtha range materials in order to produce more petrol (Nehlsen, 2005). The units used to achieve this purpose are hydro-cracking, thermal cracking, catalytic cracking, coking and visbreaker units (Kraus, 2011). Usually the cracked naphtha materials contain a high concentration of sulfur compounds since the cracking unit feed stream is the heavy crude fraction that contains polynuclear aromatic sulfur molecules (Nehlsen, 2005). Therefore the cracked naphtha materials are taken to the treatment unit.

- **Treatment process**

The treatment process separates aromatics and naphthenes, as well as removing impurities and contaminants. The units used for this purpose include crude desalting, hydrodesulfurization (HDS), hydrotreating, acid treatment units among others (Kraus, 2011). As mentioned previously, the cracked fractions contain sulfur compounds which are removed through the HDS process. This process is either performed before catalytic cracking or after depending on the refinery designs (Nehlsen, 2005). Sulfur compounds also poisons the catalysts found in the reforming units and hence HDS is usually performed before the reforming process (Nehlsen, 2005).

2.2.3 Formulation and blending process

This process involves the reshaping of molecules by changing their configurations (also known as alteration) and the combination of smaller molecules into larger molecules that are used in petrol (also known as unification) (Leffler, 2008). The units that carry out the alteration reaction include the catalytic reforming and isomerization units while those that carry out the unification reaction include the alkylation and polymerization units (Leffler, 2008). The catalytic reforming unit uses platinum catalyst to isomerize linear paraffins into branched paraffins with a high octane number. The catalysts are more vulnerable to sulfur poisoning and hence HDS process should be done before the reforming process (Nehlsen, 2005). The Alkylation unit uses acidic liquid catalysts to convert isobutene and butylenes into high-octane components (alkylate) of petrol which are further blended into other petrol streams (Nehlsen, 2005).

2.2.4 Petroleum products

Refineries produce a variety of products depending on the market demand (Fahim *et al*., 2009). All the petroleum products find use but the greatest demand is on the fuels. For instance, fuel products are used as both transportation and non-transportation fuels and they account for 75% to 80% of the total refinery products. Among the fuels, there is a huge demand for transportation fuels such as petrol, diesel and jet fuel and hence they are the mostly produced products in the refineries (Song, 2003). Hence, the desulfurization process is usually carried out on the streams forming these products (Babich & Moulijn, 2003).

The sulfur specifications on non-transportation fuels are less strict as compared to those on diesel and petrol. This is due to the reason that non-transportation fuels are used in stationary applications that uses gas cleaning processes to reduce the sulfur emissions (Babich & Moulijn, 2003). Transportation demands require the conversion of about 50% crude oil into petrol and diesel (AFPM, n.d.). Since the demand for transportation fuel is high, sulfur levels in diesel and petrol should be lowered for the environmental protection purposes. This study will thus focus on the desulfurization process of diesel. Diesel was chosen instead of petrol because most refractory sulfur compounds that are hard to remove are found mostly in diesel fuel than in petrol (Dan Liu, 2007). This makes the sulfur removal process of diesel a challenging task.

2.2.5 An example of an oil refinery

A typical example of a crude oil refinery and its ultimate products is shown in Figure 2.2 below.

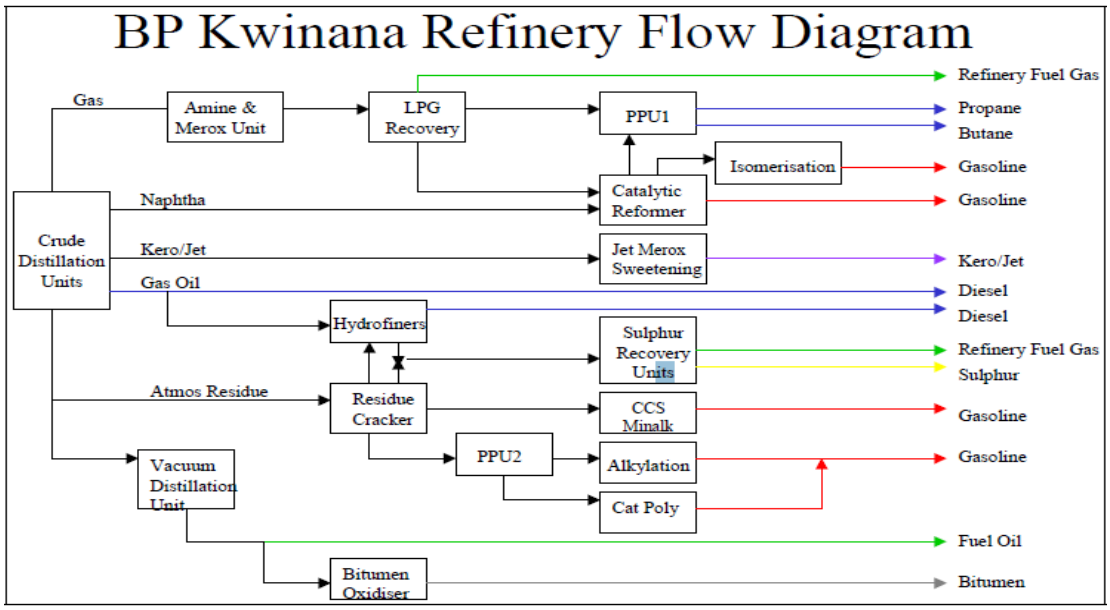

Figure 2.2: Simplified flowchart of crude processing at BP Kwinana Refinery, from crude distillation units to the resulting products output (Liew, 2007)

A general explanation of this flowchart is given below and was obtained from Liew (2007).

The first step is the separation of crude oil into different fractions through distillation. This occurs in the Crude Distillation Unit (CDU). Crude oil is pumped from the storage tank into the CDU and it gets heated. The heated gases are passed into the bottom of the distillation column and they cool as they move up the height of the column and hence condense into a liquid. Lighter

ends are removed at the top of a distillation column and they consist of Light Petroleum Gas (LPG). These lighter ends are then fed to the Propane Production Unit 1 (PPU1) for separation into propane and butane. The PPU1 converts mercaptans (i.e. linear sulfur compounds) in petrol into less odorous disulfides (H_2S).

The remainder of the crude oil fed to the CDU is further heated in the stripping column. The products are separated according to their different boiling points and they include naphtha, kerosene (jet fuel), and light and heavy gas oils. Kerosene is taken to the Merox Unit wherein mercaptans are removed. Naphtha is taken to the Catalytic Reformer where it is upgraded to produce suitable components for blending into petrol. The gas oils as well as the light residue oil from the Residue Cracking Unit (RCU) are taken to the Hydrofiner Unit. The Hydrofiner Unit uses hydrotreating process to remove organic sulfur, nitrogen and oxygen compounds from the feed. The resultant product is the sweetened oil that is used to make diesel.

The remaining products that are not vaporized in the CDU (i.e. atmospheric residue) forms the feedstock to the Vacuum Distillation Unit 2 (VDU 2) and the Residue Cracking Unit (RCU). The atmospheric residues that are fed to the RCU are converted into lighter, valuable components while those that are fed to the VDU are taken to the bitumen plant. In the RCU, alumina catalysts and high operating temperatures are used to crack the long chain molecules of the residues into petrol, and other components of fuel oils and gas oils. The LPG from RCU is then taken to the PPU2 to remove mercaptans and H_2S. The PPU2 product (which is the mixed LPG) is then split into C3 and C4 streams. TheC3 stream is either sold or taken to the Catalytic Polymerization Unit (CPU) and the bulk of the C4 stream goes to the Alkylation Unit while its remainder goes to the CPU. The CPU converts the mentioned products into polygas which is used for petrol blending while the Alkylation Unit produces high-octane petrol.

In addition to the mentioned units, the plant has two Sulfur Recovery Units that remove sulfur from gas streams, refinery flares that safely dispose excess gas, waste management area for treatment of solid wastes and waste water treatment plant.

2.4 Sulfur compounds

Of all the heteroatom species in crude oil, the removal of sulfur species is the most popular topic due to its devastating effects on the environment as well the refinery. Sulfur compounds in diesel and petrol are grouped as linear, cyclic (refractory) and polynuclear compounds. Linear compounds have a high reactivity and are easy to remove from fuels, e.g. sulfides, disulfides, mercaptans and light thiophenic compounds (Dan Liu, 2007). Refractory compounds are hard to remove and they include benzothiophene (BT), dibenzothiophene (DBT), 4-methyl dibenzothiphene (4-DMT) and 4,6-dibenzothiophene (4,6-DMDBT) (Hernández-Maldonado *et al*., 2005). The last group, polynuclear compounds, are complex and their mechanisms are partly understood in the scientific community (Babich & Moulijn, 2003).

During the combustion process in auto-mobiles, SO_2 and SO_3 collectively known as SO_x is released to the atmosphere and is a major air pollutant (Babich & Moulijn, 2003). The presence of these gases in the atmosphere at high concentrations causes respiratory diseases in human beings and animals and they also damage the leaves of plants (Fadhel, 2010). Furthermore, they react with water in the atmosphere and form acid rain which acidifies the soil and also damages the buildings (Nehlsen, 2005). Sulfur also causes problems in the refinery since it poisons the catalysts and leads to corrosion of the pipelines, pumping, and refining equipment (Huang *et al*., 2006). Removing sulfur from transportation fuels is becoming a challenging task due to the abundance of heavy sulfur content reserves and the strict environmental regulations.

2.5 Desulfurization process

2.5.1 Traditional process

The traditional process used by many refineries for sulfur removal is the hydrodesulfurization (HDS) process. This is a hydrogenation process that uses catalysts to remove contaminants such as sulfur, oxygen, nitrogen and metals from petroleum hydrocarbons (Fadhel, 2010). This process uses hydrogen gas as a reactant and it is known to be very effective in removing linear sulfur compounds than refractory sulfur compounds (Rodrigues *et al*., 2014). A typical HDS unit

has a series of reactors, separators and strippers. In a simplified HDS unit, light oil is mixed with hydrogen gas, then heated and then fed to the reactor which is packed with solid catalysts (Fadhel, 2010). This mixture of light oil and hydrogen is fed at the top of the reactor and it flows downward through the reactor coming into contact with the catalyst. Figure 2.3 below shows the simplified hydrodesulfurization process.

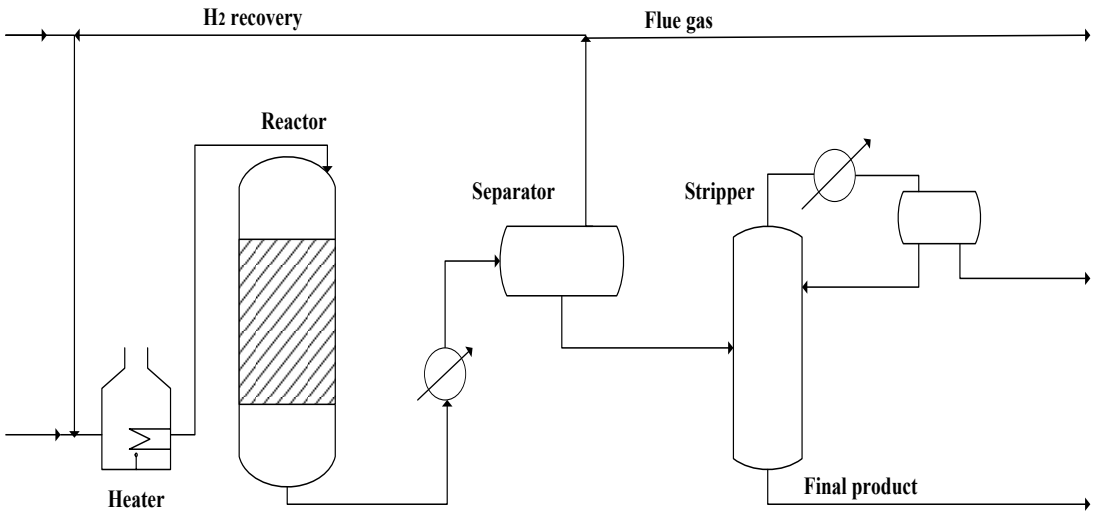

Figure 2.3: A simplified HDS process, adapted from Fadhel (2010)

The HDS reactor is usually operated at a temperature range of 300 to 400 ºC and a pressure range of 35 to 270 bar (Nehlsen, 2005). The commonly used catalysts are the sulphide Co-Mo/Al_2O_3 or Ni-Mo/Al_2O_3 catalysts (Hernández-Maldonado *et al*., 2005). An overall reaction that occurs in the reactor is the reaction of hydrogen gas with the light oil wherein hydrogen sulfide gas (H_2S) and smaller hydrocarbon compounds are liberated. This reaction takes place in two common reactions pathways. The first pathway is the direct removal of sulfur (hydrogenolysis) which occurs in linear sulfur compounds (Babich & Moulijn, 2003). The second reaction path is mainly for thiophenic compounds wherein the aromatic ring is hydrogenated first and then sulfur is removed (Babich & Moulijn, 2003).

Various researchers had shown that substituted DBT species are less reactive because of the presence of the methyl groups that create steric hindrance during the interaction of sulfur with catalysts' active sites (Ito & van Veen, 2006). It is also known that the reactivity of the aromatics decreases with the substituent's addition to the DBT structure (Ito & van Veen, 2006). Hence 4-methyl dibenzothiphene (4-DMT) is less hard to remove than 4, 6-dibenzothiophene (4,6-

DMDBT). The reaction pathways for different types of sulfur compounds are shown below (Key *et al*., 2003).

Mercaptans : $RSH + H_2 \xrightarrow{catalyst} RH + H_2S$

Sulfides : $R_2S + 2H_2 \xrightarrow{catalyst} 2RH + H_2S$

Disulfides : $(RS_2) + 3H_2 \xrightarrow{catalyst} 2RH + 2H_2S$

Thiophenes : $C_4H_4S + 4H_2 \xrightarrow{catalyst} C_4H_{10} + H_2S$

Aromatics : $ArS + 2H_2 \xrightarrow{catalyst} Aromatic + H_2S$

(excludes ring saturation)

The reactor products are then taken to a separator wherein the liquid and gas phases are separated. The gas phase stream is a mixture of hydrogen and H_2S gases. The hydrogen is recycled and the H_2S gas stream is sent to the gas treatment unit wherein it is then used as fuel for process furnaces (Fadhel, 2010). The liquid phase stream is sent to the stripping column wherein H_2S is stripped to produce clean final product (Mochida & Choi, 2004). The problem with the HDS catalysts is that they lose their activity slowly and should be replaced every two to three years (Fadhel, 2010).

2.5.2 Challenges that the traditional process is facing

The traditional hydrotreating process is relatively inexpensive and effective (Babich & Moulijn, 2003). However, there are several challenges that this process is facing and one of the biggest challenge is its inability to achieve ultra-deep desulfurization level (<10ppm). This was associated with the fact that after the traditional hydrotreating process, the refractory thiophenic sulfur compounds remain in the treated stream (Ma *et al*., 2005). What makes this treatment process even more challenging is that diesel fuel and petrol contain less than 1% sulfur compounds and about 30% aromatic compounds and the sulfur compounds have to be removed without removing or saturating the aromatic compounds (Fadhel, 2010). The catalysts used need to be replaced more frequently since they become deactivated and lose their activities (Stanislaus *et al*., 2010).

Additionally, the similar boiling point range of diesel and sulfur compounds make this separation process even more challenging. The boiling point of diesel is in the range of 163 to 357 °C which is very close to that of the refractory sulfur compounds as it can be seen in the Table 2.3 (IARC, 1989).

Table 2.3: Boiling point of various sulfur compounds, adapted from Key *et al.* (2003)

Sulfur species	Boiling points (°C)
Thiophene	85
Benzothiophene	221
Dibenzothiophene	310
Methyl dibenzothiophene	316 – 327
Dimethyl dibenzothiophene	332 – 343
Trimethyldibenzothiophene	349 – 360

Operating the hydrotreating process at mild operating conditions results in the formation of recombinant mercaptans which are formed when H_2S reacts with olefins (Nehlsen, 2005). Another challenge that the traditional process is facing is its inability to achieve ultra-deep desulfurization while preserving fuel properties such as benzene content, oxygen content, overall aromatics content, cetane number, density and etc. (Babich & Moulijn, 2003). However, for diesel hydrotreating process, sulfur removal is of great interest because other fuel specifications are successfully met (Babich & Moulijn, 2003). In general, the main challenge in petrol desulfurization is to selectively remove sulfur without saturating the olefins while in diesel is to selectively remove the refractory sulfur compounds thus achieving ultra-deep desulfurization levels (Ito & van Veen, 2006).

2.5.3 Proposed solution to the challenges

In order to achieve ultra-deep desulfurization, there were some proposed solutions such as operating the HDS reactor at severe operating conditions, i.e. high temperature, high pressure and high hydrogen consumption (Ma *et al*., 1994; Velu *et al*., 2003). However, this proposed solution was objected largely due to its several disadvantages. For instance, under these conditions, the olefins are hydrogenated resulting in a significant reduction in octane number and high consumption of hydrogen (Nehlsen, 2005). Additionally, it has been acknowledged that operating at these conditions will thus require the increase in the reactor size (Ma *et al*., 2005) as

well as the improvement of catalysts used since at severe conditions they become deactivated and lose their activities (Stanislaus *et al*., 2010). Furthermore, it was also argued that operating at high temperatures and pressures will also lead to safety issues in the refinery (Fadhel, 2010). In order to address these challenges, many researchers are focusing on the improvement of the traditional HDS process as well as the advancement of the alternative processes.

2.6 Factors that are driving attention to ultra-deep desulfurization

In this section, factors that are driving attention to ultra-deep desulfurization are discussed. These factors are also creating a hindrance in the improvement of the traditional HDS process and the development of other alternative processes. There are a lot of factors but this section will only focus on the low quality of crude oil, environmental concerns, the cost for upgrading HDS and the demand for fuel cells.

2.6.1 Quality of crude oil

Due to the rapid energy demand, there is an abundance of heavy crude oil reserves with high sulfur content (Nehlsen, 2005). Many refineries are not equipped to process the heavy sour crude oil and this puts them in a position of not wanting to purchase that type of crude oil (Al-Sahlawi, 1992). This is the case even though the heavy sour crude oil is much cheaper than light sweet crude oil (Speight, 2011). But since there is less light sweet crude oil available, refineries are left with no choice but to purchase the heavy sour crude oil. As a result most refineries are under financial strains since they need to upgrade their desulfurization processes.

2.6.2 Environmental concern

The major source of SO_x emission is the presence of high sulfur content in fuels (Sarda *et al*., 2012). As a way of addressing this, the government in many countries has tightened further the sulfur specification in transportation fuel (Ma *et* al., 2002). It is believed that most of the health and environment hazards are caused by the gas emissions from transportation fuel. As a result it is also believed that tightening the sulfur specifications in transportation fuels will reduce those

hazards (Sarda *et al*., 2012). Due to these regulations, many refineries that produce transportation fuels are faced with high costs of compliance (Takahashi *et al*., 2002).

2.6.3 Cost for upgrading HDS process

The upgrading process requires high costs and as a result most refineries are resistant on upgrading while some are now considering not producing transportation fuels (Takahashi *et al*., 2002). As a result there is ongoing research on complementary or alternative processes to the HDS that are economically viable. The viability of the refineries is determined by the type of crude oil used, refinery configuration, quality of products produced, refinery utilization rates and also the environmental considerations (Speight, 2011). Hence the best technology should allow the refiner to meet sulfur specifications at low costs (Key *et al*., 2003).

2.6.4 The use of fuel cells

Fuel cells are energy conversion devices that are used to generate electricity to both mobile vehicles and stationery power plants (Ma *et al*., 2002). They are becoming popular in power production and distribution (Hernández *et al*., 2008). These fuels are used in automotive and portable fuel cells, particularly the proton exchange membrane fuel cell (PEMFC) and the solid oxide fuel cell (SOFC) (Ma *et al*., 2005). Sulfur compounds in liquid fuels poison the catalysts used in fuel processor and those used in fuel cell stack (Ma *et al*., 2002; Gong *et al*., 2009). Due to the catalysts susceptibility to sulfur compounds, the most preferable sulfur level in diesel and petrol fuels is below 0.1 and 0.2ppm (Hernández-Maldonado *et al*., 2005). The traditional HDS is not suitable for meeting this fuel cells' sulfur requirement.

2.7 Classifications of the desulfurization processes

Desulfurization processes have been classified into many categories in different studies (Babich & Moulijn, 2003; Stanislaus *et al*., 2010). This study will only classify this process as catalysis based HDS and non-HDS processes. The catalysis based HDS uses hydrogen to convert organosulfur compounds with sulfur elimination. This is a traditional processes and it has been advanced by looking at the catalysts, reactor designs and fuel specification recovery (Babich &

Moulijn, 2003). Examples of non-HDS technology include catalytic distillation, alkylation, extraction, oxidation, precipitation and adsorption (Babich & Moulijn, 2003).

2.8 Catalysis based technology

As mentioned in Section 2.5.2, severe operating conditions leads to many problems such as undesirable side reactions and catalyst deactivation. Instead of operating at these severe conditions, the use of advanced catalysts and advanced reactor designs had been proposed and were investigated in both academia and industrial institutions. Some of the findings are shown in Section 2.8.1 and 2.8.2. However some catalysts and reactor designs have only been developed in the lab scale and were not yet proven practicable for commercialization. Ito & van Veen (2006) stipulated that in order for a design to be commercialized, there are certain criteria that have to be met and usually they are not measured during the lab tests. Some of these criteria include:

- Low capital cost. Processes with less operational units and inexpensive materials are highly favored since they imply less cost.
- Low operational costs. This requires processes that use less hydrogen, less expensive chemicals and minimizes the generation of wastes.
- Processes should produce a high product volume.
- Less technical complex processes.
- The feed stream to the process should be flexible.
- Reasonable process cycle life.
- The process should have an overall value to the refining companies.

Due to these criteria and many more, Armor (2005) argued that it is not easy to compare lab-scale and commercial catalysts since they depend on many factors beyond examining parameters such as temperature, yield and selectivity. Hence it is important to study these criteria if the new process designs and catalysts ought to be considered for industrial use. The following sub-sections discuss the advanced catalysts and reactor designs developed in academia and for commercial use.

2.8.1 Advanced HDS catalysts

Traditional catalysts consist of molybdenum supported on γ-alumina and are promoted on cobalt and nickel (Stanislaus *et al*., 2010). Between these catalysts, Co-Mo catalysts perform better at low pressure and high temperature while for Ni-Mo catalysts it is the opposite (Song, 2003). These catalysts have two main components which are the support and active metals (Stanislaus *et al*., 2010). The support provides high surface area and mechanical strength while the active metals provide the activity for hydrogenation and hydrogenolysis reactions (Stanislaus *et al*., 2010).

Major catalyst suppliers had developed a variety of effective catalysts for commercial use. These catalysts were developed through the modification of catalyst formulations and the addition of acidic features (Song, 2003). An examples of these catalysts is the STARS (Super Type II Active Reaction Sites) catalyst developed by Akzo Nobel in 1998 (Brevoord *et al*. (2001) cited in Babich & Moulijn (2003)). These catalysts are active CoMo and NiMo STAR catalysts. The CoMo STAR is suitable for fuel with fairly high sulfur level (100 to 500 ppm) at low pressure while NiMo STAR is suitable for low sulfur (<100ppm) at high pressure. These catalysts can reduce the sulfur level to ~20ppm and can process feeds with 30% higher than what the equipment is designed to process without damaging the equipment. Another example is the NEBULA (New Bulk Activity) catalyst developed by Akzo Nobel. This type is suitable at both medium severity condition and high pressure (Eijsbouts *et al*., 2003).

Researchers use different methods to develop new catalysts such as by combining the active catalysts species (such as Mo and W) with advanced catalysts supports (such as the amorphous silica-alumina, carbon, mixed oxides and zeolites), by using promoters (such as P, B, F) and also by using noble metals such as platinum (Song, 2003; Stanislaus *et al*., 2010). Based on these principles, many catalysts companies have introduced highly active catalysts in the market. Examples of some of these companies are Haldor Topsøe, Axen-IFP Group Technology and Kuwait Catalyst Company (KCC) (Stanislaus *et al*., 2010).

Furthermore, in academic research institution similar methods were used to develop different catalysts. For example, some catalysts were developed by altering the preparation methods such as the development of alternative catalyst carriers such as mixed oxides as well as novel active

phases like thulium phosphides (Fadhel, 2010). Carbon material has gain popularity as a support for Co-Mo catalysts (Pawelec *et al*., 2001; Farag *et al*., 2000; Farag *et al*., 1999). The features that make carbon a great support are its high surface area, reduced coking activity, and controllable surface functionality (Abotsi & Scaroni, 1989).

Though there is a wide range of highly selective catalysts developed, there is still a room of improvement such as the development of supports with appropriate texture and surface area and also finding an appropriate design of active sites (Babich & Moulijn, 2003; Song, 2003). Due to this, the development of new highly active commercial catalysts is expected to grow rapidly.

2.8.2 Advanced HDS reactor

The traditional HDS process uses fixed bed reactor with co-current supply of the oil stream and hydrogen which is known to cause unfavorable hydrogen and hydrogen sulfide concentration profile throughout the reactor (Sie, 1999). Due to this and many more challenges, some researchers had proposed the use of two stage processes (Sie, 1999). An example is that developed by Haldor Topsøe Company which consists of a first stage reactor, an intermediate stripper, a second stage reactor and a second stage stripper (Stanislaus *et al*., 2010). However, this configuration has received some critiques since it requires the addition of an additional reactor and a high pressure hydrogen disulfide scrubber between the old and new reactor in the existing refinery (Song, 2003). As a result, counter-current reaction operation modes were proposed.

In the counter-current reactor configuration, oil is fed at the top of the reactor, hydrogen at the bottom and hydrogen sulfide is removed at the top (Babich & Moulijn, 2003). This configuration reduces the recombination of hydrogen sulfide and olefins at the reactor outlet to form sulfur compounds. An example of this reactor design is the SynSat Technology developed by ABB Lummus Global (Song, 2003). The SynSat reactor has three catalysts beds which are placed in separate reactors but within one reactor shell with both the co-current and the counter-current flows.

Another example is the Iso-therming process developed by Process Dynamics and Linde BOC process plant LLC (LBPP) (Key *et al*., 2003). This process has a pre-treat reactor before the

furnace and the main HDS reactor. The pre-treat reactor desulfurize the oil feed into low sulfur and nitrogen content and the resultant products are taken to the HDS reactor where sulfur is further removed to less than 10ppmw. In this design, the feed stream is mixed with some recycled product and then hydrogen gas is dissolved in the mixture thus reducing mass transfer problems. The reactor used is the tubular reactor which is very small as compared to the conventional large trickle bed reactor (Fadhel, 2010). As a result, there is no additional hydrogen requirement and there is minimum capital investment and plot requirements (Key *et al*., 2003). There are many other concepts that have been used in developing various reactor configurations which have resulted in commercial use and have been left out due to the scope of this work.

2.9 Non-HDS based technology

These are the technologies that do not use hydrogen for catalytic conversion of sulfur compounds. Examples are bio-desulfurization, oxidative-extractive, precipitation and adsorption process. These techniques have undergone intense research and some had been proven as better alternatives or complementary processes to the traditional HDS method while some have been commercialized. There is continuous exploration of these techniques and a few are summarized in the following paragraphs.

2.9.1 Oxidative desulfurization (ODS)

Oxidative desulfurization process is considered as one of the most promising approaches to deep desulfurization of fuel (Wang *et al*., 2003). This process involves two steps, which are oxidation of sulfur compounds to sulfones or sulfoxides followed by extraction or purification (Ali *et al*, 2009). Usually, it is operated at ambient pressure and low temperatures (0 to 30 °C) using oxidants and any polar solvent (Fadhel, 2010). The widely used oxidants are hydrogen peroxide and peroxy-acids. However, the problem with using these oxidants is that they require to be added in high concentrations which then cause the loss of product quality and safety issues (Yazu *et al*., 2001). Amongst other factors owing to its enormous interest as a promising technique is that the refractory DBTs sulfur compounds are oxidized to sulfones which have different physical and chemical properties from the light oil and thus they can be easily removed

by separation processes (Yazu *et al.*, 2001; Wang *et al*., 2003). Furthermore, this method is receiving much attention because itis operated at low temperatures and atmospheric pressures (Wang *et al*., 2003).

There are several studies on the development and the testing of different oxidants which were conducted. Some of the oxidants were used with catalysts while some were used without catalysts. Examples include tert-butyl hydroperoxide (t- BuOOH) in the presence of Mo/Al_2O_3 catalyst (Wang *et al*., 2003), hydrogen peroxide in the presence of 1,2-tungstophosphiric acid (PTA) (Yazu *et al*., 2001), hydrogen peroxide in the presence of acetic acid and formic acid as catalysts (Ali *et al.*, 2009), molecular oxygen with an emulsion catalyst (Lü *et al*., 2006) and ozone (Stanislaus *et al*., 2010). For the extraction of sulfones from light oil, the solvents are chosen based on their polarity, surface area, boiling and freezing point (Fadhel, 2010). These factors allow for the easy separation and the recovery of the solvent. The mostly used solvents are the water-soluble polar solvents such as acetonitrile and DMF.

Based on the results obtained from the above studies, most researchers recommended ODS as a potential additional process to the HDS. For instance, a study conducted by Otsuki *et al.* (2000) shows that about 92% sulfur compounds can be removed at mild conditions i.e. atmospheric pressure and room temperature. Furthermore, Campos-Martin *et al.* (2010) proposed that the integration of ODS has a potential for reducing the operational costs of the existing HDS unit by 15%. However, several limitations were identified such as the yield loss due to extraction, the management of chemical waste (sulfone waste) and the limitation of feed flexibility (Ito & van Veen, 2006). In addition, Campos-Martin *et al.* (2010) stated that the need to feed hydrogen peroxide to the existing refinery has created some drawbacks for implementing this method. This is due to the fact that hydrogen peroxide is relatively expensive and the implementation of this process will require possible integration of hydrogen peroxide synthesis in the current process.

Some of the developed ODS processes have been commercialized, for example Sulphco process, Unipore process, Lyondell chemical process, Petrostar process and Enichem/UOP process (Stanislaus *et al*., 2010). The Sulphco process uses ultrasound energy to enhance the oxidation of sulfur compounds. Hydrogen peroxide is used as an oxidation agent with tungsten phosphoric acid as a catalyst. This technology is able to meet the sulfur specification of 10ppm (Gunnerman, 2003). The Lyondell chemical process uses t-butyl hydroperoxide (TBHP) as an oxidizing agent.

The diesel feed together with the TBHP are fed co-currently in a fixed bed catalyst which operates at mild temperatures (<200 °F) and pressures (<100psig) (Karas *et al*., 2008). This process is well suited to be used as a final step for subsequent removal of hydrotreated fuel with about 500ppm sulfur content (Stanislaus *et al*., 2010). The ENI-UOP process uses organic peroxide as an oxidizing agent and more than 98% organic sulfur is converted (Gosling *et al*. (2007) cited in Stanislaus *et al*. (2010)).

In this field, there is ongoing research on improving the selectivity and the efficiency of both the oxidant and the solvent. For instance, some researchers are considering using assisting components (e.g. active carbon) or using physical methods like microwave or ultra-sound (Ito & van Veen, 2006).

2.9.2 Extractive desulfurization

This method relies on the choosing of a solvent in which sulfur compounds are more soluble as compared to the hydrocarbons (Babich & Moulijn, 2003). A variety of extractants (liquid solvents) ranging from common polar organic solvents to ionic liquids have been investigated by many researchers (Ito & van Veen, 2006). The mostly used extractants include acetonitrile, lactones, dimethylformamide (DMF), nitrogen-containing solvents (e.g. amines) and sulfur-containing solvents (e.g. sulfone) (Ito & van Veen, 2006; Stanislaus *et al*., 2010). A general process flow diagram of extractive desulfurization is shown in Figure 2.4.

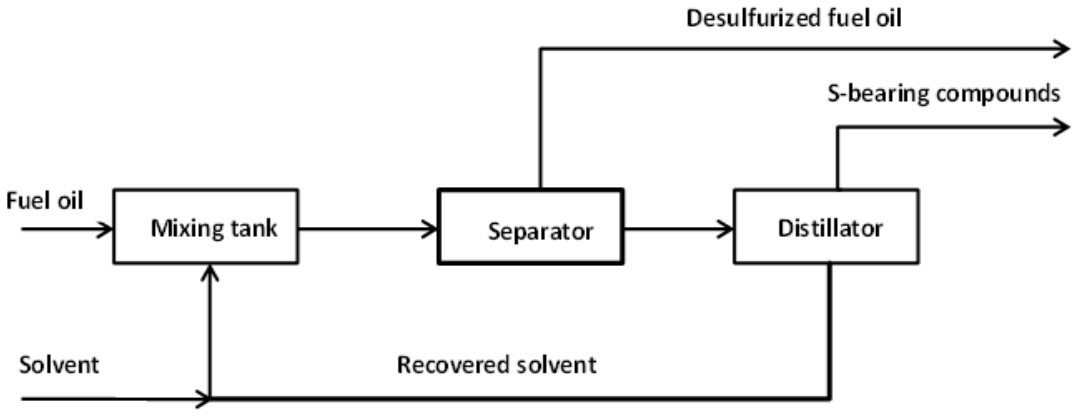

Figure 2.4: General process flow diagram for extractive desulfurization process, adapted from Babich & Moulijn (2003)

The extractive desulfurization process consists of a mixing tank, separator and a distillation column. In a mixing tank, fuel oil is fed with a solvent wherein the transfer of sulfur compounds takes place from the fuel to the solvent. Then the mixing products are taken to a separator wherein the hydrocarbons and the solvent are separated. The desulfurized hydrocarbon stream is taken to other process units to make final products whereas the spent solvent is taken to the distillation column for solvent recovery (Babich & Moulijn, 2003).

This method is receiving much attention as an alternative desulfurization technique due to its applicability at low temperatures and pressures. According to Babich & Moulijn (2003), another aspect that makes this process attractive is that it can easily be integrated into the conventional refineries since it uses conventional equipment which does not require any special requirements. However, one of the biggest challenges that this method is facing is the choosing of an appropriate solvent in which only sulfur compounds are soluble.

An example of an extractant which has been tested in the past is the polyethylene glycol. Several studies conducted showed that when using this extractant, 50 to 90% of sulfur compounds were removed from light oil (Forte, 1996, Funakoshi & Aida, 1998, Horii *et al*., 1996). Even though the sulfur removal was high, a study by Stanislaus *et al*. (2010) argued that the ultra-low sulfur levels of 10ppm could not be achieved. Furthermore, there was co-extraction of aromatics molecules resulting in a high loss of diesel products (Stanislaus *et al*., 2010). As a result, Babich & Moulijn (2003) suggested that this challenge should be addressed by choosing a selective solvent and (or) by transforming sulfur compounds into more soluble compounds.

The transformation of sulfur compounds can be done via oxidative desulfurization. Ali *et al*. (2009) conducted two experiments consecutively, the first one was extraction without oxidation and the second one was extraction with oxidation. It was found that extraction without oxidation resulted in about 45% sulfur removal whereas the other one resulted in 92% removal. Extraction without oxidation also removed other aromatic hydrocarbons which are useful in diesel. Hence, this method should be coupled with oxidation or a better solvent should be investigated. Ito & van Veen (2006) supported this by mentioning that a better approach to extraction is to oxidize sulfur compounds prior to extraction. There is no chemical reaction involved thus separation is possible and it is less costly to dispose wastes products.

Another group of extractant, i.e. ionic liquids has become an interesting research field. Examples of ionic liquids tested include chloroaluminate, hexafluorophosphate and tetrafluorobate (Bösmann *et al*., 2001). Holbrey *et al*. (2008) tested various ionic liquids changing the classes from imidazodium, pyridinium to pyrrolidium using dodecane as a model fuel. These ionic liquids showed good selectivity towards sulfur compounds. However, one of the shortcomings identified was the use of expensive chlorinated ionic liquid. Another challenge identified is that regeneration by distillation is not easy due to low vapour pressure of sulfur compounds and also the re-extraction requires large amounts of solvents (Fadhel, 2010). Even though ionic liquids were proven to be successful in extraction, Adinaya *et al*. (2013) recommended that further understanding of their properties and regeneration ability is still needed.

2.9.3 Desulfurization via conversion and extraction

This method involves mixing the fuel with an oxidant, usually peroxoacetic acid wherein the sulfur compounds get converted into sulfones followed by liquid – liquid extraction process. The process occurs at mild temperatures (up to 120 ºC) and atmospheric pressure (Ali *et al*., 2009). This method was also mentioned in the previous section (Section 2.9.2) when comparing extraction without oxidation and extraction with oxidation. This method has been found to be effective in sulfur removal but the problem is the use of expensive oxidants. In order to make the process economic feasible, it was suggested that the oxidant cost should be reduced (Babich & Moulijn, 2003). Another suggestion is to use a mixture of solvents (i.e. solvent cocktail) but further research is needed in order to identify appropriate compositions of different solvents (Babich & Moulijn, 2003).

2.9.4 Biodesulfurization (biocatalytic desulfurization)

The desulfurization is done by several microorganisms that have the ability to metabolize sulfur species for growth and biological activities (Campos-Martin *et al*., 2010). This process is operated at mild operating conditions in the presence of oxygen and water (Stanislaus *et al*., 2010). The widely used microorganism is the Rhodococcus bacteria and its closely related species because it can easily remove both linear and refractory sulfur compounds (McFarland *et al*., 1998; Monticello, 2000). A typical BDS process has a reactor, product recovery unit as well

as oil and water separation unit. This method is receiving a lot of interest as one of the promising alternative techniques due to low operating conditions, less energy requirements, no generation of undesirable side reactions and less emission of harmful gases (Stanislaus *et al*., 2010; Mohebali & Ball, 2008). Furthermore, in petrol desulfurization, this method does not degrade the octane number (Monticello, 2000).

Despite the advantages associated with this technique, there were some critiques and several limitations identified. For instance, it was argued that it is very hard to fully understand how the bacteria metabolize sulfur species (Campos-Martin *et al*., 2010). In addition, Mohebali & Ball (2008) argued that the implementation of this method in the refineries is not practical since BDS involves sanitary handling, shipment, storage and the use of living bacterial cells within the refinery environment. Several studies show that this process is not yet able to achieve ultra-low desulfurization (Guobin *et al*., 2006; Grossman *et al*., 1999; Chang *et al*., 2001; Grossman *et al*., 2001). It was proposed that this process should be placed after the HDS reactor so that the remaining refractory sulfur compounds that are resistant to hydrotreating can be removed (Monticello, 2000). In addition, Stanislaus *et al*. (2010) also proposed that this process should be conducted prior the HDS process so that all refractory sulfur compounds are removed before they are taken to the HDS unit. However, further research is still needed in order to enable adequate commercialization of this method.

Researchers have identified some gaps that still need to be filled in order to enhance this technique. Examples include the improvement of the thermal stability of the enzymes, improving the sulfur compounds transportation rate from the oil phase to the bacterial cell membrane, developing efficient separation methods of the oil fraction from the enzyme and the recovery of the biocatalyst (Stanislaus *et al*., 2010). Another gap include finding ways of integrating this process within the existing refinery (Monticello, 2000). Some of the developments in this process include the use of multi-stage airlifted reactors as a way of overcoming poor reaction kinetics and the use of a reactor system that offers continuous growth and the regeneration of the biocatalyst (Monticello, 2000). It has been proven that the activity of the naturally occurring micro-organisms is low and hence the concept of genetic manipulation is being widely used by many researchers (Kilbane II & Borgne, 2004; Ma *et al*., 2006). Some of the recent development in the biocatalysts are mentioned in a review article by Stanislaus *et al*. (2010).

2.9.5 Desulfurization by precipitation

This method is based on the formation of insoluble charge-transfer complexes followed by its subsequent removal (Babich & Moulijn, 2003). These complexes are formed through the charge transfer process between the alkylated DBTs and the π acceptor precipitate. An example of the π acceptor precipitate which has been explored in the past is 2, 4, 5, 7-tetranitro-9-fluorene (TNF). Preliminary studies of TNF were conducted using hexane and gas oil in a batch reactor (Meille *et al*., 1998; Milenkovic *et al*., 1999). An insoluble charge transfer complex of π acceptor precipitate and DBT sulfur compounds was formed which was then removed from the gas oil via filtration. The regeneration of the TNF was done using a solid adsorbent. Though the results obtained showed that TNF can be used as a potential precipitate, only 20% of the sulfur compounds were removed from gas oil.

Several issues were identified by various researchers on using this process. One of the problems is that there is competition in the complex formation between the DBT sulfur compounds and the non-sulfur aromatics (Babich & Moulijn, 2003). Furthermore, other limitations include the formation of side reactions through chlorination of aromatics, the use of expensive solvents and the treatment of the organic wastes (Ito & van Veen, 2006). As a result, there is ongoing research on the development of the new complexing materials that are cheap, safe to use and recyclable. Another precipitation approach was reported by Shiraishi *et al*. (2001) that uses alkylating agents (CH_3I and $AgBF_4$) to form N-tosylsulphimides in the presence of methanol.

There are a lot of desulfurization techniques and only a few were covered due to the scope of the work. Some include membrane processes, photochemical desulfurization and the decomposition of sulfur compounds using energy sources such as microwaves and x-rays (Ito & van Veen, 2006).

2.10 Desulfurization by adsorption (ADS)

2.10.1 Introduction

Adsorption process is a separation process which involves the transformation of a mixture of substances into products with different compositions (Yang, 2003). Other separation processes include distillation, evaporation and precipitation. These separation processes account for the most major production costs in chemical, petrochemical and pharmaceutical industries. Amongst the separation process, adsorption has become popular as a desulfurization technique. Desulfurization by adsorption (ADS) is the selective removal of organosulfur compounds from the refinery streams with the use of a solid adsorbent (Stanislaus *et al*., 2010). In order for this process to be practical and economical viable, the adsorbents should be highly selective towards sulfur compounds and should also be available in high quantities at a low cost (Ruthven, 1984).

There are three mechanisms in which the adsorption process takes place which are the steric, kinetic and equilibrium effect. The steric effect involves the diffusion of small, properly shaped molecules into the adsorbent while hindering other molecules. "The kinetic separation is achieved by the virtue of the differences in diffusion rates of different molecules", e.g. air separation. Equilibrium effect involves the analysis of the adsorbents' properties and the comparison with other molecules in the mixture (Yang, 2003). These mechanisms are widely used to classify as well as to study the adsorption process. In this study, the ADS process is divided into two groups which are the adsorptive desulfurization (physisorption) and the reactive adsorption desulfurization (chermisorption). This is based on the classification described by Babich & Moulijn (2003).

2.10.2 Adsorptive desulfurization

In this process, organosulfur compounds are physically adsorbed on the solid adsorbent (Fadhel, 2010). The regeneration of the adsorbent is possible and is usually done by flushing the adsorbent with a desorbent (Babich & Moulijn, 2003). A simplified adsorption process is shown in Figure 2.5 which is known as the IRVAD process developed by Black and Veatch Pritchard engineering company.

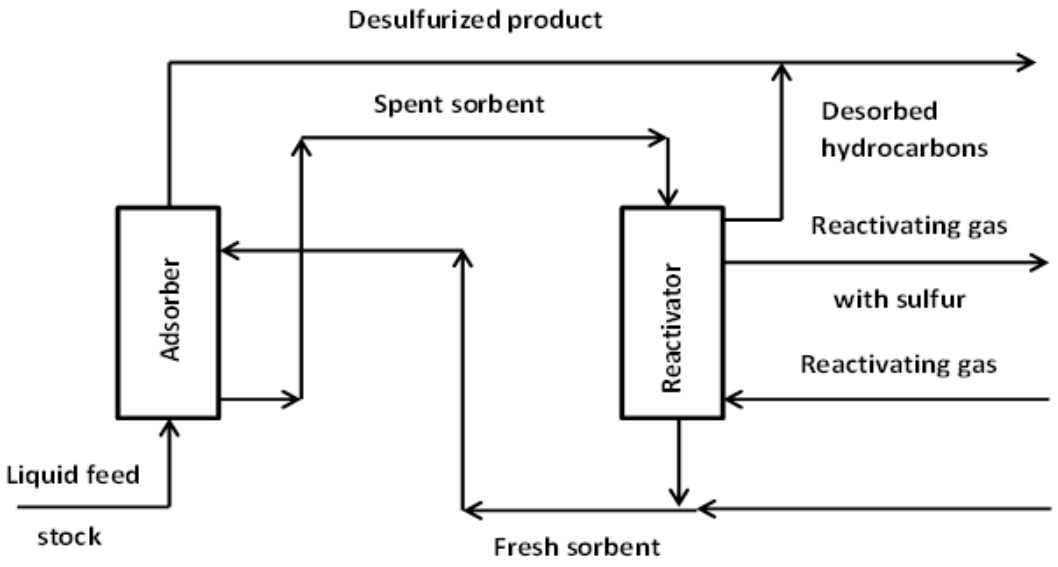

Figure 2.5: A simplified process flow diagram for adsorption process, adapted from Babich & Moulijn (2003)

This process is the counter-current operation process wherein the sulfur-rich feed stream is fed at the bottom and the solid adsorbent at the top of the adsorber column. The desulfurized hydrocarbon stream is produced and removed at the top and the spent adsorbent is removed at the bottom of the adsorber. The spent adsorbent is then taken to the re-activator column where the activating gas is used to desorb the organosulfur compounds and the adsorbed hydrocarbons. The regenerated adsorbent is then re-circulated back to the adsorber column (Babich & Moulijn, 2003). The IRVAD process uses alumina based adsorbents and the process operates at low pressure, temperatures up to 240 ºC and the hydrocarbon to adsorbent ratio of about 1:4 {Irvine (1998) cited in Babich & Moulijn (2003)}.

Physisorption process is reversible due to the weak van der Waals forces and its extent of adsorption is small at higher temperatures (Fadhel, 2010). In addition, it reaches equilibrium rapidly than chemical adsorption. The limitations of this process are the adsorbent's low selectivity towards sulfur compounds and the use of high amount of adsorbent (Babich & Moulijn, 2003). Some of the parameters that can be optimized as described by Babich & Moulijn (2003) are the adsorbent particle size, reactivation temperature, number of adsorption-reactivation steps, hydrocarbon to adsorbent weight ratio and the appropriate design for the adsorption process.

2.10.3 Reactive adsorption desulfurization

Reactive adsorption involves the formation of chemical bonds. During this process, the sulfur atom is removed from the hydrocarbon to the adsorbent without changing the structure of the hydrocarbon (Babich & Moulijn, 2003). The reaction pathway of this process is shown in Figure 2.6.

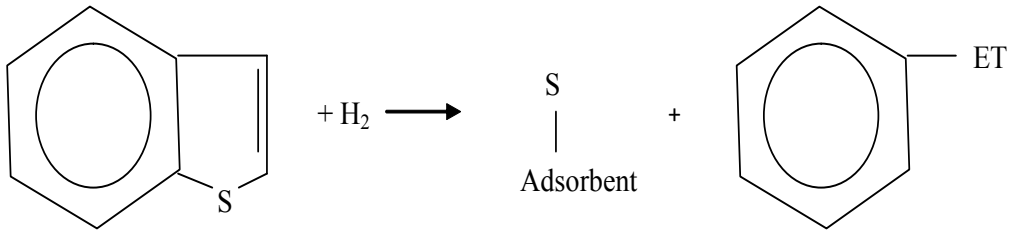

Figure 2.6: Reaction mechanism for reactive adsorption, adapted from Babich & Moulijn (2003)

The reaction largely depends on the temperature due to the requirement of the activation energy. The chemical bonds between the adsorbent and the adsorbate are very strong such that the adsorbent might not be recovered after use (Fadhel, 2010). Chemical adsorption has high enthalpy change (40-800 KJ/mol) as compared to physical adsorption.

A typical reactive adsorption process is the Phillips S Zorb technology developed by Philips Petroleum Co (USA). This process' flow diagram is similar to the ARVAD process (Figure 2.5) and hence it is not re-produced. However, the difference is that the S Zorb process operates at more severe conditions such as 310 to 410 ºC and 2 to 20 bar, and hydrogen is needed (Babich & Moulijn, 2003; Ito & van Veen, 2006). One of the limitation of this process is that the adsorbent can be overloaded quickly if the hydrocarbon stream contains high level of sulphur (Babich & Moulijn, 2003).

2.10.4 Challenges that adsorption process is facing

Though the adsorption process is a well-established process, there are some challenges that many researchers are still facing such as:

- The improvement of the adsorbents' selectivity and the adsorption capacity (Ma *et al*., 2002; Gong *et al*., 2009).
- The development of less energy – intense regeneration methods (Ma *et al*., 2002; Hernández-Maldonado & Yang, 2003)
- Developing adsorbents that are not easily blocked during the desulfurization process (Park *et al*., 2008).
- Developing adsorbents that can perform without being affected by the presence of aromatics and olefins (Ma *et al*., 2005; Hernandez-Maldonado & Yang, 2003; Wang *et al*., 2009; Wang *et al*., 2012).

2.10.5 ADS adsorbents

Most highly selective adsorbents are developed byusing porous materials impregnated with metals/ionic compounds or taking in consideration the chemical forces between thiophenic ring molecules and adsorbents (Shen *et al*., 2007). Adsorbents are grouped into separate classes depending on the micropore size and the distribution of pore size (Ruthven, 1984). Among these adsorbents, only four types have dominated the commercial industries which are the activated carbon, zeolites, silica gel and activated alumina (Yang, 2003). This section will only focus on silica gel, zeolites, carbon adsorbents, polymers and a combination thereof.

(a) Silica gel

The use of transition metals supported on silica gel as adsorbents in fuel desulfurization is well established. Various researchers have studied this adsorbent and only a few are described in this section. A preliminary work conducted by Ma *et al*. (2002) tested transition metal compounds supported on silica gel on petrol, diesel and jet fuel. This process was named the SARS process and it was found to be successful. Ito & van Veen (2006) mentioned that Song and co-workers tested many adsorbents other than transition metal chlorides on silica gel such as activated nickel adsorbents (e.g. Ni-SiO_2), metal ions in zeolites (e.g. CeY, NiY). The problem identified with these adsorbents is their low uptake capacity (Ito & van Veen, 2006).

In line with the SARS process, McKinley & Angelici (2003) further investigated the use of silver metal on the adsorption of DBT and 4,6-DMDBT on a model fuel. Different salts supported on

amorphous silica or mesoporous SBA-15 were tested and $AgNO_3$ supported on amorphous silica was the most effective. It was found that the greatest advantage of this adsorbent is that it is easy to regenerate and it does not lose its adsorption capacity after the first regeneration cycle. However, the test was done on a model (mimic) fuel which does not give a true representation of the commercial (authentic) fuel. The development of transition metal supported on silica is an on-going process and many improvements in these adsorbents have been reported. Amongst others is the use of $PdCl_2$ supported on mesoporous silica SBA-15 (Rodrigues *et al*., 2014), Ni/SiO_2-Al_2O_3 (Hernández *et al*., 2008) and the nanoparticles Ni (Ni/MCF) (Ko *et al*., 2007).

(b) Zeolites

Among the mentioned adsorbents, zeolite-based adsorbents have received much attention due to their high ion exchange as well as thermal and mechanical stabilities (Wang *et al*., 2009). There is a variety of well-established zeoilites which are widely used in different applications as adsorbents. One of the pioneer zeolites tested for the desulfurization purpose is the ZSM-5. The problem with this zeolite was that it has low selectivity due to its small pore volumes that hinder the organic sulfur compounds with more than one ring (Weitkamp *et al*. (1991) cited in Yang *et al*. (2001)). This then led to the testing of large pore volume zeolites which are 13X zeolite (NaX) and Faujasite zeolites which adsorb sulfur species based on the van der Waals forces (Salem & Hamid (1997) cited in Yang *et al*. (2001)). The adsorption capacity of thiophene on these zeolites were compared and it was found that the adsorption capacity of NaX, NaY, activated carbon and activated alumina are about the same (Yang *et al*., 2001). Thereafter, most investigations focused on the zeolites with much stronger forces (i.e. chemical complexation bonds) than the van der Waals interactions.

A study by Yang *et al*. (2001) reported the first results on the new adsorbents which employ π-complexation (CuY, AgY). Afterward, there were studies reported which compared these new adsorbents with commercial adsorbents and the adsorption capacity followed the order: Cu-Y & Ag-Y >> Na-ZSM-5 > activated carbon > Na-Y > modified alumina & H-USY (Takahashi *et al.,* 2002; Hernández-Maldonado & Yang, 2003a; Hernandez-Maldonado &Yang, 2003b). The adsorptive capacity of the π-complexation zeolites was then improved by using activated carbon as a guard bed (Hernández-Maldonado & Yang, 2004a). Another method used to improve the

adsorption capacity of these zeolites was through the modification of the method used to introduce copper ion in zeolites. For instance, in previous studies, the copper ion was introduced into the zeolite via liquid phase ion exchange (LPIE). However, Hernández-Maldonado & Yang (2004b) stated that complete ion exchange is difficult in aqueous phase due to the hydration state of cupric ions. They introduced copper ion via vapor phase ion exchange (VPIE) and solid phase ion exchange (SPIE).

Other zeolites that were developed include Cu (I)- & Ag (I)- Beta zeolites, Cu (I)-Y, Ce (II)-Y and Ni (II)-Y (Gong *et al*., 2009; Wang *et al*., 2011). These zeoilites were found to have a high selectivity towards sulfur compounds but it was found that their performance is reduced by the addition of aromatics and olefins (Ma *et al*., 2005). Similarly Park *et al*. (2008) found that the selectivity of π-complexation adsorbents depends on fuel compositions and moisture content. This implies that these adsorbents might not always perform well since the fuel content always varies depending on the type of crude oil processed in refineries. As a way of addressing this problem, Park *et al*. (2008) suggested reactive adsorption. They tested Ni particles supported on mesoporous silica KIT-6 and SBA-15. The results showed that the adsorbents could lower the sulfur content from 11.7ppmw to <0.1ppmw. However, the problem with these adsorbents is that their pores can be blocked during the process and thus it was recommended that the performance has to be maximized by changing nickel concentration and pore structure. Wang *et al*. (2009) in turn studied an adsorbent with cocation (Ce/Ni-loaded Y zeolite) in response to the stated problem. This adsorbent has two types of adsorption modes which are π-complexation between Ni^{2+} ions and direct coordination of S atoms with Ce ion. This addressed the problem well since the results proved that the adsorbent's performance was not reduced by the presence of the aromatics.

(c) Carbon material

Activated carbons are recently being used as adsorbents in both gas- and liquid-phase adsorption processes. Owing to its popularity is the fact that carbon has a high surface area, large pore volumes and adjustable surface properties that can be tailored by the introduction of surface groups (Bu *et al*., 2011). In addition, carbon adsorbents are much cheaper compared to other adsorbents and can be easily regenerated. Among varies studies on activated carbons, Kim *et al*.

(2006) tested three adsorbents which are nickel supported on silica-alumina (Ni/SiO_2-Al_2O_3), activated alumina and activated carbon using a model diesel fuel in a fixed-bed adsorption system. The results obtained showed that supported nickel is excellent for selective removal of sulfur compounds without alkyl steric hindrance and thus can be applied for petrol, kerosene and jet fuel. On the contrary, activated alumina was found to be excellent for selective removal of nitrogen compounds while activated carbon is selective for both nitrogen and sulfur compounds especially alkyl compounds such as 4,6-DMDBT. Mužic *et al*. (2009) conducted an experiment to compare the performance of activated carbon with that of aluminum oxide and found that activated carbon perform better.

It was found that the performance of carbon can be enhanced by the deposition of metals on the surface of the activated carbon. For example, the deposition of oxygen in the activated carbon leads to the formation of sulfoxides and sulfones which are more polar than their parent compounds (Ania & Bandosz, 2006; Seredych & Bandosz, 2010). Some of the metals or compounds that have been deposited in the activated carbon include copper (Ania & Bandosz, 2006), iron oxides and copper oxides (Seredych & Bandosz, 2010), sulfur (Seredych *et al*., 2011; Seredych & Bandosz, 2011) and silver (Seredych *et al*., 2009). The incorporation of these metals yielded positive results on the performance of the adsorbents. That is, the selectivity and adsorption capacity of the adsorbent was increased.

There are many factors that affect the performance of activated carbon such as the surface chemistry, surface area, competition between species and porosity. Most of these factors can be altered through preparation methods. Bu *et al*. (2011)investigated the adsorption competition between poly-aromatic sulfur heteroatoms (PASH) and poly-aromatic hydrocarbon (PAH) as well as the effect of diffusion kinetic restrictions arising from pore size and size distribution of activated carbon.The results obtained showed that mesoporous activated carbon has a higher adsorption capacity than microporous activated carbon. Activated carbons with pores which are smaller than 0.7 or 1nm are desirable since their sizes are similar to that of DBT and DMDBT and thus enhance the adsorption potential (Seredych *et al*., 2012). Also large pores can have high adsorption capacity when the functional groups are incorporated in the carbon matrix.

(d) Polymers

There are different groups of polymers that have been studied for the desulfurization purpose such as imidation agents, Microporous Coordination Polymers (MCP). According to the best of our knowledge, the use of an imidation agent (Chloramine T) for the desulfurization of fuel was first reported by Shiraishi *et al*. (2001). This study was conducted using both model and commercial light oil in the presence of methanol and acetic acid. In the model fuel, the sulfur compounds were converted into N-tosylsulfimides via imidation with Chloramine T and these compounds were found to be polar and thus they dissolved in methanol allowing them to be easily removed from the light oil. However this was not the case for the commercial light oil. This is due to the presence of DBT with alkyl substituents in commercial diesel which are hydrophobic and remain in the light oil. Due to the mentioned problem, adsorption process using alumina or silica was done in order to further remove the sulfur compounds from the light oil. Due to this combination of two processes (imidation and adsorption), Shiraishi *et al*. (2002) suggested that the adsorption of sulfimides should be avoided in order to make this process energy efficient. This novel process was proven as feasible and Chloramine T lowered the sulfur content of light oil from 1900ppm to 400ppm.

To avoid subsequent adsorption of sulfur, Shiraishi *et al*. (2003) investigated the use of a polymer-supported imidation agent (PI). This imidation agent was found to be insoluble to the light oil solution and the formed sulfimides were successfully anchored on PI and hence they could be easily removed by filtration. The diagram showing the difference between Chloramine T and PI is shown in Figure 2.7. This study compared the activity of PI and Chloramine T and it was found that PI performs better. Furthermore, the sulfur content in commercial fuel was lowered from 400ppm to 54ppm in 40 hours reaction time. Another study by Fadhel (2010) further investigated the sulfur removal efficiency of both PI and Chloramine T by looking at the effect of sorbent dose, initial sulfur concentration and the reaction time. He found that the efficiency increases with decreasing sulfur concentrations and increasing the sorbent dose. For commercial hydrocracked diesel, sulfur was lowered from 1900ppm to 180ppm while for a feed with 12354ppm sulfur content; deep desulfurization could not be achieved. Since there is a reaction involved, waste management of by products is an issue. But the advantage of using the

PI is that the sulfimide formed can be used as novel material in medicine suppliers (Shiraishi *et al*., 2003).

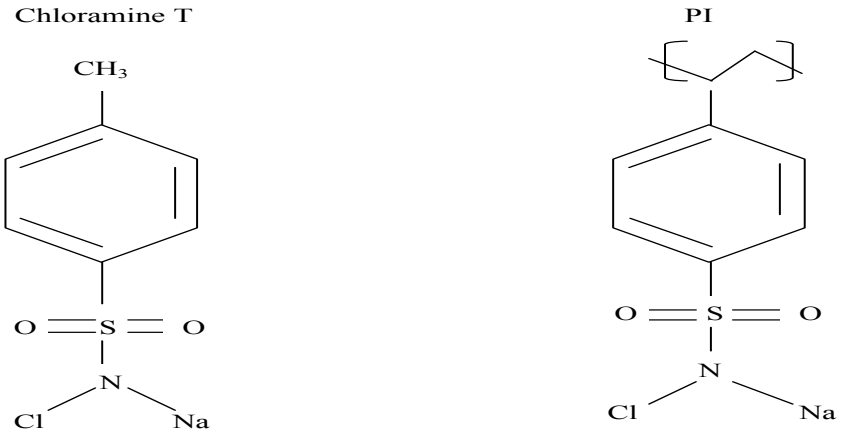

Figure 2.7: The difference between chloramine T and PI, adapted from Shiraishi *et al.* (2002)

Another group of polymers that have gained popularity in the adsorption process is called the Microporous Coordination Polymers (MCP). A study conducted by Kitagawa *et al*. (2004) proved that the MCP adsorbents have a greater adsorption capacity than that of activated carbon and Na-Y zeolites during gas adsorption experiment. Another study by Cychosz *et al*. (2008) tested five different MCPs that differed in pore sizes, shapes and the metal clusters. The MCPs tested were found to have high affinity for DMDBT than BT and DBT at 300ppmw S in isooctane solution. These results are interesting since the DMDBT compounds are hard to remove from fuel as compared to BT and DBT. Since a model fuel does not give a full representation of the commercial fuel, Cychosz *et al*. (2009) tested both the model and authentic diesel using packed-bed flow experiments. The results obtained showed that MCPs are efficient adsorbents and can be regenerated for subsequent use by using solvent and heat.

There is a new technique that has emerged known as the molecular imprinting and it allows for the creation of tailor-made binding sides for certain molecules (Lee *et al*., 2008). The resulting molecular imprinted polymers (MIPs) can be used in a wide range of applications such as the use in biosensors, separation media (Yang *et al*., 2011). These molecules are prepared via polymerization wherein a mixture of a target molecule (template), functional monomers which interact with the template's functional groups and an excess of crosslinkers are polymerized and then the template is removed from the crosslinked polymer network (Lee & Kim, 2009). These

molecules have been widely used in electrochemical sensor systems but their low cost, stability and the easy preparation methods are increasing its popularity in other applications (Haupt & Mosbach, 2000). The traditional MIPs were found to have a lower adsorption capacity and in order to improve their binding rate as well as the adsorption capacity, thin polymers have been grafted onto various support such as polymer beads, silica-based materials and carbon nanotubes (Lee & Kim, 2009; Lee *et al*., 2008). The combination of different supports resulted in outstanding adsorption capacities.

2.10.6 Factors affecting the adsorption process

The extend of adsorption process is affected by factors such as surface area, nature of adsorbate, solution pH, temperature, inferring substances and adsorbent's dose (Lofrano, 2012). Other factors that influence the adsorption process include pressure or concentration (Fadhel, 2010), mixing rate (Singh & Zahra, 2014), residence time (Wang *et al*., 2009), degree of ionization and the size of the molecules with respect to the pore size (Piero, n.d.).

Adsorption is a surface phenomenon and hence a finely divided surface area and more porous solid offer a greater adsorption rate (Lofrano, 2012). Furthermore, limitation of mass transfer penetration rate and internal diffusion rate is reduced by using adsorbents with smaller particle size (Piero, n.d.). Physical adsorption process is generally exothermic and hence increasing the temperature lowers the adsorption rate while for endothermic reaction high temperatures are favourable (Lofrano, 2012). Organic and inorganic compounds that are present in the solution may interfere with one another or may mutually enhance adsorption. For example, Wang *et al*. (2009) showed that the presence of aromatics in the fuel decreases the adsorption capacity. The nature of the adsorbent is also important since the adsorbent with a high solvent solubility reduces the extent of adsorption (Lofrano, 2012).

In batch adsorption system, making a proper contact of adsorbent sites with the surrounding adsorbate is very important. Hence agitation is one of the important parameters that influence the adsorption process since the distribution of the solute in the bulk solution and the formation of external bounding film are dependent on it (Singh & Zahra, 2014). There are several studies that have investigated the effect of mixing speed on the adsorption capacity of different adsorbents (Singh & Zahra, 2014; Saha & Datta, 2009; Ahmad *et al*., 2005). The obtained results showed

that increasing the stirring speed result in an increase in the adsorption capacity until a point is reached wherein a further increase in mixing speed decrease the adsorption capacity. This was explained by the fact that increasing the mixing speed increases the mass transfer rate while rigorous mixing speed desorbs the adsorbate due to strong centrifugal force.

Another important parameter that influences the adsorption process is the adsorbent dosage. Most of the adsorption studies investigated the effect of varying the adsorbent dosage on the adsorption capacity. The increase in the adsorbent amount results in a greater availability of the surface area and hence more adsorbates get adsorbed until a certain point is reached wherein the removal efficiency won't change due to the overlapping of adsorption sites (Kumar and Kirthika, 2009).

2.11 Adsorption kinetics and adsorption isotherms

2.11.1 Adsorption capacity

The adsorption capacity of sulfur compounds on PI was investigated by varying the contact time, temperature, mixing speed and the adsorbent amount. The equations that are used to calculate the adsorption capacity at any time and at equilibrium are given below (Jiwalak *et al*., 2010).

$$q_t = (C_o - C_t)\frac{V}{W} \qquad \textbf{Equation 2-1}$$

$$q_e = (C_o - C_e)\frac{V}{W} \qquad \textbf{Equation 2-2}$$

Where q is the amount of sulfur compounds adsorbed per gram of an adsorbent at any time (q_t) and at equilibrium (q_e),C_o is the initial concentration (mg/l), C_t is the concentration at time t (mg/l), V is the volume of a solution (l), and W is the weight of an adsorbent used (g).

The sulfur removal efficiency, η (%) can be calculated using the following equation:

$$\eta = \frac{C_o - C_t}{C_0} x\ 100 \qquad \textbf{Equation 2-3}$$

2.11.2 Adsorption kinetics

The study of the adsorption kinetics helps to examine the controlling mechanism of the adsorption process such as mass transfer and chemical reaction and also determines the time required to achieve equilibrium during the adsorption process (Mittal *et al*., 2007; Kumar & Kirthika, 2009). In this study, the pseudo-first-order and pseudo-second-order equations were used to model the kinetics of sulfur adsorption onto PI. The best fit model is then selected based on the linear regression correlation coefficient i.e. R^2 (Jiwalak *et al*., 2010).

Pseudo-first-order kinetic model

The pseudo-first-order rate expression of the Lagergren equation is given below {Lagergren (1898) cited in Jiwalak *et al*. (2010)}.

$$\frac{dq_t}{dt} = k_1(q_e - q_t) \qquad \textbf{Equation 2-4}$$

Where k_1 is the rate constant for pseudo-first-order adsorption (min).

When integrating this equation and applying the initial conditions of $q_t = 0$ at $t = 0$ and $q = q_t$ at t=t, the following equation is obtained:

$$\ln(q_e - q_t) = \ln q_e - k_1 t \qquad \textbf{Equation 2-5}$$

A linear relationship of $\ln(q_e - q_t)$ versus t implies that this model is applicable to fit the experimental data. The pseudo-first-order constants (k_1 and q_e) can be calculated from the slope and intercept of the line.

The preferred form of this equation is given below (Lakshmi *et al*., 2009).

$$\log(q_e - q_t) = \log q_e - \left(\frac{k_1}{2.303}\right) t \qquad \textbf{Equation 2-6}$$

Pseudo-second-order kinetic model

The pseudo-second-order kinetic model is given as follows (Lakshmi *et al*., 2009):

$$\frac{dq_t}{dt} = k_2(q_e - q_t)^2 \qquad \textbf{Equation 2-7}$$

Where k_2 is the rate constant for pseudo-first-order adsorption (g/mg.min).

Integrating the equation and applying the initial conditions which are also applied in pseudo-first-order kinetic model, the following equation is obtained.

$$\frac{t}{q_t} = \frac{1}{k_2 q_e^2} + \frac{1}{q_e} t \qquad \textbf{Equation 2-8}$$

A linear relationship of t/q_t versus t implies that this model is applicable to fit the experimental data. This model relies on the assumption that the rate-limiting step might be chemisorptions (Kumar & Kirthika, 2009).

2.11.3 Equilibrium adsorption

Adsorption isotherm is a mathematical model that describes a relationship between the quantity of a substance adsorbed and its equilibrium concentration in the solution at constant temperature (Jiwalak *et al*., 2010). It shows how the adsorption molecules distribute between the liquid and the solid phase during equilibrium. These isotherms are based on the assumptions that are associated with the homogeneity/heterogeneity of the adsorbents, the type of coverage and the possible interaction between the adsorbate species (Kumar & Kirthika, 2009). The two models that are frequently used are the Langmuir and Freundlich models.

Langmuir Isotherm

This model assumes that adsorption takes place at specific homogeneous sites on the surface (Jiwalak *et al*., 2010). Furthermore, it assumes that once an adsorbate occupies a site, there is no further adsorption that will take place at that site. The theoretical equation of this isotherm is shown below (Hameed *et al*., 2008).

$$q_e = \frac{QbC_e}{1+bC_e} \qquad \textbf{Equation 2-9}$$

Where Q is the maximum amount of an adsorbate per unit weight adsorbent to form complete monolayer coverage on the surface bound; b is a Langmuir constant related to the affinity of binding sites (l/mg).

The above equation can be rearranged into a linear form as shown below:

$$\frac{C_e}{q_e} = \frac{1}{Qb} + \frac{1}{Q}C_e \qquad \textbf{Equation 2-10}$$

$$\frac{1}{q_e} = \frac{1}{Q} + \frac{1}{QbC_e} \qquad \textbf{Equation 2-11}$$

From a plot of ($1/q_e$) versus ($1/C_e$), the Langmuir constants (Q and b) can be calculated from the intercepts and the slopes. The separation factor can be calculated in order to examine the progression of the adsorption dimensionless constant using the following equation (Weber & Chakravorti, 1974).

$$r = \frac{1}{1+bC_o} \qquad \textbf{Equation 2-12}$$

The value of r indicates the type of an isotherm. The decrease in r-value as the temperature is increasing indicates that the adsorption process is favorable at higher temperatures (Mittal *et al*., 2007). The table below shows the r-values and their relative isotherm type.

Table 2.4: r-values and their relative isotherm type

Values of r	**Type of isotherm**
r > 0	Unfavorable
r = 1	Linear
0 < r < 1	Favorable
r = 0	Irreversible

Freundlich Isotherm

This isotherm describes the adsorption equilibrium on heterogeneous surfaces. It is based on the assumption that adsorption takes place at different sites with several adsorption energies (Kumar & Kirthika, 2009). Unlike the Langmuir Isotherm, it does not assume a monolayer capacity (Jiwalak *et al*., 2010). The theoretical equation of this isotherm is shown below (Hameed *et al*., 2008).

$$q_e = Q_f C_e^{\,1/n} \qquad \textbf{Equation 2-13}$$

Where Q_f is an indicator of the adsorption capacity (mg/g) and 1/n is the adsorption intensity (l/mg).

In linear form, this equation is represented by:

$$\log q_e = \log Q_f + \frac{1}{n}\log C_e \qquad \text{Equation 2-14}$$

The Freundlich constants (Q_f and 1/n) can be determined from slopes and intercepts of a plot of log q_e versus log C_e. The n-value gives an indication of the favorability of the adsorption process wherein n >1 implies that the adsorption process is favorable at the given conditions (Chiou & Li, 2002).

2.11.4 Activation energy

The activation energy of the process can be calculated by using the empirical van't Hoff and Arrhenius equation as given below (Jiwalak *et al*., 2010).

$$k = Ae^{-E_a/RT} \qquad \text{Equation 2-15}$$

Where A is the pre-exponential factor, E_a is the activation energy (KJ/mol), R is the gas constant (8.314 J/mol.K), k is either the pseudo-first- or second-order rate constant depending on R^2 value and T is the temperature in Kelvins.

The logarithmic form of this equation is given as follows:

$$\ln k = \ln A - \frac{E_a}{RT} \qquad \text{Equation 2-16}$$

An Arrhenius plot of ln k versus 1/T is used to calculate the activation energy. The magnitude of this activation energy indicates whether the process is physisorption or chemisorption. For physisorption processes, the activation energy is usually between 5 and 40 KJ/mol (Nollet *et al*., 2003). This is due to weak intermolecular forces and hence low energy requirement for breaking the bonds. For chemisorption processes, the activation energy usually ranges from 40 to 800 KJ/mol due to much stronger bonds involved (Nollet *et al*., 2003; Jiwalak *et al*., 2010).

2.11.5 Thermodynamic parameters

The thermodynamic parameters considered in this study are the Gibbs free energy (ΔG˚), enthalpy (ΔH˚) and entropy (ΔS˚). They were determined using the following equations.

$$K_c = \frac{C_{ads,e}}{C_e} \qquad \text{Equation 2-17}$$

$$\Delta G^o = -RT \ln K_c \qquad \text{Equation 2-18}$$

$$\ln K_c = \frac{\Delta S^o}{R} - \frac{\Delta H^o}{RT} \qquad \text{Equation 2-19}$$

$$\Delta G^o = \Delta H^o - T\Delta S^o \qquad \text{Equation 2-20}$$

Where K_c is the equilibrium constant, $C_{ads,e}$ is the sulfur concentration adsorbed at equilibrium (mg/l), C_e is the sulfur concentration remaining in diesel at equilibrium (mg/l), R is the gas constant (8.314 J/mol.K) and T is the temperature in Kelvin (Jiwalak *et al*, 2010).

The equilibrium constant, K_c was calculated from the experimental data. The Gibbs free energy was calculated using Equation 18. A van't Hoff plot of $\ln K_c$ versus 1/T was plotted and the entropy as well as the enthalpy were determined from the intercept and slope of the graph.

2.12 Background on PI

2.12.1 Introduction

The development of ion exchange resins based on the copolymerization of styrene cross-linked with divinylbenzene is an ongoing research field which is known to have originated in the middle 1940 (Kumar & Jain, 2013). Ever since that period, the application of these resins has evolved rapidly from laboratory tools to the industrial products. These resins can be classified based on their appearance, whether they are organic or inorganic; natural or synthetic and so forth (Kumar & Jain, 2013). Toro *et al.* (2008) classified ion exchange resins based on their structural characteristics into gel-type and macroreticular (macroporous) cation exchange resins. The difference between the two resins is that gel-type resins usually have a DVB content of lower than 12% hence high swelling capacity and fast diffusion rates while macroporous resins

have higher percentage of DVB hence higher chemical and mechanical stabilities (Chakrabarti & Sharma, 1993).

Many researchers have shown a lot of interest in the use of ion exchange resins due to their stability, greater exchange capacities and simple preparation methods compared to their predecessors (Kumar & Jain, 2013). The properties of ion exchange resins vary depending on its suitability for a particular application. Macroporous chlorosulfonated resins are widely used as intermediates in the preparation of several polymer-supported reagents (Bacquet *et al.*, 1991). As a result chlorosulfonation is a very wide spread reaction used to functionalize polymers.

2.12.2 Applications of macroporous chlorosulfonated resins

The mostly used intermediate in the preparation of several polymer-supported reagent such as sulfonamides and sulfuric acid is the macroporous chlorosulfonated poly (styrene-co-divinylbenzene) (Emerson & Ifalade, 2005). Among these resins, halo-sulfonamide resins have gained popularity in water treatment due to their functional groups that enhance their oxidizing action as well as their simple preparation and regeneration methods (Emerson *et al.*, 1978). Furthermore, this resin is insoluble in water unlike other active chlorine compounds used in water treatment. An example is the macroporous N-chlorosulfonamide resins used for bactericidal action (Emerson *et al.*, 1978), removal of residual sulfides and residual nitrates from water (Kociołek-Balawejder, 2002a; Bogoczek *et al.*, 2005). A similar resin prepared by different researchers is N,N-dichlorosulfonamide which is used as an oxidant for residual sulfides and nitrates removal (Kociołek-Balawejder, 2002b; Bogoczek *et al.*, 2006) and a stimulant for sulfur mustard removal (Gutch *et al.*, 2008).

Another approach used in the preparation of resins is the grafting of linear polymers onto cross-linked polymer resin particles using the atom transfer radical graft polymerization (ATRP). The resulting graft polymer has a combination of the resin's properties and the graft polymer functional group thus making them suitable for various applications. An example is the use of acrylamide grafted on polystyrene resin-supported on N-chlorosulfonamide for selective mercury removal (Bulbul Sonmez *et al.*, 2003). Furthermore, the grafted sulfonamide based polystyrene resins are popular in dye removal from water (Senkal *et al.*, 2007; Senkal & Yavuz, 2006).

2.12.3 Preparation method of the chlorosulfonated resins

The following sections explain the chlorosulfonation of polystyrene (also known as poly (styrene-vinylbenzene)) and the conversion of the subsequent sulfonyl chloride into the sulfonamide. These conversion methods of polystyrene are the same as that of styrene-divinylbenzene copolymers. Therefore, these terms will be used interchangeable in the following sections.

(a) Preparation of sulfonyl resin (sulfonation reaction)

Some starting materials are purchased in the form of sulfonate-type resins and hence the sulfonation reaction is omitted. For starting materials such as benzene and polystyrene, the sulfonation and chlorosulfonation reactions can be carried out at one stage using chlorosulfonic acid (Bacquet *et al.*,1991). There are two reaction steps involved and are shown as follows:

$$step\ 1: C_6H_6 \xrightarrow{HSO_3Cl} C_6H_5 - SO_3H + HCl \qquad \text{Equation 2-21}$$

$$step\ 2: \xleftrightarrow{HSO_3Cl} C_6H_5 - SO_2Cl + H_2SO_4 \qquad \text{Equation 2-22}$$

The second step is an equilibrium reaction, and as a result a mixture of sulfonated (-SO_3H) and chlorosulfonated (-SO_2Cl) products can be obtained. An excess of chlorosulfonic acid is added in order to obtain a fair yield of chlorosulfonyl resin.

Sulfonated polystyrene can also be synthesized using different sulfonating agents such as acetyl sulfateand concentrated sulfuric acid (H_2SO_4) with organic solvents such as 1, 2-dichloroethane (DCE) and chloroform (Carretta *et al*., 2000; Kucera & Jancar, 1996). The sulfonation reaction was carried out by first dissolving polystyrene in dried DCE and heating the solution to 48 to 50 °C. Acetyl sulfate was placed in DCE solution and finally transferred to polystyrene and DCE solution. The reaction was carried out at 50 °C for one hour. The resulting polystyrene sulfonate was isolated from the reaction mixture and then dried at 50 °C under vacuum for three days.

(b) Preparation of chlorosulfonyl resins (chlorosulfonation)

The chlorosulfonation reaction is given below (Bogoczek & Kociołek-Balawejder, 1986):

$$P - SO_3H \xrightarrow{A\,(Cl)} P - SO_2Cl \qquad \textbf{Equation 2-23}$$

Where P refers to the polymeric chain.

The general method involves the addition of an excess of chlorinating agent to the sulfonate resin. The mixture is then stirred for a desired time at a desired temperature. Thereafter the resin is washed, filtered and taken to the vacuum oven for drying. In order to obtain a high yield of sulfonyl chloride, many researchers observed that higher temperatures and an excess of the chlorinating agent should be used.

For instance, a study conducted by Bogoczek and Kociołek-Balawejder (1986) reported on the chlorosulfonation of sulfonate cation exchange resin (poly (ST-co-DVB)). 3 grams of the resin were mixed at boiling temperature (75 to 110 ºC) with 25 ml of a chlorinating agent. Chlorinating agents which were tested include phosphorus pentachloride (PCl_5), phosphoryl chloride ($POCl_3$), thionyl chloride (SO_2Cl), sulfurylchloride ($SOCl_2$), mixture of $POCl_3$ with either SO_2Cl, $SOCl_2$ or PCl_5. The results obtained showed that the highest conversion (99%) is obtained when using a mixture of $POCl_3$ and PCl_5 at 110 ºC. Amongst these chlorinating agents, SO_2Cl with and without solvents did not yield any sulfonyl chloride resin.

Another study by Emerson *et al*. (1978) gave a detailed report on the preparation of poly (ethenylbenzenesulfonic acid). The starting material was an ion-exchange resin in the acidic form. The chlorinating agents tested are chlorosulfonic acid (HSO_3Cl), $SOCl_2$ and SO_2Cl_2 dissolved in solvents, either dimethylformamide (DMF), carbon tetrachloride (CCl_4), chloroform ($CHCl_3$) or dichloromethane (CH_2Cl_2). The chlorinating agent was added in excess (4 to 10 fold molar excess) and the temperature was maintained at 10 to 80 ºC. The highest conversion (80%) was obtained when using chlorosulfonic acid without a solvent at 70 to 80 ºC.

(c) Preparation of sulfonamide resins (sulfonamidation reaction)

Emerson *et al*. (1978) prepared poly (ethenylbenzenesulfonamide) using two methods. The first one involves pouring the mixture of previously prepared sulfochlorinated resin and chlorosulfonic acid into cracked ice. Then the resin was filtered and taken to concentrated ammonium hydroxide and allowed to stand for 2 or more hours. The second method involves the addition of the sulfochlorinated acid (after washing with THF) to the cold concentrated ammonium solution and allowing the mixture to stand for 2 or more hours. The resulting resin was separated from the excess ammonium solution, washed with water and then treated in a flow system with 15% sulfuric acid. This was done in order to convert the residual sulfonic acid groups into H^+ form. Then the final product was washed with water and vacuum dried.

(d) Preparation of halo-sulfonamide (N-chlorination reaction)

The final step is the conversion of sulfonamide into N-chlorosulfonamide and N, N-dichlorosulfonamide. This was done by placing the resin in a column and then passing through household bleach with a concentration of 5.25% through the resin bed. Gutch *et al*. (2008) carried out this step by stirring polystyrene sulfonamide in sodium hypochloride solution in an acidic medium (using acetic acid) for 2 to 4 hours. The reaction was carried out at 5 °C and the resulting product was filtered and dried in air.

These preparation methods have received some critiques such as the safety issues since most reactions use chlorosulfonic acid which reacts violently with water (Emerson & Ifalade, 2005). Furthermore, the use of phosphorus pentachloride in phosphorus oxychloride followed by the reaction with thionyl chloride as well as the use of other solvents causes serious problems for disposing of reaction byproducts. As a result, various researches emerged with the aim of improving the conversion rate and the safety involved during the synthesis process.

2.12.4 Factors affecting the chlorosulfonation reaction

The knowledge on several factors affecting chlorosulfonation reaction is useful in the production of desired products. Depending on the application of the resin, some resins having both the sulfonic acid groups and the sulfonyl chloride groups might have some advantages on some

applications (Emerson *et al*., 1978). This is because sulfonyl chloride groups are very reactive and hydrophobic while the presence of sulfonic acid group which are hydrophilic might facilitate the reaction with water-soluble reagents. The degree of sulfonation is affected by time, reaction temperature and porosity (Fritz & Story, 1974; Ahmed *et al*., 2004). The porosity is known to be controlled by the amount and type of the parogen used and the cross-linkage (i.e. DVB content) (Coutinho *et al.*, 1990). Increasing the DVB content (from 15 to 60%) decreases the capacity of the corresponding resin. The studies conducted by Ahmed *et al*. (2004) and Toro e*t al*. (2008) confirmed that the cross-linkage has a significant effect on chlorosulfonation than the porosity. From these studies, it was deduced that the degree of crosslinking, the porosity and type of DVB isomers have an influence on the catalytic activity of the resins (Toro *et al*., 2008).

Chapter 3 Experimental work

3.1 Introduction

In this study, the adsorption of sulfur compounds from commercial diesel fuel using a polymer–supported imidation agent (PI) (sodium N–chloro–polystyrene sulfonamide) was tested. This polymer was synthesized in the laboratory and then its sulfur removal capability with and without CNTs was studied at varying contact time, adsorbent amount, temperature and stirring speed. This chapter covers a description of the experimental materials, procedure and the analysis techniques that were used to obtain results.

3.2 Materials

Diesel fuel: The experiment was carried out using commercial diesel fuel obtained from Natref refinery. Two types of diesel fuels were tested, which are the inlet feed stream to the HDS reactor and the outlet product stream from the HDS reactor. Its typical physical and chemical properties are shown in Table 3.1. The inlet and outlet HDS reactor streams contain a total sulfur content of 5200 mg/kg and 670.6 mg/kg respectively. The sulfur content in the outlet stream is higher than the 10 mg/kg target specification.

Table 3.1: Properties of diesel fuel tested in this study

Property	**Value**
Cetane index	46.0
Density @ 15°C, $kg.m^{-3}$	820.0
Polycyclic aromatic hydrocarbons, wt%	2.1
Total sulfur, $mg.kg^{-1}$	5200 HDS feed, 120 HDS outlet
Ignition point, °C	>55
Kinematic viscosity @40°C, $mm^2.s^{-1}$	3.98
Distillation: Vol.% distilled until 250°C Vol.% distilled until 300°C End of distillation, °C	 <40 75 342

Polystyrene: Polystyrene was supplied from Sigma Aldrich (South Africa). The procedure for the synthesis of PI involved using polystyrene as a starting material. It was used as such without additional purification. It was obtained in a form of white beads with a DVB content of 1%.

Carbon nanotubes: Multi-walled carbon nanotubes were supplied from Sigma Aldrich (South Africa). They were used as received without being activated.

Chemicals: The synthesis procedure of PI required the use of certain chemicals. All these chemicals were supplied from Sigma Aldrich (South Africa). They were used as received without extra purification. Different chemicals used are shown in Table 3.2 along with their purity.

Table 3.2: A list of chemicals used during the synthesis of PI and their purity

Chemicals	Chemical Formula	Purity
Chlorosulfonic acid	$ClSO_2OH$	≥ 99.5%
Diethylether	$C_4H_{10}O$	≥ 99.5%
Calcium Chloride dehydrated	$CaCl_2$	≥ 99.0%
1,2 Dichloroethane(DCE)	$C_2H_4C_{l2}$	99.8%
Acetic acid glacial	CH_3COOH	≥99.9%
Aqueous ammonia solution	NH_3	30% NH_3 basis
Methanol (MeOH)	CH_4O	99.8%
Sodium hypochloride	NaOCl	10-15% Cl

3.3 Experimental procedure

3.3.1 Synthesis of sodium N-chloro-polystyrene sulfonamide (PI)

The polymer was synthesized following a procedure given by Fadhel (2010) which is a modification of that presented by Bogoczek and Kociołek-Balawejder (1986). This procedure consists of three stages which are described as follows:

Stage 1: Preparation of polystyrene sulfonyl chloride (P-SO_2Cl) – PI_1

This consists of two reactions shown below:

Step 1: $Ps - H + ClSO_3H \rightarrow Ps - SO_3H + HCl \uparrow$ **Equation 3-1**

Step 2: $Ps - SO_3H + ClSO_3H \leftrightarrow Ps - SO_2Cl + H_2SO_4$ **Equation 3-2**

In the shown reactions, polystyrene is represented by the letter Ps. According to Fadhel (2010), the first reaction (step 1) is driven towards the right by the evolution of HCl. The second reaction (step 2) is an equilibrium reaction, and as a result, in order to have a fair yield of the desired product, chlorosulfonic acid has to be added in excess (Bacquet *et al*., 1991). The preparation method is given below (Iimura *et al*., 2003; Vogel *et al*., 1996 cited in Fadhel, 2010).

1. 3 g of polystyrene was placed into 25 ml of DCE solution. Polystyrene was obtained in a form of beads and it did not dissolve instantly. The solution was left to dissolve at room temperature (23 °C) for one day.
2. 15 ml of chlorosulfonic acid was added dropwise in 10 ml of DCE to make a total volume of 25 ml. The solution was cooled to 0 °C in crushed ice.
3. Polystyrene in DCE solution was placed in a dropping funnel and was introduced dropwise into a solution of chlorosulfonic acid and DCE. The reaction is exothermic and to ensure that the temperature does not rise, the three-necked flask was placed in crushed ice. The dropwise addition of polystyrene solution lasted for an hour with continuous stirring at 172 rpm. The stirring speed was not specified in other studies and hence this could probably lead to some distinctions between this PI and that synthesized by other researchers.
4. After the addition of polystyrene solution, the 3-necked flask was removed from crushed ice and was placed in a water bath kept at a temperature of 25 °C. The reactor content was stirred until a light brown colour was seen. Then the temperature was increased to 80 °C with continuous stirring. The mixture was allowed to stand overnight with the reflux condenser attached to it.
5. After the completion of the reaction, there was an excess of chlorosulfonic acid in the flask. This was removed by introducing the reactor product into 20 ml acetic acid. The solution was then filtered with suction, washed with diethyl ether and then dried at 50 ºC overnight in a vacuum oven.

The figure below shows some of the pictures that were taken in the laboratory.

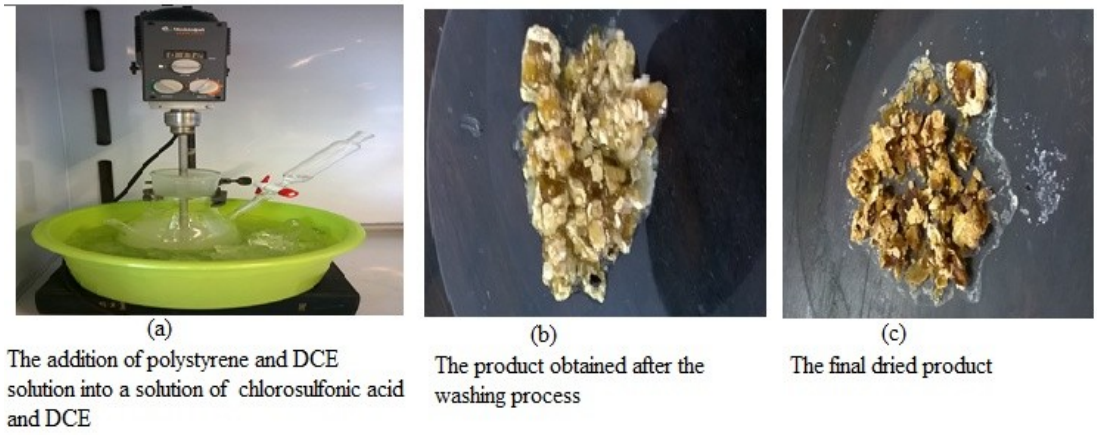

(a) The addition of polystyrene and DCE solution into a solution of chlorosulfonic acid and DCE

(b) The product obtained after the washing process

(c) The final dried product

Figure 3.1: Pictures taken in the laboratory during the synthesis of polystyrene sulfonyl chloride

Stage 2: Preparation of polystyrene sulfonamide (P-SO_2NH_2) – PI_2

The preparation method is given below (Iimura *et al*., 2003; Vogel *et al*., 1996 cited in Fadhel, 2010).

1. The product obtained from stage 1 was stirred with an excess of aqueous ammonia solution of 50 ml.
2. The mixture was stirred at room temperature for 24 hours.
3. The resulting mixture was filtered with suction. Afterwards the product was washed several times with distilled water. Then the product was taken to the vacuum oven and was dried at a temperature of 25 °C overnight. The product was obtained in a form of yellowish-brownish beads.

Stage 3: Preparation of sodium N-chloro-polystyrene sulfonamide (PI) (P-SO_2NClNa) – PI_3

The preparation method is given below (Iimura *et al*., 2003; Vogel *et al*., 1996 cited in Fadhel, 2010).

1. The product obtained from stage 2 was mixed with 50 ml sodium hypochloride aqueous solution at room temperature for 10 hours.
2. The resulting product was washed several times with distilled water. It was then vacuum dried at a temperature of 26 °C.

The dried final product was then crushed into fine powder using a pestle and mortar. This product is shown in Figure 3.2.



Figure 3.2: The synthesized PI

A certain portion of the obtained mass was weighed and taken for different characterization techniques. A mass of 0.2 g was weighed for BET analysis; 0.2 g was weighed for FTIR and about 10 mg for each of the TGA and SEM analysis.

3.3.2 Characterization techniques

There are a lot of characterization techniques that are used to obtain the physical and chemical properties of the catalysts. The present study only focused on the following techniques: FTIR, BET, SEM-EDS and TGA. These techniques were used to determine the adsorbent's physico-chemical properties for its application in the desulfurization process. They were also used to confirm if the obtained PI is the same as that obtained by other researchers. Properties that were analysed include the functional groups, surface area, pore volume, particle size, morphology and thermal stability. These properties are important since they affect the adsorption capacity of the synthesized PI in sulfur removal process.

Fourier Transform Infrared Spectroscopy (FTIR)

A Brüker Tensor 27 Fourier Transform Infrared spectrometry was used to identify the types of functional groups present in the final product (PI) and its intermediate products. All the samples analysed were in powder form. The spectra were recorded at a range of 550 to 4000 cm^{-1}. During this analysis, a beam containing many frequencies of light was shined at the sample and then the

amount of that beam absorbed by the sample was measured. This resulted in an infrared adsorption spectrum which was then used to identify the chemical bonds in a sample.

Brunauer-Emmet and Teller surface area measurement (BET)

A Micromeritics Tristar-Surface area and Porosity analyser was used to measure the adsorption/desorption isotherms of nitrogen at 77K. Sample with a mass of approximately 0.2 g was degassed in nitrogen at 150 ºC for 4 hours prior to analysis using a Micromeritics flow Prep 060 sample degas system. The degassing process is crucial since it removes gases and vapours that may have been adsorbed during the manufacture and handling process. After degassing, the gas adsorption experiment was conducted in order to determine the surface area, total pore volume and average pore size. This analysis was only done on the final product, i.e. PI.

Scanning Electron Microscopy (SEM) equipped with Energy Dispersion Spectroscopy (EDS) Analysis

A Carl-Zeiss Sigma Field Emission-Scanning Electron Microscopy (FE-SEM) equipped with an Oxford X-act Energy dispersion Spectroscopy (EDS) detector was used for analysis. A small amount of each sample was mounted on a carbon adhesive tape. After mounting, the samples were coated with gold-palladium under vacuum to induce conductivity. Thereafter the samples were taken to SEM-EDS for analysis. Before the samples were analysed, the system was purged with nitrogen gas in order to remove moisture and air. This process took about 10 minutes and was done at room temperature. The analysis was done at an acceleration voltage of 10 kV. SEM was used to observe the external morphologies of the samples while EDS was used to determine the elemental composition of the samples. This analysis was done for all three stages products.

Thermo-gravimetric analysis (TGA)

A Perkin Elmer Pyris 1 TGA Thermo-gravimetric analyser was used for thermal analysis of a sample. A sample with a mass of approximately 10 mg was analysed in nitrogen at a constant heating rate of 10 ºC/min in the temperature range of 25 to 900 ºC. A constant air flow rate of 100 ml/min was used. The analysis was done on the final stage product.

3.3.3 Desulfurization process

The desulfurization of diesel fuel was investigated using PI according to the method described by Shiraishi *et al*. (2003). The method employed is the batch adsorption process which was carried out in two sets of experiments. The first set (Case 1) was carried out at the HDS inlet stream and the second set (Case 2) at the HDS outlet stream. For each set, two adsorbents were tested which are PI and PI with CNTs. The experiments for the two adsorbents were conducted simultaneously and also in a similar manner with the only difference being that for PI with CNTs, 0.01 g of CNTs was added 30 minutes after the addition of PI. Four parameters were investigated which are contact time, adsorbent amount, temperature and stirring speed. Hence the experiment is composed of four experimental runs. Since all these parameters are crucial for this study, it was decided to use a small sample size i.e. four samples per run. This was limited by the availability of chemicals and analysis costs. The experimental set-up is shown in Figure 3.3 and the procedure is described thereafter.

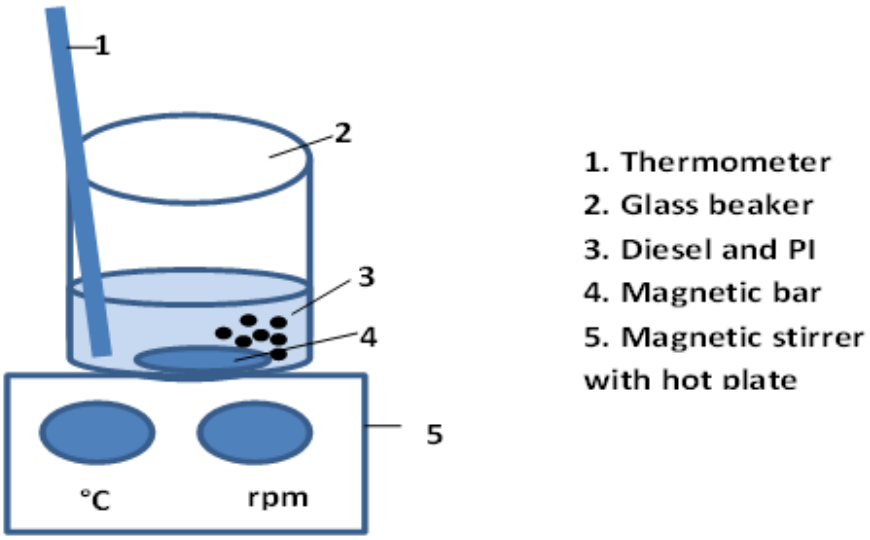

Figure 3.3: Experimental set-up for batch adsorption process of sulfur from diesel using PI

CASE 1: THE TEST ON THE HDS REACTOR INLET STREAM

The first part of this experiment was the test of the adsorbents' sulfur removal capacity on the HDS inlet stream with a sulfur content of 5200 mg/kg.

Part 1: The desulfurization process using PI

Run 1: Effect of contact time

1. 50 ml of diesel fuel was mixed vigorously with 50 ml of methanol and the mixture was heated to the desired temperature. The mixing speed and temperature were kept constant at 625 rpm and 50 ºC respectively.
2. 1 g of PI and 2 ml of acetic acid were carefully added to the mixture.
3. The mixture was stirred and the samples were collected after every 10 hours for 40 hours. The collected samples were allowed to cool to room temperature.
4. After the mixture had cooled, the mixture was filtered to recover the resulting PI.
5. Diesel was then separated from methanol. The diesel was washed with water several times to remove the suspended residues.
6. The diesel samples were then taken for analysis to determine the residual sulfur concentration.

Run 2: Effect of temperature

1. 15 ml of diesel fuel was mixed with 15 ml of methanol at a mixing speed of 625 rpm. The mixture was heated to a temperature of 30 °C.
2. 0.3 g of PI and 0.6 ml of acetic acid were carefully added to the mixture.
3. The mixture was stirred for a desired contact time of 40 hours and afterwards the mixture was cooled to room temperature.
4. Steps 4, 5 and 6 from experimental run 1 were repeated.
5. The same procedure was repeated at a temperature of 50, 70 and 80 °C while keeping other parameters constant.

Run 3: Effect of mixing speed

The procedure is the same as that of run 2 with the difference being that for this experimental run, the temperature and adsorbent amount were kept constant at 50 °C and 0.3 g respectively while changing the mixing speed. The mixing speed of 150, 300, 450 and 625 rpm were used.

Run 4: Effect of adsorbent amount

For this experimental run, the temperature and the mixing speed were kept constant at 50 °C and 625 rpm respectively while the adsorbent amount was varied. The procedure is the same as that of run 2. The mass of PI used was 0.1, 0.3, 0.6 and 1 g keeping that of CNTs constant.

Part 2: The desulfurization process using PI with CNTs

The experimental procedure is the same as that in part 1 with the only difference being that CNTs were added 30 minutes after the addition of PI in all the experimental runs.

CASE 2: THE TEST ON THE HDS REACTOR OUTLET STREAM

This is the second part of this experiment which was conducted on the HDS outlet stream with a sulfur content of 670.6 mg/kg. For this part, some of the parameters (adsorbent amount, temperature, mixing speed) were investigated as a function of contact time while some were investigated at a fixed contact time of 30 hours. Similarly, this case is also divided in two parts which are the test on PI and the test on PI with CNTs.

Part 1: The desulfurization process using PI

Run 1: Effect of adsorbent amount as a function of contact time

1. 50 ml of diesel fuel was mixed with 50 ml of methanol at a mixing speed of 625 rpm. The mixture was heated to the desired temperature of 50 ºC.
2. 1 g of PI and 2 ml of acetic acid were carefully added to the mixture.
3. The mixture was stirred and the samples were collected after every 10 hours for 40 hours. The collected samples were allowed to cool to room temperature.
4. After the mixture had cooled, the mixture was filtered to recover the PI.
5. Diesel was then separated from methanol followed by the washing with water. The washing process was done several times to remove suspended solids.
6. The same procedure was repeated at 0.5 g keeping other parameters constant.
7. The diesel samples were then taken for analysis to determine the residual sulfur concentration.

Run 2: Effect of temperature as a function of contact time

The procedure is the same as that of run 1 with the difference being that for this experimental run, the adsorbent amount and mixing speed were kept constant at 1 g and 625 rpm respectively while changing the temperature. The temperature of 25, 50, 70 and 80 °C were used.

Run 3: Effect of mixing speed as a function of contact time

The procedure is the same as that of run 1 with the difference being that for this experimental run, the adsorbent amount and temperature were kept constant at 1 g and 50 °C respectively while changing the stirring speed. The stirring speed of 300 and 625 rpm were used.

Run 4: The effect of process parameters at a fixed contact time of 30 hours

For the investigation of amount of adsorbent, the remaining adsorbent mass of 0.1, 0.3 and 0.6 g were investigated following the procedure given in Case 1 (Part 1 run 4). Similarly, for the investigation of stirring speed, the remaining speed of 150 and 450 rpm were investigated following a procedure given in Case 1 (Part 1 run 3).

Part 2: The desulfurization process using PI with CNTs

The experimental procedure is the same as that in part 1 with the only difference being that CNTs were added 30 minutes after the addition of PI for all the experimental runs.

3.3.4 Sulfur analysis method

The analysis of the total sulfur compounds remaining in diesel fuel was done using an Inductively Coupled Plasma – Atomic Emission Spectrum (ICP-AES) instrument. For the analysis of the HDS reactor inlet stream, the analysis was conducted at the Inductively Coupled Plasma – Mass Spectrum (ICP-MS) & XRF Laboratory at the University of Stellenbosch. Prior the analysis, the samples were prepared using a microwave digestion instrument. The entire procedure followed is given as follows:

Microwave digestion

The instrument used for the digestion is the MARS microwave digester manufactured by CEM Corporation. The sample was weighed out in the microwave vessel, and then 5 ml of nitric acid (HNO_3) and 2 ml of hydrochloric acid (HCl) were added. This was let to stand open for 20

minutes in order to predigest it. Thereafter the vessel was sealed, placed in the digester and then heated from 25 to 185 °C based on the settings shown in Table 3.3.

Table 3.3: Settings for microwave digester

Power level	1600 W, 100%
Ramp time	25 min
Pressure	800 psi
Temperature	215 °C
Hold time	15 min
Cool down time	25 min

After microwaving, 43 g of deionized water was weighed into a sample bottle that was cleaned in 10% HNO_3 and then it was added to the digested sample in the microwave vessel to make a volume of 50 ml. The solution was then stirred and transferred to the sample bottle.

ICP-AES

The sulfur in diesel was analyzed using a Thermo ICap 6200 ICP-AES. Prior analysis, the instrument was calibrated using National Institute of Standards and Technology, Gaithersburg MD, USA (NIST) traceable standards to quantify selected elements. Thereafter, a NIST-traceable quality control standard from a different supplier was analysed to verify the accuracy of the calibration. For the samples that have undergone digestion, the results were corrected for the dilution factor resulting from the digestion procedure.

For the analysis of the HDS reactor outlet stream, the analysis was conducted at the Environmental and Analytical Chemistry Laboratory at the University of the Witwatersrand. Prior the analysis, the samples were prepared using a microwave digestion instrument. The sulfur analysis was conducted using a Spectrogenesis_EOP ICP-AES instrument. The analysis procedure is the same as that described above with the difference being that HCl was not added during the digestion step. In addition, the standard used is the Multi-elements standard supplied by De Bruyn Spectroscopic Solutions.

Chapter 4 Results and discussion

This study intended on improving an adsorbent's sulfur removal capacity in diesel fuel and to evaluate its applicability in achieving ultra-low sulfur specifications after the HDS process. This section discusses the characterization results of the synthesized PI and the testing of the adsorbents at both high and low sulfur content fuel as elaborated in Chapter 3. Furthermore, the optimum operating conditions were chosen and the adsorption isotherms and kinetics were also discussed.

4.1 Adsorbent characterization results

4.1.1 BET results

Surface area and the porosity of the synthesized material were characterized using a Micromeritics Tristar-Surface area and Porosity analyzer. This experiment was conducted using nitrogen at 77K in a liquid nitrogen cryostat. The obtained structural properties of the synthesized PI are summarized in Table 4.1.

Table 4.1: Structural properties of the synthesized PI

Properties	**Values**
BET surface area (m^2/g)	0.5333
Total pore volume (cm^3/g)	0.00369
Average pore diameter (nm)	25.80

The obtained surface area and pore volumes are much lower than that of the PI synthesized by Fadhel (2010) which are 34.02 m^2/g and 0.6994 cm^3/g respectively. This difference could have been caused by the different solvents concentrations used during the preparation method, the stirring rate and different analysis gases since Fadhel (2010) did not specify the gas used for analysis. This low porosity implies that the PI has some regions that are not porous and this was confirmed by the SEM image shown in Figure 4.4. The synthesized PI is a mesoporous material according to literature (2-50nm) (Llewellyn *et al*., 2012). The porosity of the material is an important surface feature that governs the performance of the adsorbents. Pores that are smaller

than 1nm are known for enhancing the adsorption capacity since they are similar in size with the thiophene molecules (DBTs, DMBTs) (Seredych *et al*., 2012). However, even large pores can enhance the adsorption capacity and selectivity when the functional groups and inorganic particles are present in the adsorbents' surface (Seredych *et al*., 2012). As a result, the adsorption capacity and the selectivity of the synthesized PI would be enhanced by the presence of functional groups and inorganic particles as identified by FTIR and EDS results. In summary, it can be suggested that the synthesized PI is perhaps a mesoporous powder with some nonporous regions.

4.1.2 FTIR results

The functional groups present in the synthesized PI and its intermediates were identified through the IR study. The experiment was conducted using a Brüker Tensor 27 Fourier Transform Infrared spectrometry. The IR study was done by comparison with the typical spectra of ST/DVB chlorosulfonated copolymers and with the information available from literature (Bacquet *et al.*, 1991; Bogoczek & Kociołek-Balawejder, 1986).

Some studies conducted the IR study of polystyrene and compared it to that of sulfonated polystyrene. In this study this was not done and hence sulfonated polystyrene was compared to the IR spectra of polystyrene available from literature. The IR spectra of polystyrene as conducted by Gutch *et al.*(2008) showed sharp peaks at 700 and 780 cm^{-1} which correspond to the C-H bond. Other peaks which were noticed were at 1160 and 2925 cm^{-1} which correspond to C-C bond as well as at 1340 cm^{-1} and 3000 cm^{-1} which correspond to C-H bonds. After sulfonation reaction, it was observed that all these peaks had disappeared. Similarly, this was also observed in the IR spectra obtained in this study as shown by square markers in Figure 4.1.

Stage 1 product: polystyrene sulfonyl chloride (P-SO_2Cl) –PI_1

The IR spectra shown in Figure 4.1 shows adsorption bands at wavelengths of 1800, 1686, 1593, ~1360 and ~1180 cm^{-1} as depicted by letters 1, 2, 3, 4 and 5 respectively. This figure also shows the presence of intensive adsorption bands at a range of 1400 to 850 cm^{-1} which correspond to sulfur-containing functional groups (Bogoczek & Kociołek-Balawejder, 1986). The adsorption bands at wavelengths of ~1160 and ~1360 cm^{-1} correspond to chlorosulfonated groups while

those at1800 and 1053 cm^{-1} correspond to sulfonated groups (RSO_3^-). These bands are in good agreement with those identified by Bacquet *et al*. (1991).

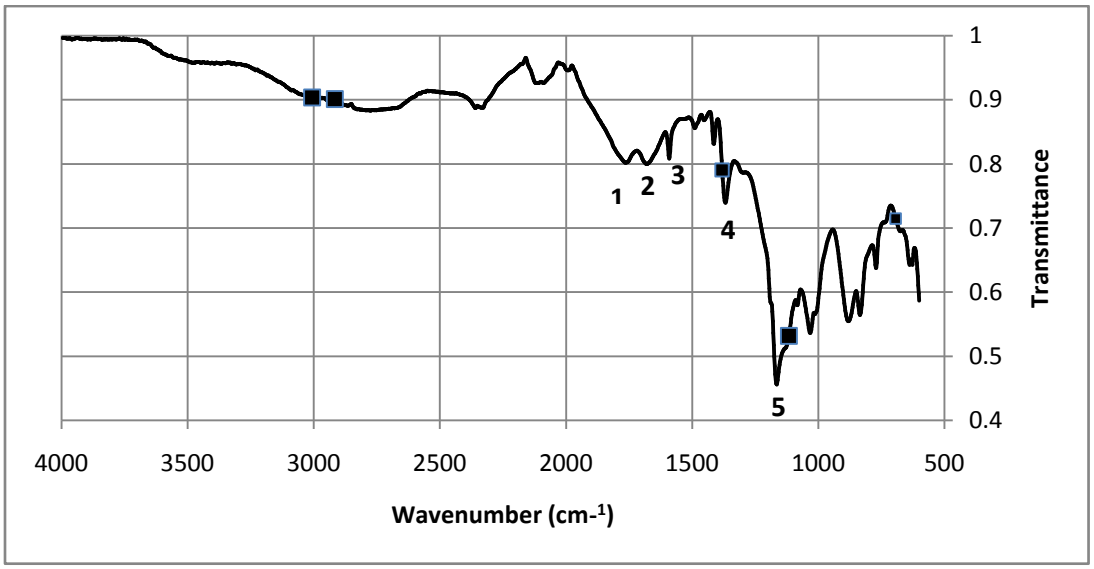

Figure 4.1: FTIR spectra of polystyrene sulfonyl chloride (P-SO_2Cl)

The few adsorption bands at a wavelength of 1686 and 1593 cm^{-1} correspond with aromatic vibrations that stretch from 1600 to 1450 cm^{-1}. The IR spectra do not show strong adsorption bands at a range of 3085 to 3025 cm^{-1} which are characteristic of hydrogen atoms in the benzene ring (Bacquet *et al.*, 1991). The absence of these bands is due to the substituents present in the functionalized resins (Bogoczek & Kociołek-Balawejder, 1986). The same applies to the other two products. The bands that are visible at 780-770, 640 and 590 correspond to C-S vibrations and they are visible in all the three products (i.e. Figure 4.1, Figure 4.2 and Figure 4.3).

Stage 2 product: polystyrene sulfonamide (P-SO_2NH_2) – PI_2

The IR spectra shown in Figure 4.2 show broad adsorption bands at a wavelength of 3209 and 3053 cm^{-1}.

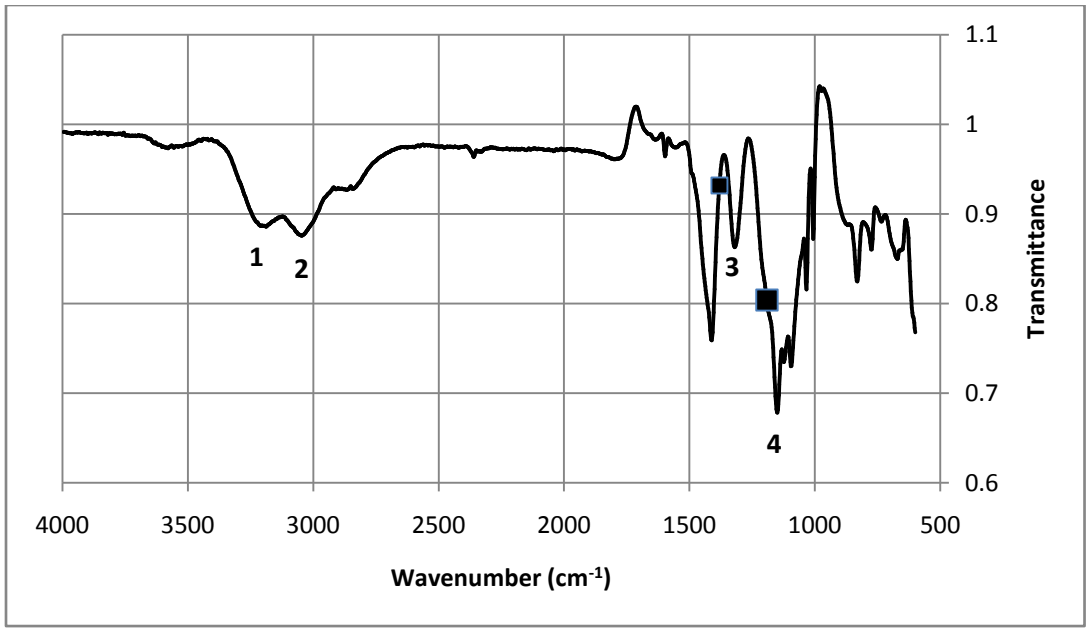

Figure 4.2: FTIR spectra of polystyrene sulfonamide

These bands correspond to N-H bond which stretches from 3250 to 3400 cm^{-1}. These bands are not present in Figure 4.1 due to the absence of amine group in polystyrene sulfonyl chloride. The adsorption bands at wavelengths of 1180 and 1380 cm^{-1} are visible in Figure 4.1, but they are absent in both Figure 4.2 and Figure 4.3 as shown by square markers. This then imply that Cl was replaced by N during the formation of polystyrene sulfonamide. This is the evident that nitrogen was successful added as a functional group. Additionally, there are intensive adsorption bands at a range of 1400 to 850 cm^{-1} which correspond to the sulfur-containing functional groups (Bogoczek & Kociołek-Balawejder, 1986). Some of these bands include bands at ~1380 and ~1126 cm^{-1} which correspond to S-OH and SO stretching in SO_3^- respectively. They are depicted by letter 3 and 4 on the figure above. The identified bands are in good agreement with those identified by Fadhel (2010) and Bogoczek & Kociołek-Balawejder (1986). These bands are also present in Figure 4.3.

Stage 3 product: sodium N-chloro-polystyrene sulfonamide (P-SO_2NClNa) – PI_3

The intensive adsorption bands which correspond to the sulfur-containing functional groups which were described previously are depicted by letters 2 and 3 as shown in Figure 4.3. There is an intense adsorption band at a wavelength of 914 cm^{-1} as depicted by letter 4 in Figure 4.3. This band corresponds to S-N functional group and was also visible in the IR spectra of the PI

synthesized by Fadhel (2010). An adsorption band at 1600 cm^{-1} as depicted by letter 1 corresponds to N-H (Shiraishi *et al*., 2001). An absorption band at 822 cm^{-1} as depicted by letter 5 corresponds to N-Cl (Gutch *et al*., 2008). However, these results do not confirm whether there is a presence of N-Na bond. Hence the results from EDS further confirmed the presence of Na.

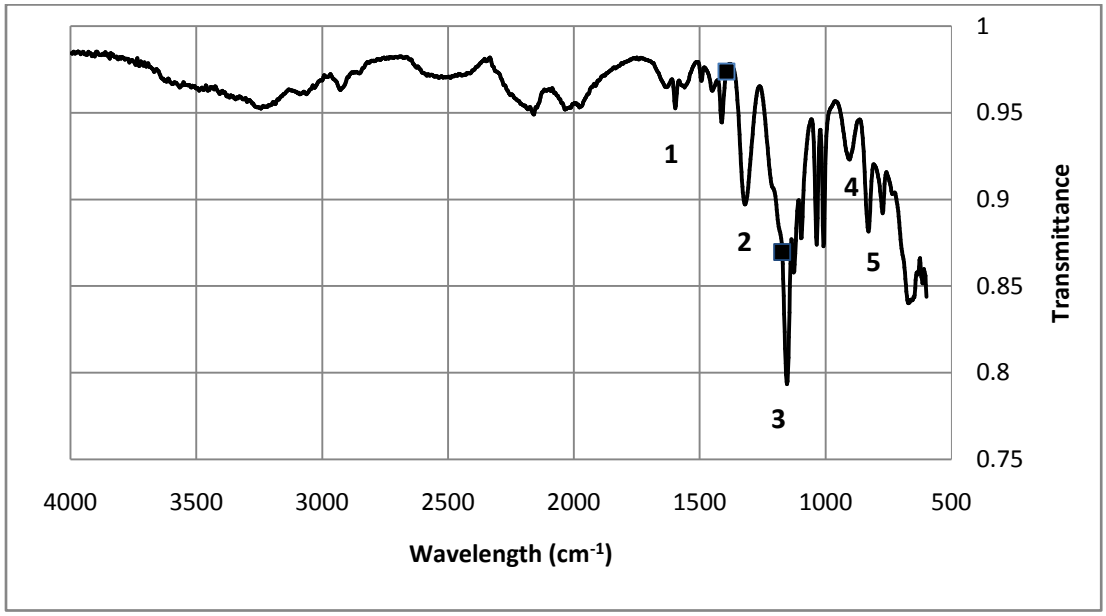

Figure 4.3: FTIR spectra of sodium N-chloro polystyrene sulfonamide

4.1.3 SEM and EDS results

The external surface morphology and topography of the three products was obtained using a Carl-Zeiss Sigma Field Emission-Scanning Electron Microscopy (FE-SEM). The SEM images obtained for all three products are shown in Figure 4.4.

The SEM images as depicted in Figure 4.4 show that all the three products have particles with irregular shape. This shape could have resulted from crushing which was done using a pestle and mortar. It can also be observed from this figure that the surfaces of these products have some porous region. This property is very important since the adsorption rate depends on the porosity of the adsorbent. However, the SEM images show that after sulfonamidation reaction (Figure 4.4 b, c, d), the structures became less porous as compared to the structure before sulfonamidation (Figure 4.4 a).

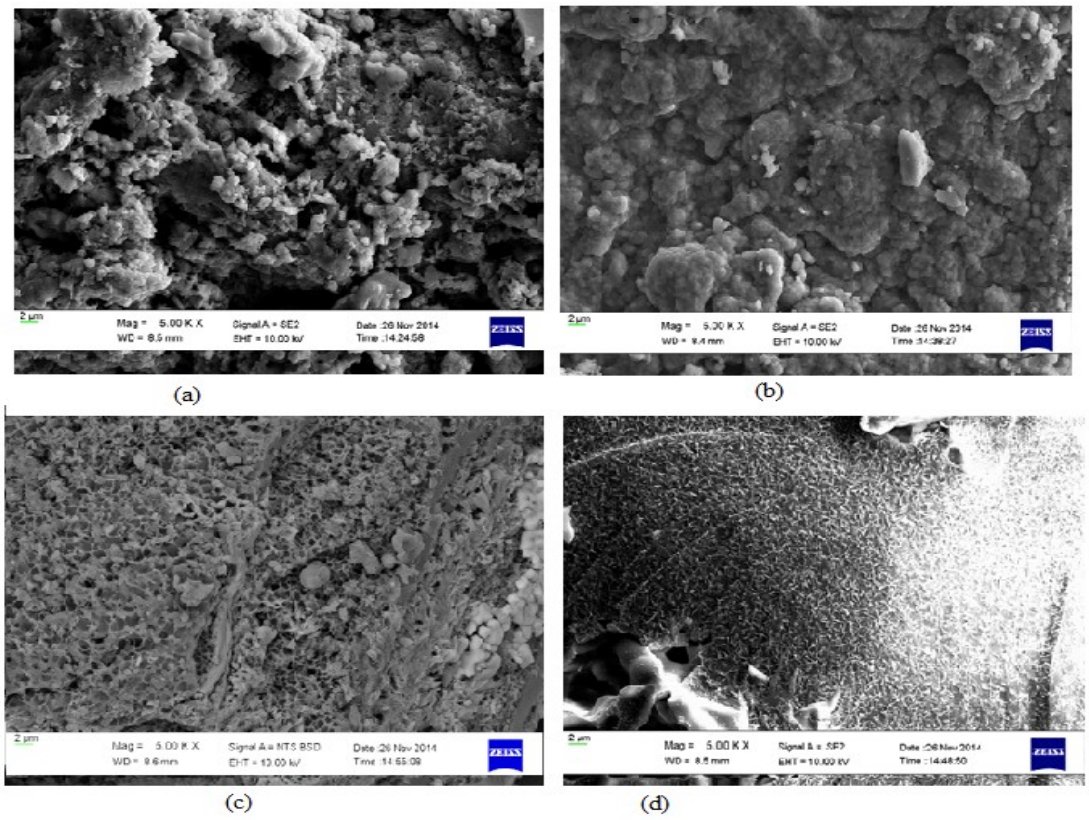

Figure 4.4: SEM images for polystyrene sulfonyl chloride (a), polystyrene sulfonamide (b) and sodium N-chloro polystyrene sulfonamide (c, d)

All the products as shown in Figure 4.4 (a, b, c) appear to have a similar rough surface structure indicating that they are polymer resins (Rabia *et al*., 1996; Bacquet *et al*., 1991). The third product, i.e. sodium N-chloro-polystyrene sulfonamide shows interesting results as depicted Figure 4.4 d. Its SEM image shows that there was a formation of a protective layer in some region of the catalyst. From a study conducted by Krylova *et al*. (1983), it was proven that passivation in catalyst is caused by the adsorption of oxygen molecules. This phenomenon could have resulted in the formation of a protective layer in this polymer. This protective layer appears to be nonporous as shown in the SEM image. This is in good agreement with the results obtained from BET analysis that stipulates that the final product perhaps have a nonporous region. The presence of this nonporous region might have a negative effect on the diffusion of sulfur species during the adsorption process.

The presence of the sulfonic groups, amine group and other elements was confirmed using an Oxford X-act energy dispersion spectroscopy (EDS) detector. The results obtained are shown in Figure 4.5, Figure 4.6 and Figure 4.7.

Stage 1 product: polystyrene sulfonyl chloride (P-SO_2Cl) – PI_1

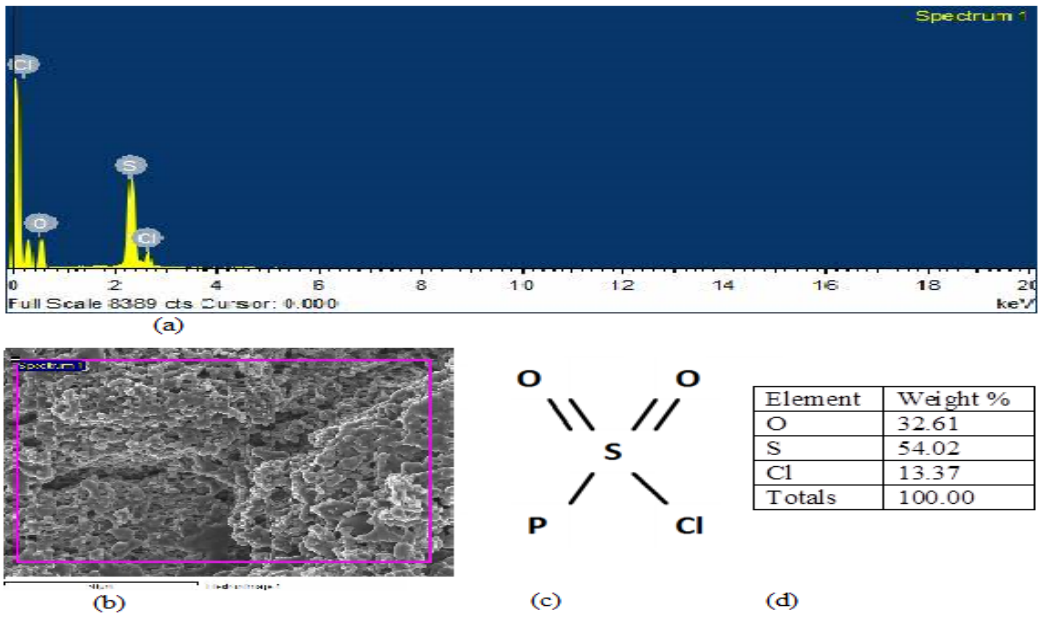

Element	Weight %
O	32.61
S	54.02
Cl	13.37
Totals	100.00

Figure 4.5: EDS spectrum (a), EDS image (b), polymer structure where P represents polystyrene (c) and EDS elemental composition (d) for polystyrene sulfonyl chloride

The EDS spectrum and its elemental composition as shown in Figure 4.5 (a, d) show that polystyrene sulfonyl chloride consists of oxygen, sulfur and chlorine. All the three elements are present in the polymer structure as shown in Figure 4.5 (c). This then imply that the desired product was obtained during chlorosulfonation reaction. These results are in good agreement with the results obtained from FTIR study which confirm the presence of chlorosulfonyl group.

Stage 2 product: polystyrene sulfonamide (P-SO_2NH_2) – PI_2

The EDS spectrum and its elemental composition shown in Figure 4.6 (a, d) shows that polystyrene sulfonamide consists of nitrogen, oxygen, sulfur and chlorine. However, the polymer structure as shown in Figure 4.6 (c) shows the presence of these elements except for chlorine. During the sulfonamidation reaction, chlorine is displaced by nitrogen but the obtained findings shows that not all the chlorine atoms were displaced by nitrogen atoms. The results obtained

from the FTIR study confirm the presence of amine group implying that nitrogen was successfully added to the polymer even though some chlorine atoms were still present.

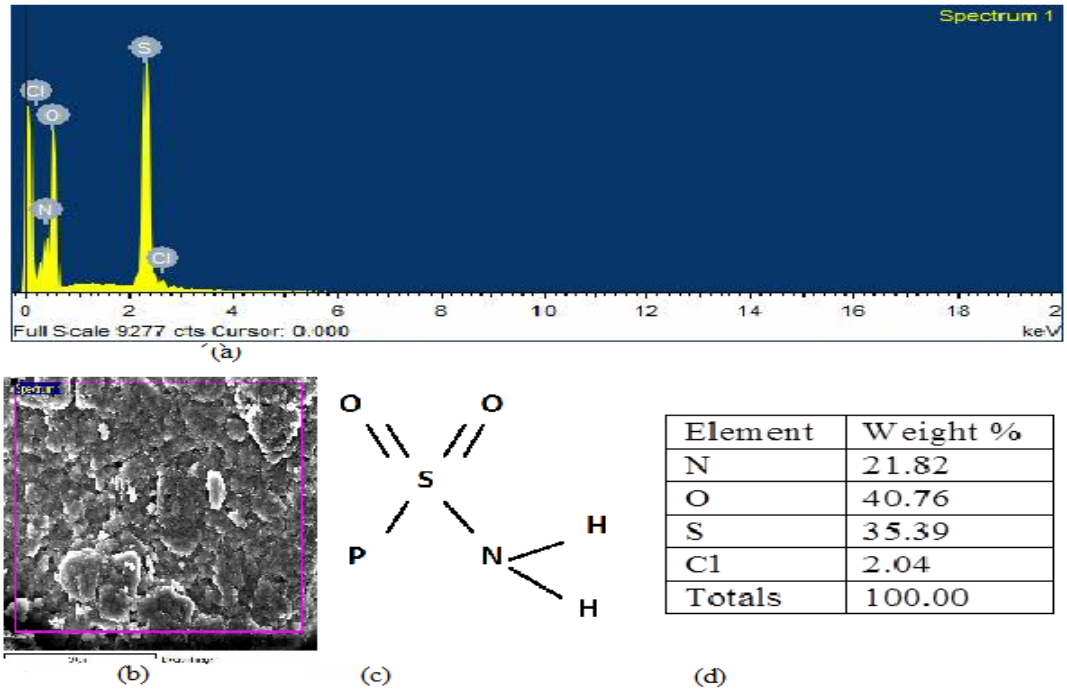

Element	Weight %
N	21.82
O	40.76
S	35.39
Cl	2.04
Totals	100.00

Figure 4.6: EDS spectrum (a), EDS image (b), polymer structure where P represents polystyrene (c) and EDS elemental composition (d) for polystyrene sulfonamide

Stage 3 product: sodium N-chloro-polystyrene sulfonamide (P-SO_2NClNa) – PI_3

The EDS spectrum and its elemental composition shown in Figure 4.7 (a, d) shows that sodium N-chloro-polystyrene sulfonamide consists of oxygen, sodium, sulfur, chlorine and calcium. The structure as shown in Figure 4.7 (c) shows the presence of these elements except for calcium. Calcium is probably an impurity since none of the chemicals used during the reaction contained calcium. The product was probably contaminated during the washing process. The region that was analyzed did not contain nitrogen atom. However the results obtained from FTIR study confirmed the presence of nitrogen. The results from EDS analysis could have been affected by the fact that EDS only requires few quantity of a material (about 10 mg). It is recommended that in future, analysis methods that require a large quantity of the adsorbent should be used such as XRD analysis.

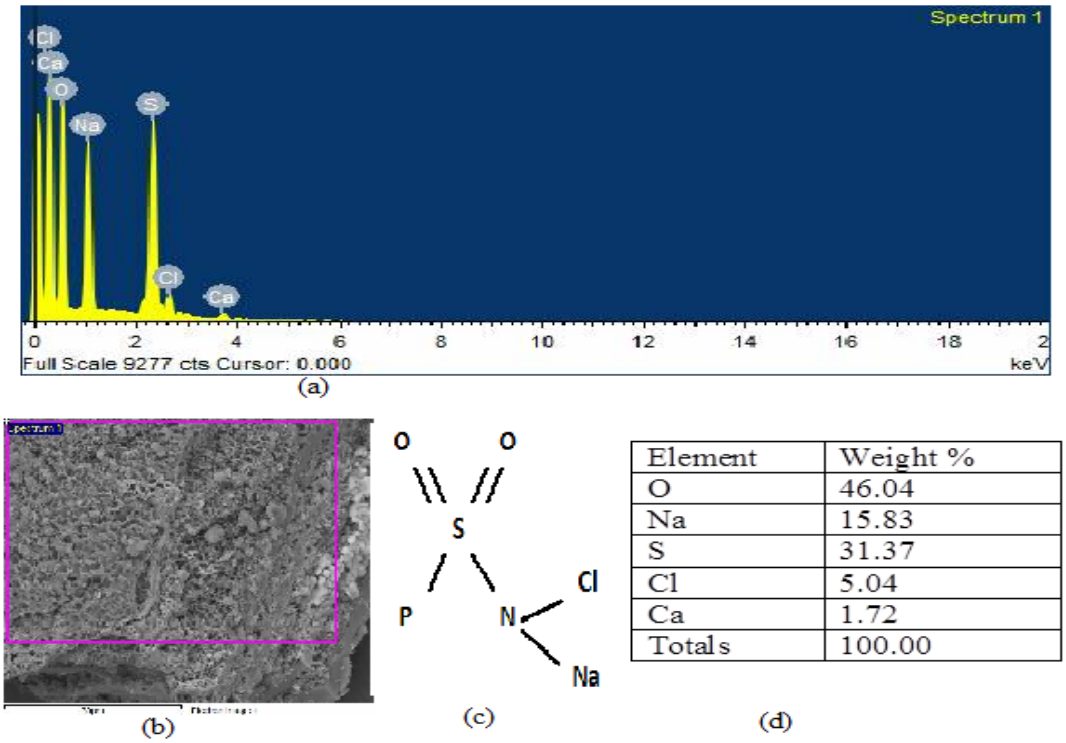

Element	Weight %
O	46.04
Na	15.83
S	31.37
Cl	5.04
Ca	1.72
Totals	100.00

Figure 4.7: EDS spectrum (a), EDS image (b), polymer structure where P represents polystyrene (c) and EDS elemental composition (d) for sodium N-chloro polystyrene sulfonamide

4.1.4 TGA analysis

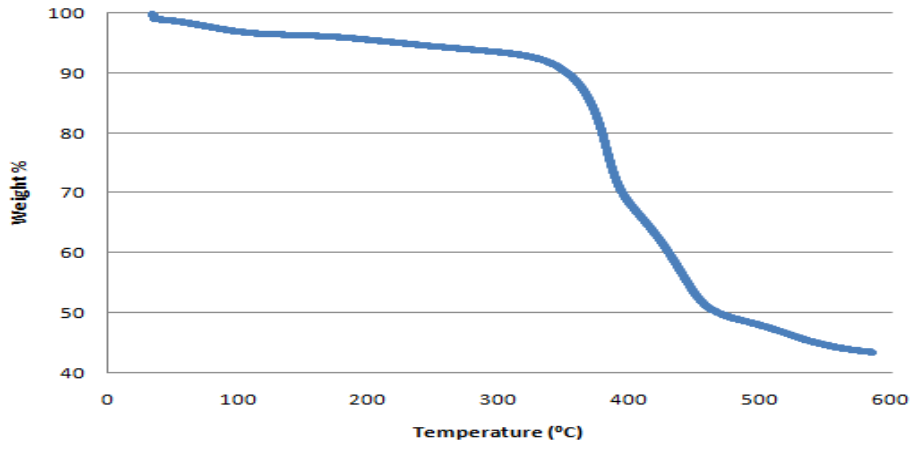

Figure 4.8: TGA analysis curve for PI_3

TGA results show that the thermal stability of the PI decreases as the temperature increases. A slight decrease is noticed starting from around 80 to 300 ºC while after 300 ºC the weight loss is significant. From 80 to 300 ºC there is a weight loss of ~6% and after 300 ºC the weight loss is 55%. Similar findings were obtained by Gutch *et al*. (2008) which showed the decomposition of the resin at high temperatures. This suggests that the PI should not be used at temperatures beyond 80 ºC.

4.2 Comparison of the desulfurization activity of different PI

As described in the synthesis procedure of PI (Chapter 3), there are three stages involved. The desulfurization activity using PI_1, PI_2 and PI_3 was tested on both the inlet and outlet reactor streams. All the process parameters were kept constant at 50 °C, 0.3 g and 625 rpm. The procedure followed is the same as the experimental procedure at a fixed contact time of 30 hours. The results obtained at an inlet reactor stream (5200 mg/kg) are shown in Figure 4.9.

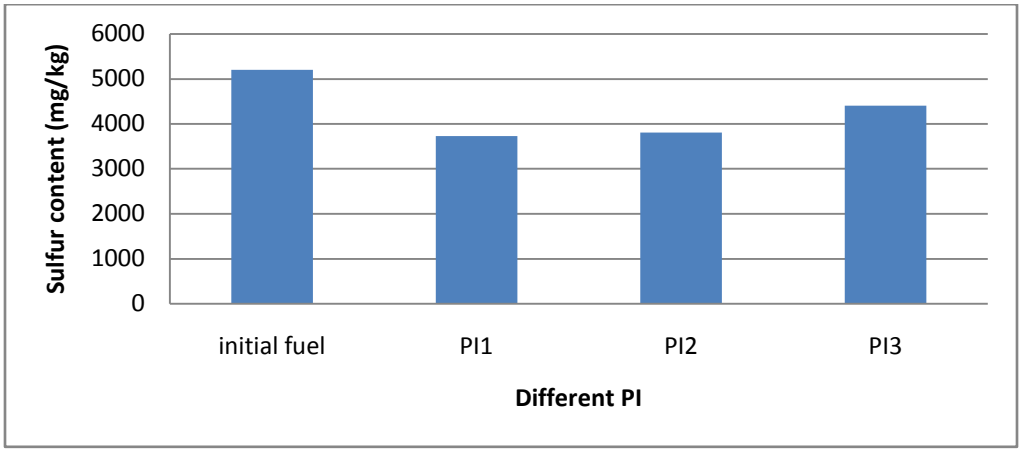

Figure 4.9: The sulfur content of treated diesel fuel with initial concentration (C_0) of 5200 mg/kg using different PI

Figure 4.9 shows that stage 1 product (polystyrene sulfonyl chloride) has the lowest sulfur content as compared to other products. However, the differences in the sulfur content in all the products are very small. This then imply that the first two products may also be used as adsorbents. In addition, it is clear that these products are not capable of lowering the sulfur

content to the desired specification of 10 mg/kg. Hence it can be suggested that these products should not be used to treat fuel with high sulfur content fuel.

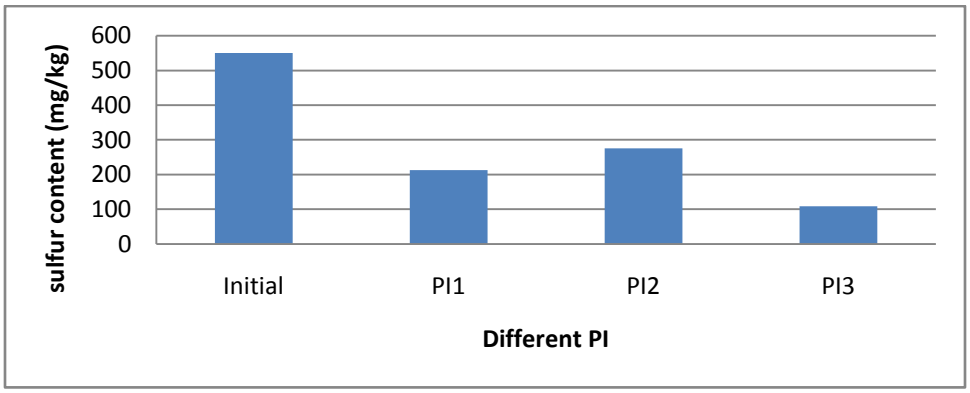

Figure 4.10: The sulfur content of treated diesel fuel with Co of 670.7 mg/kg using different PI

Figure 4.10 shows that stage 3 product (sodium N-chloro-polystyrene sulfonamide) has the lowest sulfur content as compared to other products. It can be suggested that the presence of sodium and chlorine have a positive effect on the adsorption capacity of PI. This is because after they were added, there was a reduction in sulfur content from 275 (PI_2) to 109 (PI_3) mg/kg. Similarly, various studies were conducted that shows that the incorporation of metals and (or) non-metals yield positive results on the performance of the adsorbents. Examples include copper (Ania & Bandosz, 2006), iron oxides and copper oxides (Seredych & Bandosz, 2010), sulfur (Seredych *et al*., 2011; Seredych & Bandosz, 2011) and silver (Seredych *et al*., 2009). As stated in the previous paragraph on high sulfur content fuel, the intermediates products have the capability to treat the diesel fuel. However, they should be used at low sulfur fuel content due to their high sulfur removal efficiencies as seen in Table 4.2.

Table 4.2: Sulfur removal efficiency (η) of different synthesized PI

Different PI	% η at 5200ppm	% η at 670.6 ppm
PI_1	28.21	61.35
PI_2	26.79	49.96
PI_3	15.32	80.25

4.3 Results for the HDS reactor inlet stream (Case 1)

The desulfurization activity of PI (referred as PI_3 in Chapter 3) with and without CNTs was investigated using a commercial fuel obtained from the HDS reactor inlet stream with an initial sulfur concentration (C_0) of 5200 mg/kg. Parameters such as contact time, amount of adsorbent, temperature and mixing speed were investigated and thus the optimum operating condition was determined. The adsorption isotherms were fitted to the experimental data and the kinetics were studied. The experimental results as well as the data used to plot graphs are found in Appendix A.

4.3.1 Effect of contact time

The effect of contact time was studied at 50 °C, 625 rpm and 1 g. The samples were collected every 10 hours for duration of 40 hours. The obtained results are shown in Figure 4.11 for both the adsorbents.

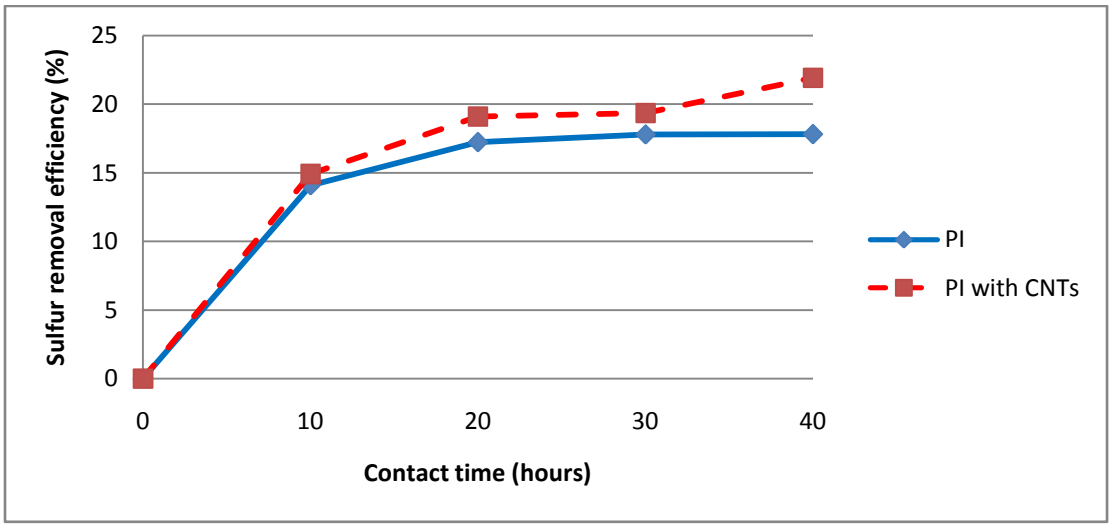

Figure 4.11: The effect of contact time on the sulfur removal efficiency at 1 g, 50 ° C, 625 rpm and C_o of 5200 mg/kg

From the figure, it can be seen that in the beginning of the reaction, there was a rapid increase in the sulfur removal efficiency for both the adsorbents. This can be probably linked to the availability of the adsorption sites in the beginning of each reaction. After 20 hours, there was a slight increase in the sulfur removal efficiency of PI until equilibrium which was reached after

30 hours. A similar trend was observed for PI with CNTs, with the difference being that there was a rapid increase in the sulfur removal efficiency after 30 hours. This slight increase in the removal efficiency probably results because almost all the adsorption sites of the adsorbent were almost filled with sulfur compounds.

An interesting behaviour was observed when CNTs were added to the solution. For instance, Figure 4.11 shows that after its addition, its sulfur removal efficiency exceeded that of PI at all contact times. This suggests that the addition of CNTs accelerated the desulfurization process such that the maximum sulfur removal efficiency was increased from 18 to 22%. However, this removal efficiency is very low and the sulfur content in clean fuel is still far from the acceptable desulfurization level of 10 mg/kg. For instance, the sulfur content was decreased from 5200 mg/kg to 4274 mg/kg using PI and to 4060 mg/kg using PI with CNTs (Appendix A, Table A1). This probably results because of the adsorbent's low reactivity to sulfur compounds at high sulfur content fuel (Fadhel, 2010). Other parameters were varied so as to find the optimum operating conditions as well as to determine the adsorbents' ability/inability to achieve ultra-deep desulfurization levels.

4.3.2 Effect of adsorbent amount

The effect of adsorbent amount on sulfur removal was studied at 50 °C and 625 rpm. The adsorbent amount was varied from 0.1 to 1 g at a fixed equilibrium time of 30 hours and the obtained results are shown in Table 4.3.

Table 4.3: Effect of adsorbent amount on sulfur removal efficiency at 50 °C, 625 rpm, 30 hrs and C_o of 5200 mg/kg

	PI		PI with CNTs	
Adsorbent amount (g)	**Sulfur content (mg/kg)**	**% η**	**Sulfur content (mg/kg)**	**% η**
0	5200		5200	
0.1	4291.56	17.47	4320.17	16.92
0.3	4403.49	15.32	3981.36	23.44
0.6	3766.33	27.57	4244.66	18.37
1	4352.58	16.30	4200.32	19.22

As shown in Table 4.3, no relationship between the removal efficiency and adsorbent amount is observed. Nevertheless, the highest sulfur removal efficiency was achieved at 0.6 g when using PI and 0.3 g when using PI with CNTs. In other studies, the effect of adsorbent amount was observed and it was found that the desulfurization process is accelerated by an increase in the adsorbent amount (Fadhel, 2010). This trend was expected because when the adsorbent amount is high, there is a greater availability of the surface area until a certain point is reached wherein the removal efficiency will not change due to the overlapping of adsorption sites (Kumar & Kirthika, 2009).

In this study, the optimum operating condition was chosen based on the parameters that give the maximum sulfur removal efficiency. Hence, for PI adsorption, the optimum condition occurs at 0.6 g while for PI with CNTs it occurs at 0.3 g. At these adsorbents amounts, the acceptable desulfurization level of 10 mg/kg could not be achieved. Furthermore, even in the presence of 10 times the adsorbent amount, the removal efficiency was still very low. This suggests that this adsorbent (PI) is not suitable to be used at high sulfur content fuel. In this investigation, the advantage offered by the addition of CNTs could not be figured out since there is no trend observed. There were some experimental errors in this run and unfortunately the run could not be repeated due to some limiting factors described in Chapter 3.

4.3.3 Effect of mixing speed

The effect of mixing speed was studied at 50 °C and 0.3 g. The mixing speed was varied from 150 to 625 rpm at a fixed equilibrium time of 30 hours. The obtained results for both the adsorbents are shown in Figure 4.12.

The graphs for the two adsorbents show that the increase in the mixing speed results in the increase in the sulfur removal efficiency. This is due to the fact that, during the adsorption process, the mass transfer rate increases with an increase in the mixing rate. This is caused by the reduction in surface film resistance as the mixing rate increase, thereby allowing the sulfur species to reach the adsorbent surface more easily (Ahmad & Sumathi, 2005). A further increase in the stirring speed resulted in a rapid decrease in the sulfur removal efficiency as shown in the figure. This is probably due to the fact that as the stirring speed increases, more of the particle

surface gets occupied with sulfur species until there are no more sites left. Furthermore, rigorous mixing speed desorbs the adsorbate due to strong centrifugal force (Saha & Datta, 2009).

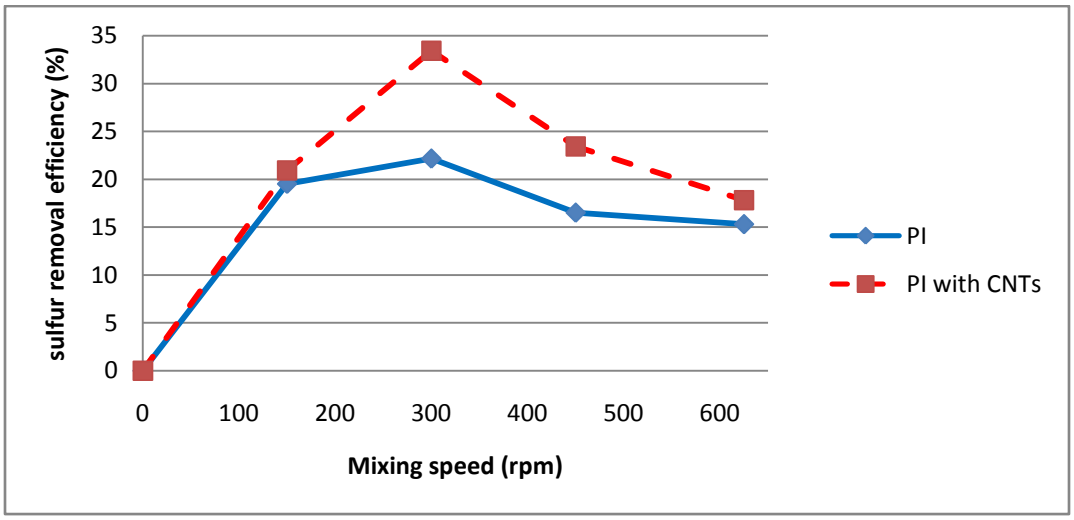

Figure 4.12: Effect of mixing speed on sulfur removal efficiency at 50 °C, 0.3 g, 30 hours and C_o of 5200 mg/kg

These results, therefore suggest that the process operates much better at lower mixing rates. On contrary, Shiraishi *et al*. (2003) specified that the desulfurization test should be carried out at rigorous mixing speed. However, our findings agreed fairly well with those obtained by other researches in the study of the effect of mixing speed on the adsorption capacity of different adsorbents (Ahmad *et al*., 2005; Saha & Datta, 2009). The comparison of the two graphs shows that the addition of CNTs has a very positive effect on the desulfurization performance. For instance, the maximum sulfur removal efficiency was increased from 22 to 33 % at 300 rpm. However, this removal efficiency is still very low since the sulfur content was lowered from 5200 mg/kg to 4048.13 mg/kg using PI and to 3462 mg/kg using PI with CNTs (Appendix A, Table A4). This is still far from the acceptable sulfur specification of 10 mg/kg.

4.3.4 Effect of temperature

The effect of temperature was studied at 625 rpm and 0.3 g. The temperature was varied from 30 to 80 °C for 30 hours and the results obtained are shown in Figure 4.13. The graphs show the rapid increase in the sulfur removal efficiency at lower temperatures and then a rapid decrease at high temperatures. The removal efficiency for PI is low. However, when CNTs were added, it

was observed that there is an increase in the sulfur removal efficiency of PI. For instance, the maximum removal efficiency of PI was increased from 20.8 % (at 50 °C) to 27.8 % (at 30 °C). This further supports the finding that the addition of CNTs has a positive effect on the desulfurization performance of PI.

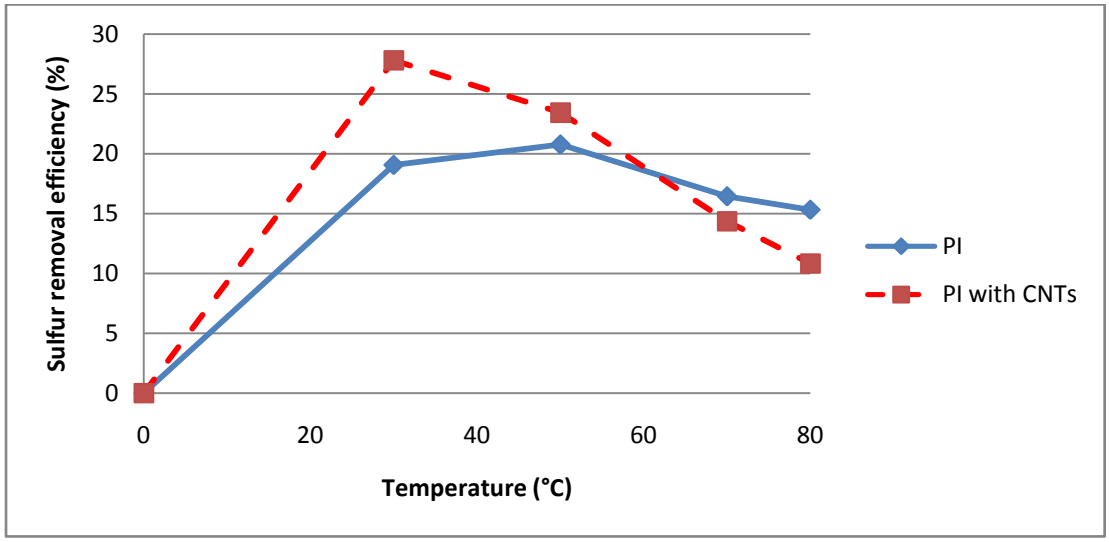

Figure 4.13: The effect of temperature on sulfur removal efficiency at 0.3 g, 625 rpm, 30 hours and C_o of 5200 m/kg

For both the adsorbents, Figure 4.13 shows that the adsorption process is highly favoured at temperatures below 50 °C. At higher temperatures, the removal efficiency decreased significantly which is probably caused by the decomposition of the sulfonium salts (Shiraishi *et al*., 2001). This relationship suggests that the adsorption process might be endothermic in nature. This is supported by the results obtained in the adsorption isotherm study (Section 4.3.6) which indicate that this adsorption process can be best described by the Freundlich model thus suggesting that the nature of the process is physioption. On the contrary, the kinetic study (Section 4.2.7) suggests that this process follows the pseudo-second-order model which suggests that the process is most likely to be chemisorption. However, even though the Freundlich model was the best fit, the Freundlich n-value indicated that the sulfur compounds were not favourably adsorbed onto the two adsorbents. Thus it can be suggested that the process is most likely to be controlled by chemisorption process.

From the obtained results, it can be suggested that the desulfurization process should be carried out at lower temperature conditions. In addition, operating the process at temperatures between

30 and 50 °C is not such a bad idea since the difference in the removal efficiencies is not too high. Hence the optimum operating temperature is 50 °C for PI and 30 °C for PI with CNTs. Additionally, at these optimum temperatures, the sulfur content was reduced from 5200 mg/kg to 4120 mg/kg when using PI and 3754 mg/kg when using PI with CNTs (Appendix A, Table A3).

4.3.5 Optimum operating conditions

The optimum operating condition for each of the two adsorbents was chosen based on the parameter that corresponds to the lowest sulfur content. These conditions are summarized in the table below.

Table 4.4: The optimum operating condition for sulfur adsorption process at C_o of 5200 mg/kg

Parameter	PI	PI with CNTs
Amount of adsorbent (g)	0.6	0.3
Temperature (°C)	50	30
Stirring speed (rpm)	300	300
Contact time (hrs)	30	40

As discussed earlier on, the use of CNTs has a positive effect on the desulfurization activity of PI. This is not the only advantage offered by CNTs; it also reduced the optimum operating temperature and the adsorbent amount used as shown in Table 4.4 above. For the adsorbent amount, the given adsorption process that uses PI with CNTs only requires half of the adsorbent (PI) and this process can be carried out at room temperature. Operating at low temperature lowers the energy requirement of the process and thus making this process attractive.

From the obtained results, it can be suggested that CNTs should be used with PI in the desulfurization process of high sulfur content fuel. Although CNTs improved the adsorption capacity, the acceptable sulfur levels could not be achieved. This was also supported by the findings from other studies (Fadhel, 2010; Shiraishi *et al*., 2003). The aim was to use CNTs to improve the adsorption capacity, and this idea worked but it was not good enough since the lowest sulfur content attained is very far from the current sulfur standard.

4.3.6 Adsorption isotherms

The adsorption isotherms show how the adsorption molecules distribute between the liquid and the solid phase during equilibrium. The two models that are frequently used are the Langmuir and Freundlich models. The graph obtained in the study of the effect of temperature on sulfur removal was fitted in these models. The calculations and data are shown in Appendix C.

Langmuir isotherm

The equilibrium data for sulfur adsorption on the two adsorbents was fitted to the linearized Langmuir equation given by Equation 2.10. Figure 4.14 shows a linear plot of specific adsorption (C_e/q_e) against equilibrium concentration (C_e).

The Langmuir constants, Q and b, were determined from the slope and the intercept of the plot and the calculated values are shown in Table 4.5. In addition, the separation factor (r) was also calculated in order to examine the progression of the adsorption dimensionless constant using Equation 2.12. The correlation coefficient, R^2, suggests that the Langmuir model can sufficiently describe the data well for both the adsorbents. However, the negative values of b and r indicate that this model is not suitable to describe the equilibrium adsorption (Ramakrishna, 1996). This is due to the fact that the constants indicate the surface binding energy and the monolayer coverage which are positive values (Kale, 2013). Similar findings of negative Langmuir constants were reported on the study of the adsorption of sulfur compounds from diesel using activated carbon (Nkosi, 2014).

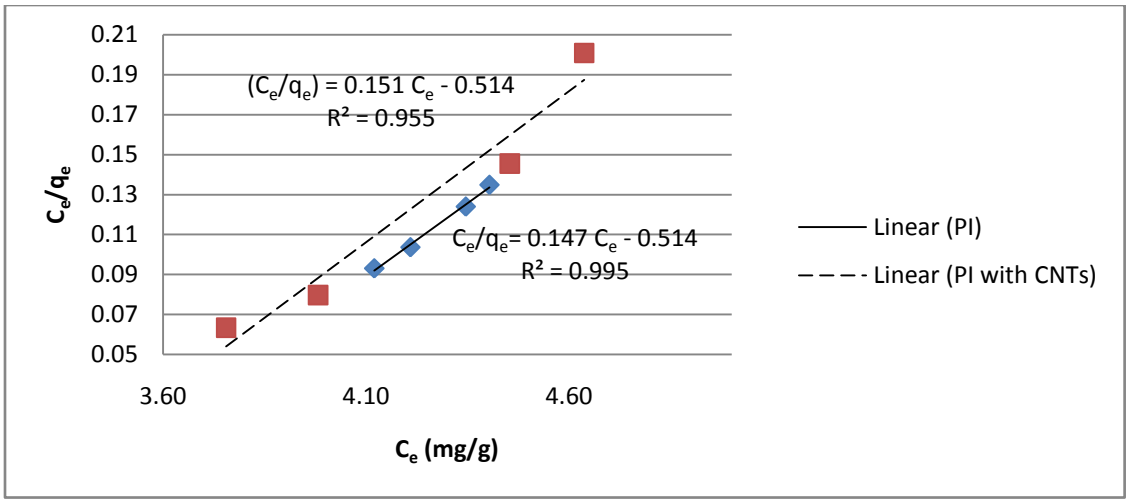

Figure 4.14: Langmuir isotherm for sulfur adsorption at C_0 of 5200 mg/kg

Freundlich isotherm

The equilibrium data were further analyzed using the Freundlich isotherm. The equilibrium data was fitted to the linearized Freundlich equation given by Equation 2-14. Figure 4.15 shows the Freundlich isotherm plot.

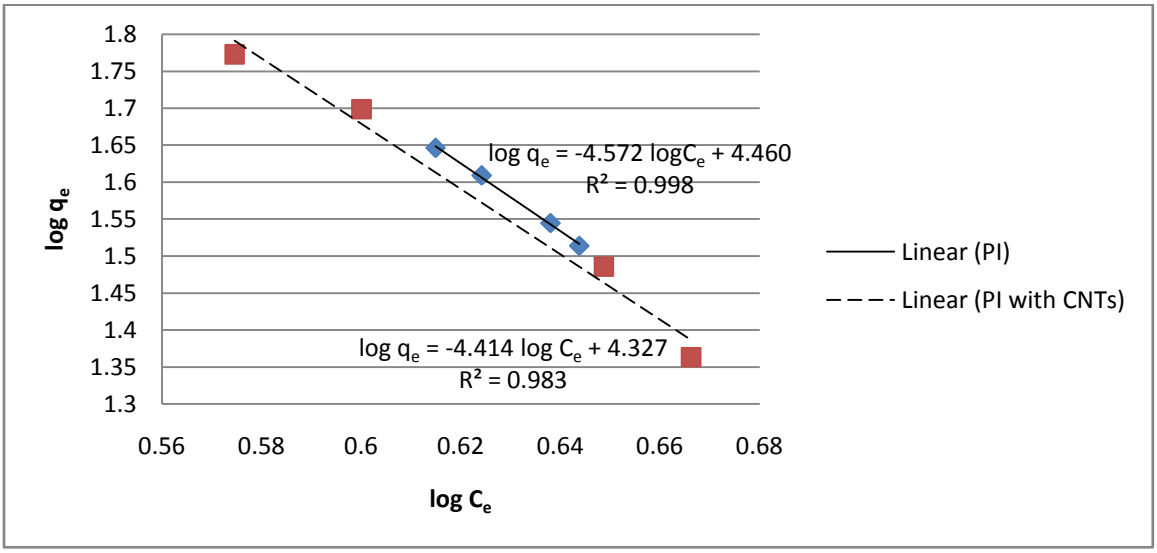

Figure 4.15: Freundlich isotherm for sulfur adsorption at C_0 of 5200 mg/kg

The Freunlich plot as shown above was used to determine the Freundlich constants, Q_f and n. These constants represent an indication of adsorption capacity (mg/g) and the adsorption intensity respectively. The interpretation of the n-value gives an indication of the favorability of

the adsorption process, wherein n >1 implies that the adsorption process is favorable at given conditions (Chiou and Li, 2002). These constants along with their corresponding correlation coefficients are higher than those calculated by Langmuir model, suggesting that the adsorption process is a physical process. These findings are similar to those obtained in the study of sulfur adsorption using activated carbon (Bu *et al*., 2011; Mužic *et al*., 2009). The calculated n-value for both the adsorbents is lower than unity, indicating that the sulfur compounds were not favourably adsorbed onto the two adsorbents.

A summary of the Langmuir and Freundlich constants is shown in the table given below. Based on the correlation coefficients, the Freundlich isotherm model best represents the experimental data.

Table 4.5: Langmuir and Freundlich isotherm constants and correlation coefficients for sulfur adsorption at C_0 of 5200 mg/kg

	Langmuir isotherm				Freundlich isotherm		
Adsorbents	**Q (mg/g)**	**b (l/mg)**	**r**	**R^2**	**Q_f ((mg/g)(l/mg)$^{1/n}$)**	**n**	**R^2**
PI	6.803	-0.2860	-2.053	0.995	28840.32	-0.219	0.998
PI/ CNTs	6.623	-0.2934	-1.895	0.995	21232.44	-0.227	0.983

4.3.7 Kinetic study

The pseudo-first-order and the pseudo-second-order model were used in order to determine the controlling mechanism of the adsorption process. These modelas are based on the assumption that the rate limiting step is either the mass transfer process or chemisorption. In addition, the rate of adsorption was determined using these models. Appendix D gives a detailed description of the kinetic data.

Pseudo-first-order kinetics

The linear form of pseudo-first-order model given by Equation 2-6 was used to describe the adsorption kinetics of sulfur. Figure 4.16 shows a linear plot of log ($q_e - q_t$) versus time for the two adsorbents.

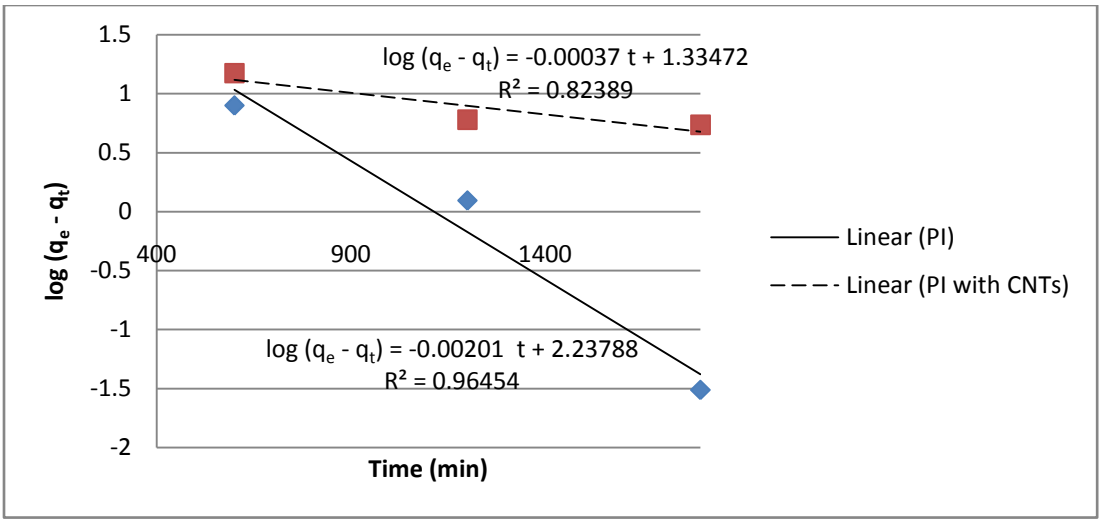

Figure 4.16: Pseudo-first-order kinetic graph for sulfur adsorption at C_0 of 5200 mg/kg

The slope and intercept of the graph were used to obtain the pseudp-first-order constants (k_1 and q_e). The rate constant (k_1) and equilibrium concentration (q_e) obtained are shown in Table 4.6 along with their correlation coefficient. Based on the correlation coefficient of 0.965 (PI) and 0.824 (PI with CNTs), the pseudo-first-order model does not fit well the experimental data as compared to the pseudo-second-order model. In addition, the calculated equilibrium concentration ($q_{e,calc}$) does not agree well with the experimental value. This suggests that the adsorption of sulfur does not follow the pseudo-first-order kinetics.

Pseudo-second-order kinetics

The linear form of pseudo-second-order model given by Equation 2-8 was used to describe the adsorption kinetics of sulfur. This model assumes that the rate-limiting step might be chemisortption (Kumar and Kirthika, 2009). A linear plot of t/q_t versus time was plotted and is given in Figure 4.17.

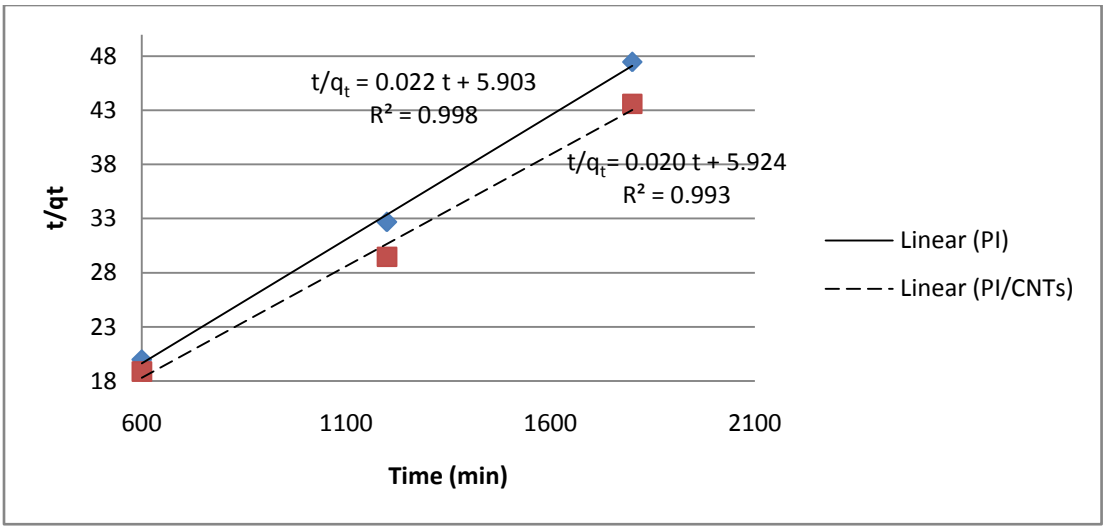

Figure 4.17: Pseudo-second-order kinetic model for sulfur adsorption at C0 of 5200 mg/kg

The slope and intercept of the graph were used to obtain the pseudo-second-order constants (k_2 and q_e). The obtained rate constants (k_2) and equilibrium concentration (q_e) along with the R^2 values are shown in Table 4.6. The correlation coefficient for the two adsorbents, 0.998 (PI) and 0.993 (PI with CNTs) are very close to unity. In addition, the calculated equilibrium concentration is very close to the experimental value. Hence these facts support that the adsorption of sulfur follows the pseudo-second-order kinetics. This then suggests that the overall sulfur adsorption is most likely to be controlled by chemisorption process (Jiwalak *et al*., 2010).

The pseudo-first- and second-order-constants as well as the correlation coefficients are shown in the Table 4.6. From the table, it is clear that the pseudo-second-order is a best model to represent the experimental data.

Table 4.6: Pseudo-first-order and pseudo-second-order constants and correlation coefficients for sulfur adsorption at C_0 of 5200 mg/kg

	Pseudo-first-order		**Pseudo-second-order**		
Constants	**PI**	**PI/CNTs**	**Constants**	**PI**	**PI/CNTs**
k_1 (min^{-1})	0.00463	0.000852	**k_1 ($g.mg^{-1}.min^{-1}$)**	8.20E-05	6.75E-05
$q_{e,calc}$ (mg/g)	172.93	21.613	**$q_{e,calc}$ (mg/g)**	45.455	50
$q_{e,exp}$ (mg/g)	37.956	46.701	**$q_{e,exp}$ (mg/g)**	37.956	46.71
R^2	0.965	0.824	**R^2**	0.998	0.993

4.3.8 Characterization of spent adsorbent

The PI used to treat the inlet stream to the HDS reactor was taken for FTIR and SEM-EDS analysis. The obtained results were compared with those of the unused PI.

FTIR analysis

Figure 4.18 shows that the two absorbents have the same functional groups with the difference at a region from 3000 to 1400 cm^{-1} wavelength. The peaks of the sulfur-containing functional groups (1400 to 850 cm^{-1}) for both the spectra are aligned thus indicating that the sulfur compounds adsorbed on PI via chemical reaction may be relatively weak. However, there are sharp peaks present at around 3000 and 1400 cm^{-1}. The peaks at ~3000 and ~2900 cm^{-1} correspond to C-H stretch in thiophene compound. Furthermore, sharp peaks can be seen at ~1450 and ~1370 cm^{-1}which can be assigned to the v_3 mode of thiophene which is a ring vibration consisting of a symmetric stretch of C=C bonds of thiophenes. These bands are in good agreement with those identified by Wu *et al*. (2002). This thus implies that sulfur compounds were indeed adsorbed during adsorptive desulfurization process.

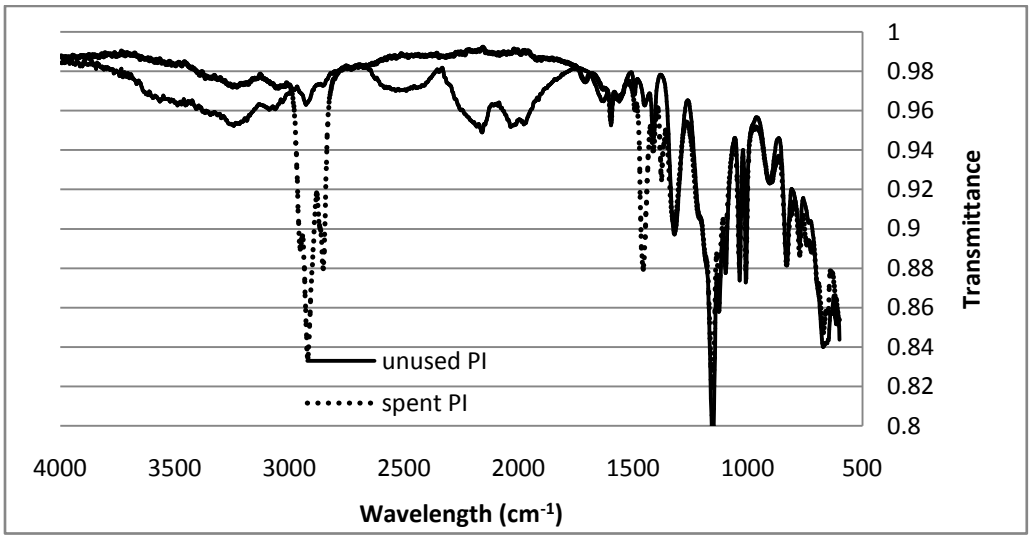

Figure 4.18: FTIR spectra of spent PI used to treat HDS reactor inlet stream with C_o of 5200 mg/kg

SEM-EDS analysis

The SEM images for the unused and spent PI show dissimilarity in their structures. The SEM images of used PI with and without CNTs (Figure 4.19 a (i) & b (i)) show a less porous structure as compared to the image of unused PI (Figure 4.19 c (i)). This is probably due to the sulfur species that are now present on the used PI. It can be noticed from the EDS spectrum that the used and unused PI comprises of the same elements though the compositions are different.

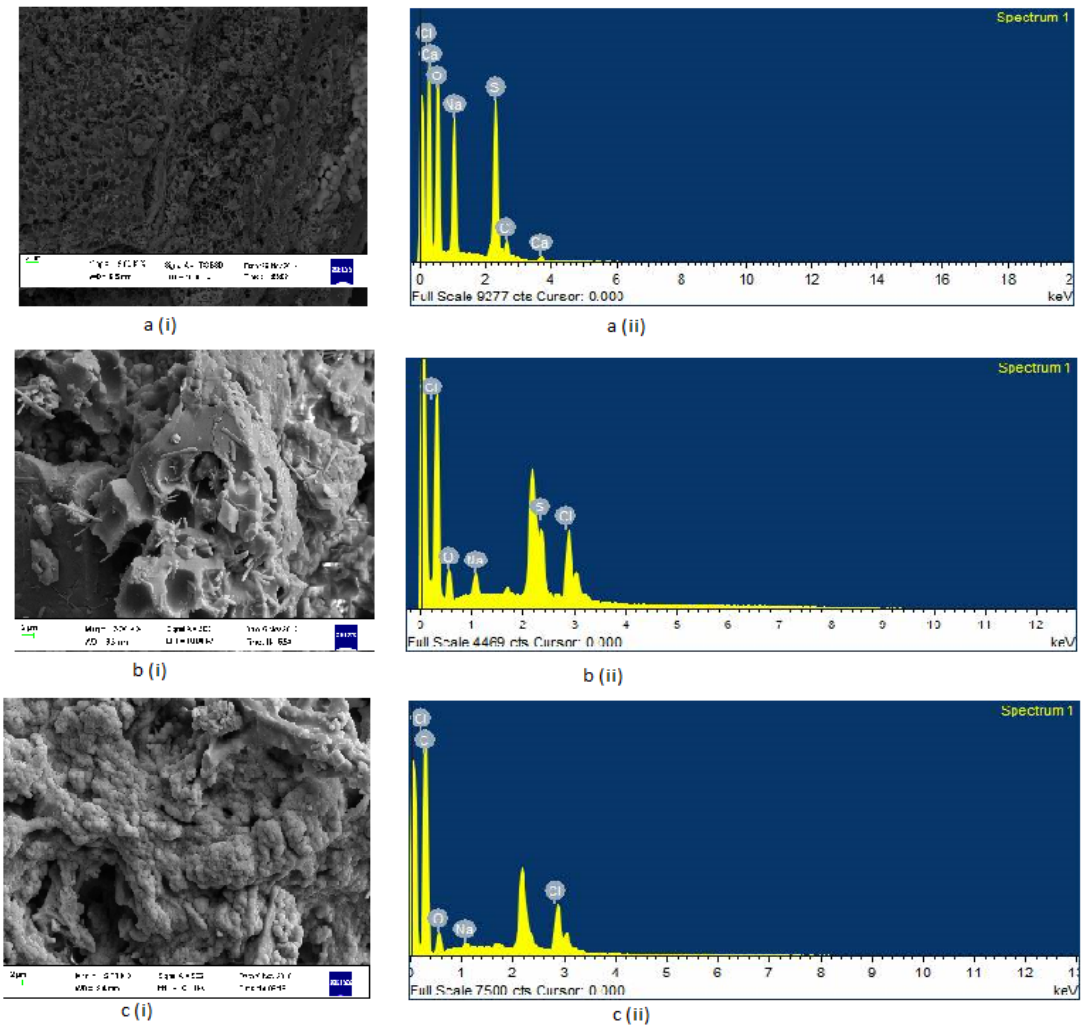

Figure 4.19: SEM images for unused PI a (i), used PI b (i) and used PI with CNTs c (i) alongside with their corresponding EDS spectra (ii) at Case 1

4.4 Results for the HDS reactor outlet stream (Case 2)

The desulfurization of commercial diesel fuel obtained from HDS reactor outlet stream with initial sulfur content (C_o) of 670.6 mg/kg was investigated using PI with and without CNTs. The investigated parameters are the same as those in Section 4.3. The experimental results as well as the data used to plot graphs are found in Appendix B.

4.4.1 Effect of contact time

The effect of doubling the stirring speed on the sulfur removal efficiency was investigated as a function of contact time in order to determine the equilibrium time. This was conducted at 50 °C and 1 g. The samples were collected after every 10 hours and the results obtained are shown in Figure 4.20. The sulfur removal efficiency for both the adsorbents was very rapid in the beginning of the reaction (i.e. first 10 hours). This is probably due to the large number of available adsorption sites in the beginning of each reaction (Kumar & Kirthika, 2009). As the contact time increases, the sulfur removal efficiency gradient decreases due to the few available adsorption sites. Most of the maximum sulfur removal efficiency was obtained after 20 hours for both the adsorbents. For instance, at 625 rpm, both the adsorbents show that equilibrium is attained after 20 hours. However, at 300 rpm, there is a slight increase in the sulfur removal efficiency between 20 and 40 hours. Increasing the contact time increases the sulfur removal efficiency and it remains almost constant after reaching an equilibrium time of about 20 hours. These results agreed well with the findings obtained from a study by (Fadhel, 2010) who obtained a saturation time of 20 hours.

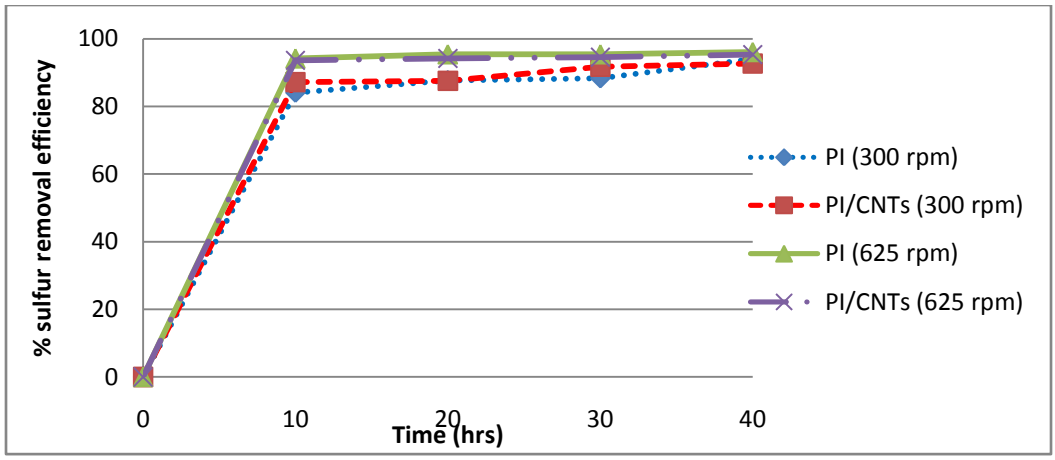

Figure 4.20: The effect of doubling stirring rate on the sulfur removal efficiency at 1 g, 50 °C and C_o of 670.6 mg/kg

It can also be observed that doubling the stirring speed results in an increase in the sulfur removal efficiency for both the adsorbents. Furthermore, it can be seen that the removal efficiency obtained using PI with CNTs at 300 rpm is slightly higher than that obtained using PI while at 625 rpm there is no improvement noticed. From the obtained results, it can be concluded that at low sulfur content fuel, CNTs do not offer any major improvement in the adsorption capacity of the PI. On the contrary, CNTs are very effective on high sulfur content fuel as proven by the results obtained in Section 4.3. All the trends show that at after 30 hours there is a slight increase in the removal efficiencies thus it is safe to use an equilibrium time of 30 hours in the proceeding investigations.

4.4.2 Effect of adsorbent amount

The effect of adsorbent amount on the sulfur removal efficiency was studied at 50 °C and 625 rpm at an equilibrium time of 30 hours. The adsorbent amount was varied from 0.15 to 1 g and the obtained results are shown in Figure 4.21.

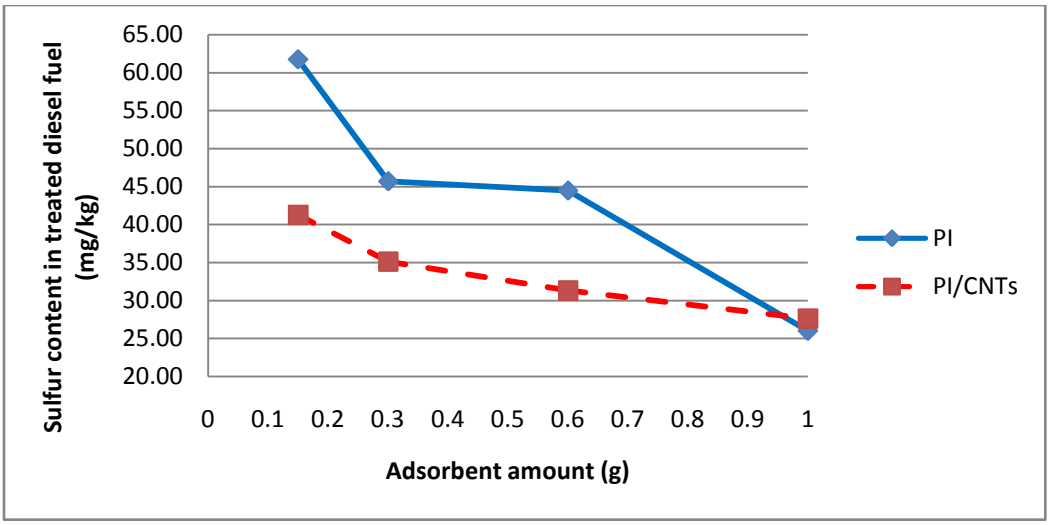

Figure 4.21: The effect of adsorbent amount on sulfur removal efficiency at 50 °C, 625 rpm, 30 hrs and C_o 670.6 mg/kg

Figure 4.21 shows that the sulfur content in treated diesel fuel decreases sharply as the adsorbent amount is increased. This trend was also observed in the desulfurization study of commercial light oil using PI (Fadhel, 2010). This is because increasing the adsorbent amount results in a greater availability of the surface area and hence more sulfur compounds get adsorbed (Kumar and Kirthika, 2009). This decrease in the sulfur content corresponds to the increase in the removal efficiency of the adsorbents. The highest sulfur removal efficiency of ~96% was obtained for both the adsorbents at 1 g. These removal efficiencies correspond to sulfur content of 26 and 27 mg/kg for PI and PI with CNTs respectively (Appendix B, Table B 3).

The obtained figure shows that the addition of CNTs improves the adsorption capacity of PI especially at the adsorbent range of 0.1 to 0.6 g. This suggests that instead of adding high dosage of PI, the process can be operated at low adsorbent dose of PI and 0.01 g of CNTs. For instance, adding 0.6 g of PI and 0.01 g of CNTs cleans the fuel to ~31 mg/kg which is very close to the target specification of 10 mg/kg. The highest removal efficiency for both the adsorbents was achieved at 1 g thus this was chosen as the optimum adsorbent dosage. From this, it can be suggested that CNTs should be added to the solution when using low adsorbents dosage. The lowest sulfur content obtained is 26 mg/kg which is very close to the target specification of 10 mg/kg thus implying that this process is a potential desulfurization process.

4.4.3 Effect of mixing speed

The effect of mixing on the sulfur removal efficiency was studied at 50 °C and 0.3 g at a fixed equilibrium time of 30 hours. The mixing speed was varied from 150 to 625 rpm and the obtained results are shown in Figure 4.22.

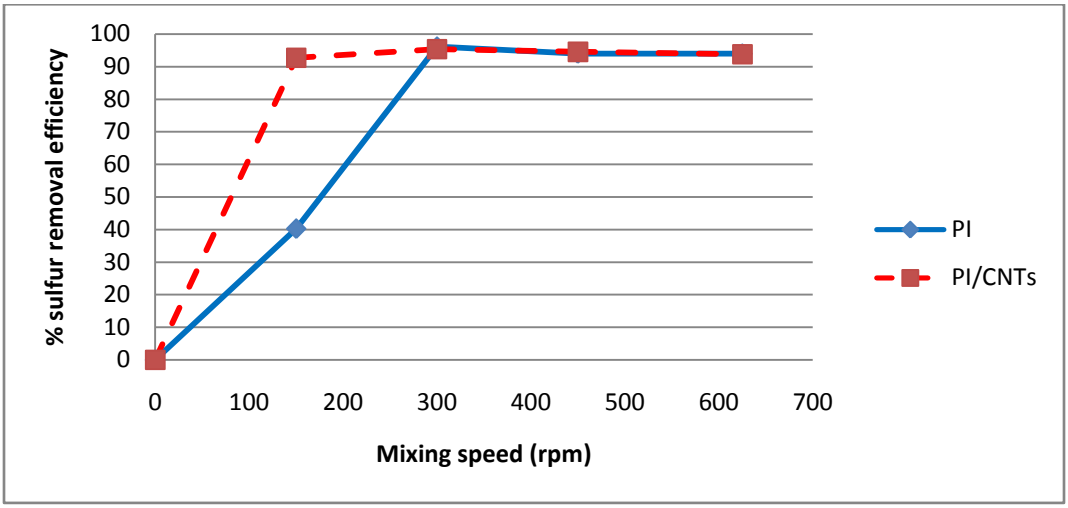

Figure 4.22: Effect of mixing speedon sulfur removal efficiency at 50 °C, 0.3 g, 30 hours and C_o of 670.6 mg/kg

As shown by the trend in Figure 4.22, the results show that the sulfur content in diesel fuel increases sharply at first (0-300 rpm) but thereafter there is no significant change in the sulfur content. This relationship can be explained by the fact that, during the adsorption process, the mass transfer rate increases with an increase in the mixing rate thereby allowing the sulfur species to reach the adsorbent surface more easily (Ahmad *et al*., 2005). As the mixing speed increases from 300 to 625 rpm, the removal efficiency remained almost constant and this may be due to the non-availability of vacant sites onto the surface of the adsorbents. The highest sulfur removal efficiency of about 96% was obtained at a mixing speed of 300 rpm for PI and at 150 rpm for PI with CNTs thus this is the optimum speed. This optimum speed was also obtained at Section 4.3.5 as well as in a study by Saha & Datta (2009). These removal efficiencies correspond to a sulfur content of 26 and 31 mg/kg for PI and PI with CNTs respectively (Appendix B, Table B 1).

Furthermore, it can be observed that at lower mixing rates, PI with CNTs performance increased from 40 to 92%. From these observations, it can be suggested that CNTs may be added if

operating at lower stirring speed is desired. These findings agreed well with those obtained when treating diesel fuel with 5200 ppm sulfur (Section 4.3). Furthermore, there is a small difference in the removal efficiencies at 300, 450 and 625 rpm thus implying that the process can be operated at any of those speeds. However, a lower mixing rate is preferred since it will save energy and hence reduce operation costs. In addition, it is known that at higher agitation speed, the adsorbed species experience a strong centrifugal force and as a result the bound species become desorbed from the surface of the adsorbent (Saha & Datta, 2009). The lowest sulfur content obtained when using both the adsorbents is very close to the target sulfur specification of 10 mg/kg.

4.4.4 Effect of temperature

The effect of temperature on the adsorption of sulfur species was investigated as a function of time at constant speed of 625 rpm and adsorbent amount of 0.3 g. The temperature was varied from 25 to 80 °C and the samples were collected every 10 hours. The obtained results for both the adsorbents are shown in Figure 4.23 and Figure 4.24.

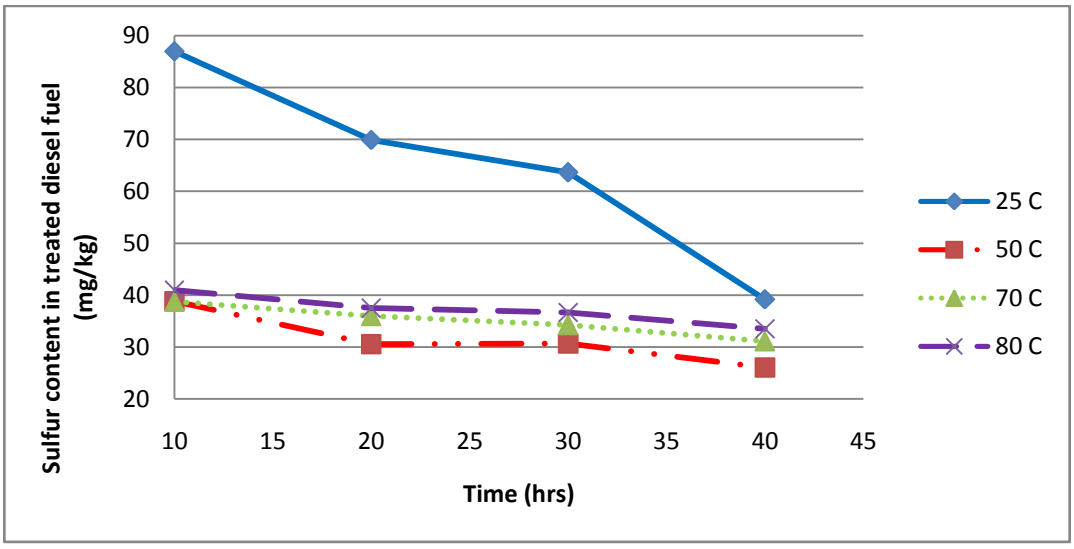

Figure 4.23: Effect of temperature as a function of time on sulfur removal efficiency at 0.3 g PI, 625 rpm, 30 hours and C_o of 607.6 m/kg

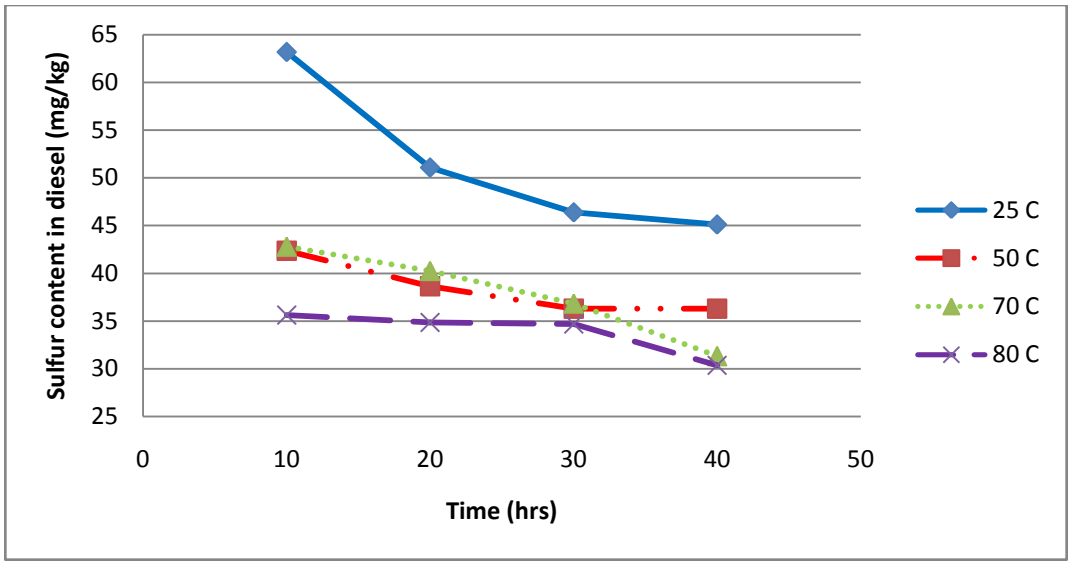

Figure 4.24: Effect of temperature as a function of time on sulfur removal efficiency at 0.3 g PI with CNTs, 625 rpm, 30 hours and C_o of 607.6 m/kg

The trend shows that the sulfur content in the treated fuel decreases with time for all the temperatures. During the first 10 hours there is a rapid decrease in the sulfur content at all temperatures. This is probably due to the availability of the large number of adsorption sites in the beginning of each reaction. After 10 hours, the sulfur content decreases slightly which is probably due to the fact that there are few adsorption sites left as the reaction progresses. However, at 25 °C, the reduction of sulfur is rapid at each contact time yet it still remains the least effective temperature for both adsorbents. When comparing the results for both the adsorbents, it can be seen that CNTs do not offer any major improvement in the adsorption capacity of PI. However, it reaches the lowest sulfur content much quicker than PI.

For each adsorbent, the effect of temperature on the sulfur removal efficiency was plotted as shown in Figure 4.25 when considering 30 hours only.

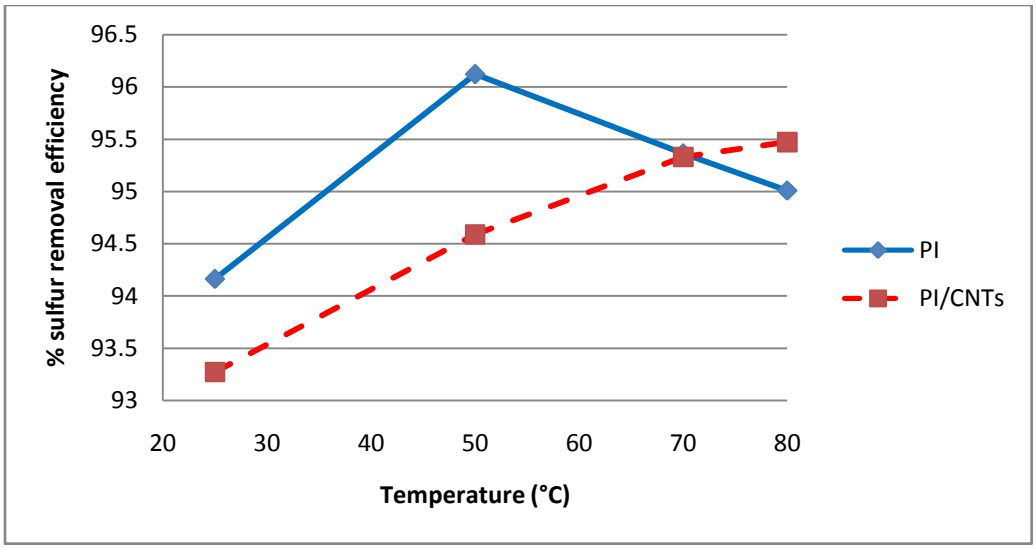

Figure 4.25: Effect of temperature on sulfur removal efficiency at 0.3 g, 625 rpm, 30 hours and C_o of 670.6 m/kg

The trend shows that when using PI as an adsorbent, there is a rapid increase in sulfur removal efficiency from 25 to 50 °C and thereafter a rapid decline in the removal efficiency. This rapid decline at high temperatures is probably caused by the decomposition of the sulfonium salts (Shiraishi *et al*., 2001). The maximum removal efficiency of 96% was achieved at 50 ºC which corresponds to 26 mg/kg. This suggests that the adsorption process of sulfur on PI might be endothermic in nature. On contrary, the trend for PI with CNTs shows that the sulfur removal efficiency increases as the temperature increases. This suggests that this process is endothermic in nature. The maximum removal efficiency of 95% was obtained at 80 ºC which corresponds to 30 mg/kg. Additionally, there is no major change in the removal efficiency at 70 and 80 ºC. And in order to make the process less energy intensive, 70 ºC is highly favoured. Hence, the optimum operating condition for PI is 50 ºC and for PI with CNTs is 70 ºC for 30 hours.

4.4.5 Optimum operating conditions

The optimum operating conditions are summarized in Table 4.7.

Table 4.7: The optimum operating condition for sulfur adsorption process at C_o of 670.6 mg/kg

Parameter	PI	PI with CNTs
Amount of adsorbent (g)	1	1
Temperature (ºC)	50	70
Stirring speed (rpm)	300	150
Contact time (hrs)	30	30

The highest sulfur removal efficiency obtained is 96% using PI (26 mg/kg). The sulfur content of the treated fuel is close to the 10ppm specification. A study conducted by Shiraishi *et al*. (2003) reported a reduction in sulfur content from 400ppm to 54ppm in 40 hours reaction time. As discussed in this section, it can be concluded that at low sulfur content, CNTs do not offer any major advancements to the adsorption capacity of PI. However, at high fuel content, it was proven that they improve the adsorption capacity of PI (Section 4.3). The aim was to use CNTs to improve the adsorption capacity of PI, and it worked in a minimal way. As a result, it can be suggested that this treatment process should be placed after the traditional HDS rector to further lower the treated fuel to acceptable desulfurization levels but the PI should not have CNTs to reduce operating costs and increase efficiency.

4.4.6 Adsorption isotherm

The adsorption equilibrium was described using the Langmuir and Freundlich models. The results obtained in the study of the effect of adsorbent amount on sulfur removal were fitted to these models. These isotherms were investigated at 50 ºC, 625 rpm and an equilibrium time of 30 hours. The data is shown in Appendix C.

Langmuir isotherm

The Langmuir constants (Q and b) were determined from the slope and intercept of the obtained linear plot as shown in Figure 4.26. In addition, the separation factor (r) was calculated. The obtained values are shown in alongside with the correlation coefficient (R^2). Based on the R^2 value, the Langmuir model does not sufficiently describe the adsorption of sulfur on PI. The same can be said on PI with CNTs. Furthermore, the negative values for the Langmuir constants indicate the unsuitability of the model to describe the equilibrium adsorption (Ramakrishna,

1996). Similarly, negative Langmuir constants were obtained in Case 3 (Section 4.3.6) and in the study of the adsorption of sulfur compounds from diesel fuel using activated carbon (Nkosi, 2014).

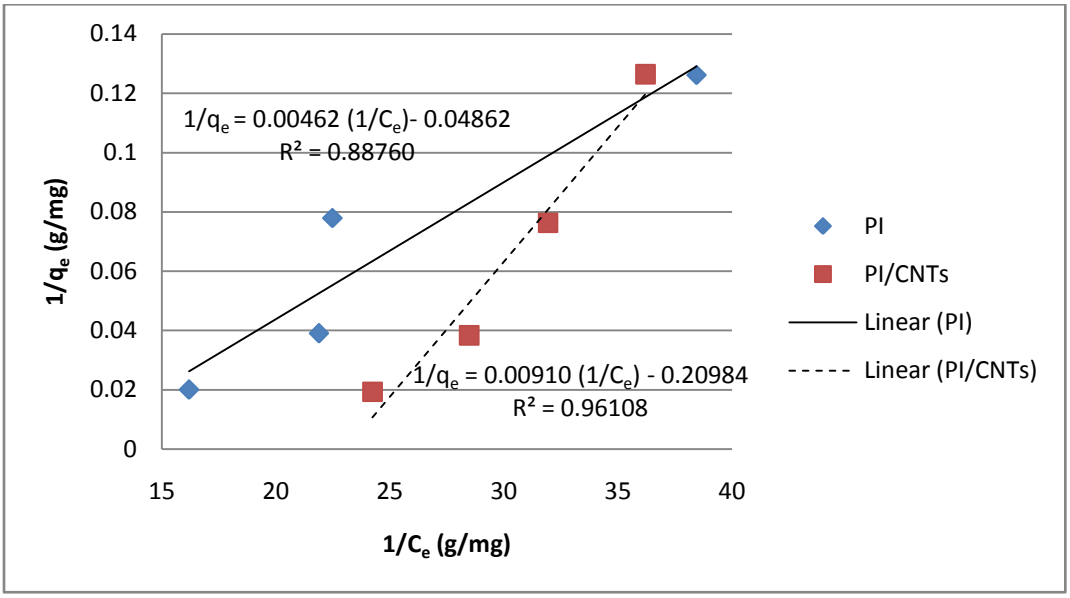

Figure 4.26: Langmuir isotherm for sulfur adsorption at C_o of 670.6 mg/kg

Freundlich isotherm

The Freundlich constants (Q_f and n) were determined from the slope and intercept of the obtained linear plot as shown in Figure 4.27. These constants as well as the R^2 value are shown in Table 4.8. The R^2 (0.837) of PI is lower than that obtained in Langmuir model (0.888) suggesting that the data is fairly fitted by Langmuir model. However, due to the negative Langmuir constants, the adsorption process obeys the Freundlich model. For PI/CNTs, the obtained R^2 for Freundlich model (0.994) is closer to unity and higher than the Langmuir R^2 thus suggesting that this process obeys the Freundlich model. This implies that the adsorption process is a physical process. This finding is in agreement with Case 1 results and those obtained in a study of sulfur adsorption using activated carbon (Bu *et al*., 2011). The calculated n-value for both the adsorbents is lower than unity, indicating that the sulfur compounds were not favourably adsorbed onto the two adsorbents.

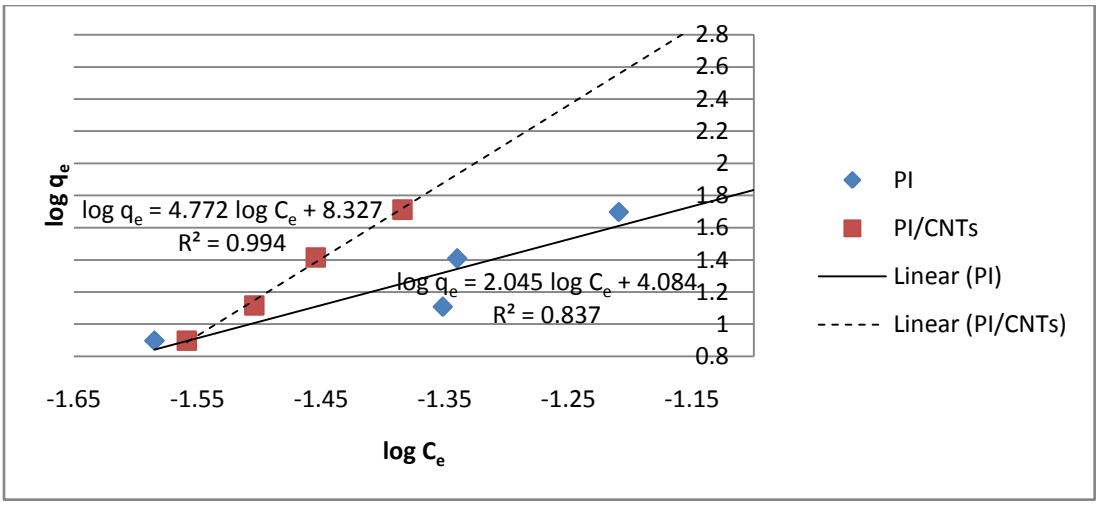

Figure 4.27: Freundlich isotherm for sulfur adsorption at C_o of 670.6 mg/kg

Table 4.8: Langmuir and Freundlich isotherm constants and correlation coefficients for sulfur adsorption at C_o of 5200 mg/kg

Langmuir isotherm					**Freundlich isotherm**		
Adsorbent	**Q (mg/g)**	**b (l/mg)**	**r**	**R^2**	**Q_f ((mg/g)(l/mg)$^{1/n}$)**	**n**	**R^2**
PI	-20.57	-10.52	-1.42E-04	0.888	12133.889	0.4890	0.837
PI/CNTs	-4.77	-23.06	-6.47E-05	0.961	212324446	0.2096	0.994

4.4.7 Adsorption kinetics

The pseudo-first- and second-order models were used in order to determine the controlling mechanism of the adsorption process. The data obtained in the effect of temperature was modelled and the data is shown in Appendix D.

Pseudo-first-order kinetics

The linear plot of log (q_e – q_t) versus time was plotted for each temperature for both the adsorbents and the figures obtained are shown in Appendix D. From the plots, the slope and intercepts were used to determine the pseudo-first-order constants (k_1 and q_e) and the obtained values are shown in Table 4.9. The calculated amount of sulfur adsorbed ($q_{e,\,cal}$) was compared to the experimental one.

Pseudo-second-order kinetics

The linear plots of t/q_t versus time were plotted for each adsorbent at different temperatures and the graphs are shown in Appendix D. From the plots, the slope and intercepts were used to determine the pseudo-second-order constants (k_1 and q_e) and the obtained values are shown in Table 4.10.

Based on the correlation coefficients, the pseudo-second order fits the data very well as compared to the pseudo-first-order for both the adsorbents at all temperatures. Furthermore, the calculated equilibrium adsorbed amount of sulfur ($q_{e,calc}$) for pseudo-second-order model are very close to the experimental values. These facts support that the adsorption of sulfur compounds on PI follows the pseudo-second-order adsorption kinetics. This then suggests that the overall sulfur adsorption process is most likely to be controlled by chemisorption process (Jiwalak *et al*., 2010). This is in good agreement with the results obtained in Case 1.

Table 4.9: Pseudo-first-order constants and correlation coefficients for sulfur adsorption at Co of 607.6 mg/kg

Pseudo-first-order (PI)					**Pseudo-first-order (PI/CNTs)**			
Constants	**25 °C**	**50 °C**	**70 °C**	**80 °C**	**25 °C**	**50 °C**	**70 °C**	**80 °C**
k_1 (min^{-1})	0.000553	0.000852	0.000760	0.000714	0.00230	0.00159	0.000599	0.000161
$q_{e,calc}$ (mg/g)	2.6441	0.72547	0.49164	0.44164	2.9902	0.64585	0.70547	0.23404
$q_{e,exp}$ (mg/g)	25.890	26.429	26.220	26.123	25.646	26.007	26.211	26.250
R^2	0.96694	0.72628	1	0.93644	0.99130	1	0.96877	0.89817

Table 4.10: Pseudo-second-order constants and correlation coefficients for sulfur adsorption at Co of 607.6 mg/kg

Pseudo-second-order (PI)					**Pseudo-second-order (PI/CNTs)**			
Constants	**25 °C**	**50 °C**	**70 °C**	**80 °C**	**25 °C**	**50 °C**	**70 °C**	**80 °C**
k_1 ($g.mg^{-1}.min^{-1}$)	0.00105	0.00353	0.00551	0.00625	0.00147	0.00408	0.00385	0.0289
$q_{e,calc}$ (mg/g)	25.641	27.027	26.316	26.316	26.316	26.316	26.316	26.316
$q_{e,exp}$ (mg/g)	25.890	26.429	26.220	26.123	25.646	26.007	26.211	26.250
R^2	1	1	1	1	1	1	1	1

4.4.8 Activation parameters

The activation energy (E_a) is used to determine whether the adsorption process is physical or chemical in nature. An Arrhenius plot of ln k versus 1/T was plotted for both the adsorbent wherein the pseudo-second-order constant (k) was used. From the Arrhenius plot, E_a was determined from the slope. The obtained Arrhenius plot is given in Figure 4.28.

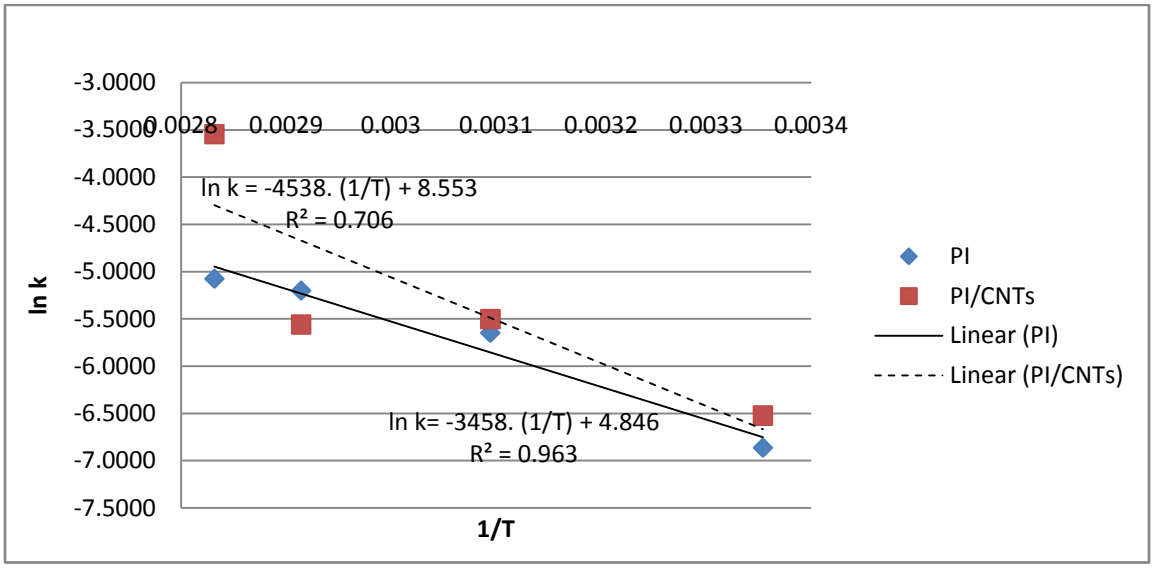

Figure 4.28: An Arrhenius plot for sulfur adsorption on PI with and without CNTs

The activation energy for physical process is usually between 5 and 40 kJ/mol due to the less energy requirement since weak intermolecular forces are involved. However, for chemical process, the activation energy ranges from 40 to 800 kJ/mol due to strong bonding forces involved. The activation energies obtained in this study are 28.7 kJ/mol and 37.7 kJ/mol for PI and PI with CNTs respectively. This then imply that the adsorption of sulfur compounds on PI involves physical process. This contradicts with the results obtained in the investigation of the effect of temperature on adsorption as well as the pseudo-second-order kinetic model. Furthermore, a study by Shiraishi *et al*., (2001) indicates that during the adsorption process, sulfur compounds reacts with the adsorbent forming N-tosylsulfimides.

4.4.9 Thermodynamic parameters

The thermodynamic parameters considered in this study are the Gibbs free energy (ΔG˚), enthalpy (ΔH˚) and entropy (ΔS˚). They were determined using Equations 2.17 – 2.20. A van't Hoff plot of ln K_c versus 1/T was plotted and the entropy as well as the enthalpy were determined from the intercept and slope of the graph. The Gibbs free energy was calculated using Equation 2.20. A sample calculation on how these parameters were calculated is shown in Appendix E. The thermodynamic parameters are given in Table 4.11 for both the adsorbents. However, for PI, the correlation coefficient is very small and far away from unity. The negative ΔG^o values indicate that the sulfur adsorption is a thermodynamically favourable process at the given temperature range. The obtained enthalpy is very high and it indicates that the adsorption of sulfur onto PI/CNTs is an endothermic process. A positive enthalpy implies that a disordered system and hence allowing processes to occur spontaneously.

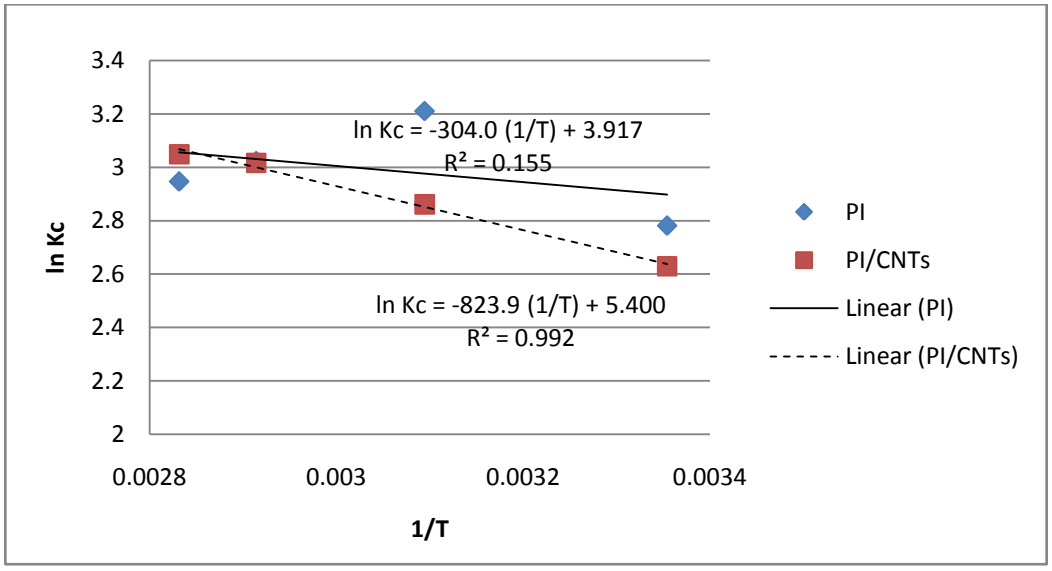

Figure 4.29: Van't Hoff plot

Table 4.11: Thermodynamic parameters

	PI				PI/CNs			
Temp (K)	lnKc	ΔG° (kJ/mol)	ΔH° (kJ/mol)	ΔS° (kJ/mol.K)	lnKc	ΔG° (kJ/mol)	ΔH° (kJ/mol)	ΔS° (kJ/mol.K)
298.15	2.78	-7182.08	2527.5	32.6	2.63	-6535.72	6849.9	44.9
323.15	3.21	-7996.23			2.86	-7658.11		
343.15	3.02	-8647.55			3.02	-8556.02		
353.15	2.95	-8973.21			3.05	-9004.98		

4.4.10 Characterization of spent adsorbent

The PI used to treat the outlet stream to the HDS reactor was taken for FTIR and SEM-EDS analysis. The obtained results were compared with those of the unused PI.

FTIR analysis

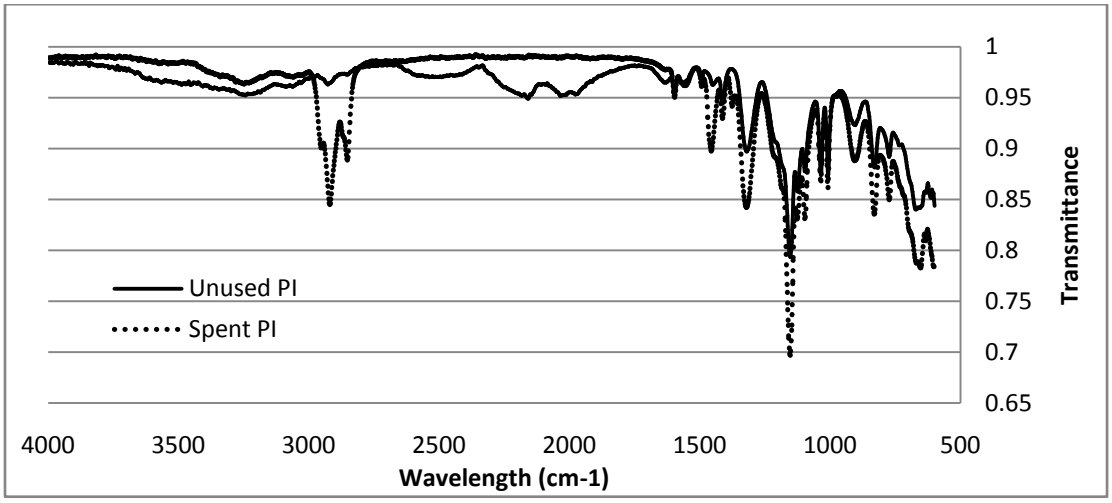

Figure 4.30: FTIR spectra of spent PI used to treat HDS reactor outlet stream with C_o of 670.7 mg/kg

Figure 4.30 above shows that the spent absorbents have the same functional groups as the unused adsorbent with the major difference at around 3000 and 1400 cm^{-1} wavelength. These IR spectra of the spent PI is very similar to the one used to treat the inlet stream with 5200 mg/kg sulfur content (Figure 4.18). Both the Spectra of the spent PI show sharp peaks at ~3000 and ~2900 cm^{-1} corresponding to C-H stretch in thiophene compound. And also another peak at ~1450 corresponding to a ring vibration consisting of a symmetric stretch of C=C bonds of thiophenes.

This thus implies that sulfur compounds were successfully adsorbed during the adsorptive desulfurization process. This is in good agreement with the findings obtained in this study as discussed in Section 4.2.8.

SEM-EDS analysis

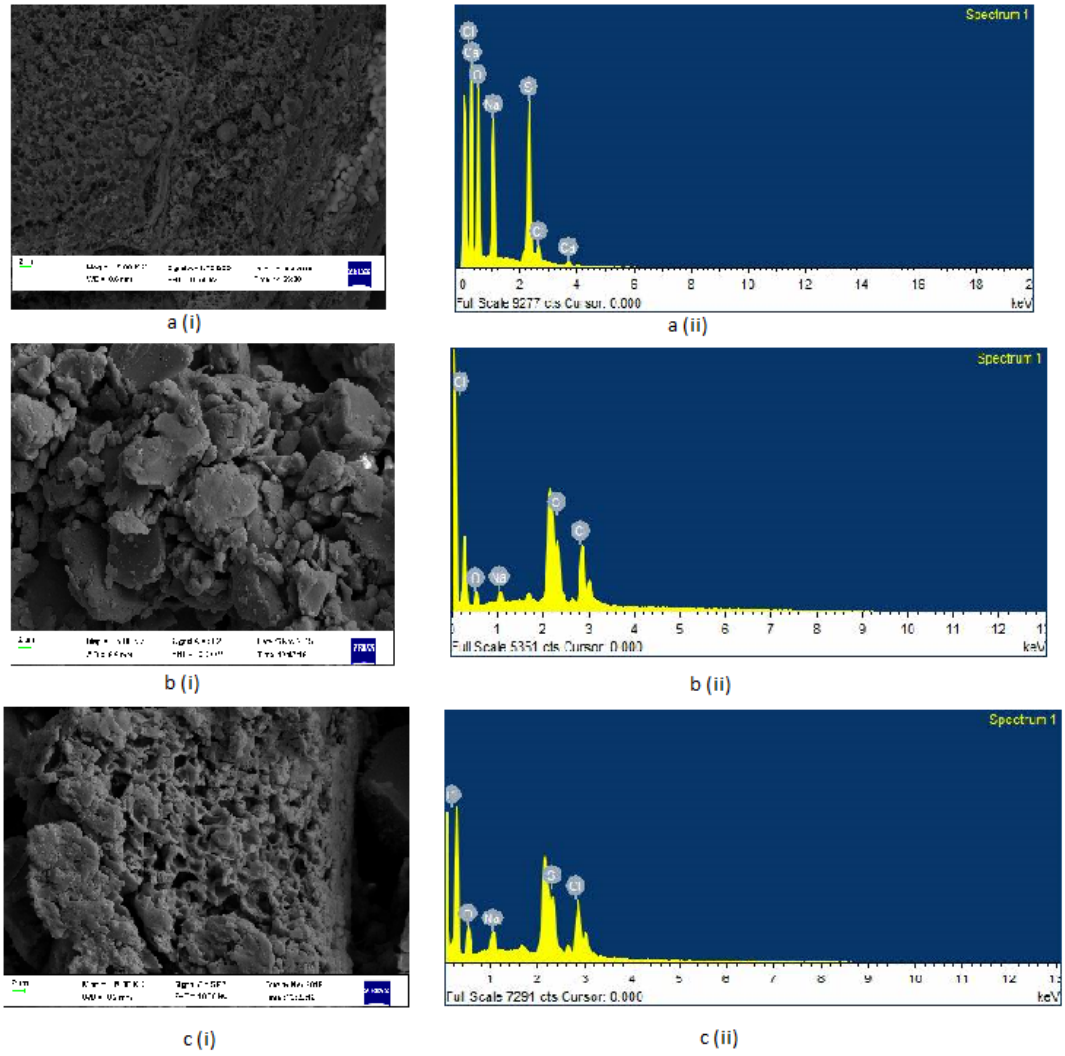

Figure 4.31: SEM images for unused PI a (i), used PI b (i) and used PI with CNTs c (i) alongside with their corresponding EDS spectra (ii) at Case 2

The SEM images for the unused and spent PI show dissimilarity in their structures. For instance, the used PI with and without CNTs {Figure 4.31a (i) & b (i)} show a less porous structure as compared to the image of unused PI {Figure 4.31 c (i)}. This is probably due to the sulfur species that are now present in the used PI.

4.4.11 Advantages offered by CNTs

Case 1

In Case 1, the addition of CNTs to the adsorption process resulted in the increase in the sulfur removal efficiency of PI. For instance, in the investigation of contact time (Figure 4.11), the sulfur removal efficiency of PI with CNTs exceeded that of PI at all contact times. It increased the maximum sulfur removal efficiency from 18 to 22%. The same trend was observed under the study of the effect of temperature and mixing speed on sulfur removal efficiency. Furthermore, the operating temperature and adsorbent amount used were reduced. For instance, only half of the amount of PI and room temperature were used. Operating at low temperature lowers the energy requirement of the process and thus making this process attractive.

Case 2

As shown in Figure 4.21, the addition of CNTs improves the adsorption capacity of PI especially at the adsorbent range of 0.1 to 0.6 g. This suggests that instead of adding high dosage of PI, the process can be operated at low adsorbent dose of PI and 0.01 g of CNTs. For instance, adding 0.6 g of PI and 0.01 g of CNTs cleans the fuel to ~31 mg/kg which is very close to the target specification of 10 mg/kg. At lower mixing rates, PI with CNTs increased the removal efficiency of PI from 40 to 92% (Figure 4.22). From these observations, it can be suggested that CNTs may be added if operating at lower stirring speed is desired. Furthermore, during the experimental runs, it was observed that it was easy to clean the fuel with CNTs. The spent adsorbent with sulfur species was suspended in methanol and hence the solution was easily decanted.

Chapter 5 Conclusions and recommendations

A polymer-supported imidation agent, i.e. PI was successfully synthesized in our laboratory. FTIR spectra were used to identify the functional groups present in the adsorbent and they corresponded with those synthesized by other researchers. The SEM results showed that the synthesized PI has nonporous region and EDS confirmed the present of all the desired elements in the polymer structure. In addition, the PI was found to have a low surface area of 0.5333 m^2/g as compared to 34.02 m^2/g of the PI synthesized by Fadhel (2010). The obtained results from this study showed that despite the low surface area and the nonporous nature of the synthesized PI, this adsorbent performed very well at low sulfur content diesel fuel. The used PI was analysed and compared to the fresh PI using FTIR as well as the SEM/EDS instruments. From the obtained results, it can be concluded that the adsorbent successfully adsorbed the sulfur species.

The synthesized PI is highly effective in treating fuel with low sulfur content as compared to the one with high sulfur content. The sulfur content of the HDS reactor inlet stream was 5200 mg/kg and the lowest content obtained after adsorption process is 3462 mg/kg (33% removal efficiency). On contrary, at a low sulfur content fuel (670.6 mg/kg), the lowest sulfur content obtained was 26 mg/kg (96% removal efficiency). For both cases, the treated amount is higher than the target specification of 10 mg/kg. However, conducting the adsorptive desulfurization in series with HDS process can yield better results than conducting the adsorptive desulfurization process before the HDS process. From the obtained results, it can be suggested that the combination of HDS and adsorptive desulfurization process can lower the fuel content from 5200 mg/kg to 26 mg/kg.

The ultra-clean fuel can be achieved by addressing several factors affecting the adsorption process. This study focused on the improvement of the adsorbent's selectivity and on finding the optimum operating parameters. The SEM images of the adsorbent indicated that its morphology was not uniform. Due to this uneven distribution of pores within the adsorbent, it was postulated before this study that the adsorption capacity of the PI would be low. This postulation was also supported by the low surface area obtained from BET results. As a result, the CNTs were added to the solution to improve the adsorption capacity of the PI. The results obtained in Case 1

showed that CNTs offered various advantages to the process. For instance, it improved the adsorption capacity of PI, reduced the operating temperature and also it improved the efficiency at lower adsorbent amounts. While at low sulfur content fuel, there were no significant improvements that were noticed. However, even with the use of CNTs in the adsorption process of high sulfur content fuel, the acceptable desulfurization level of 10 mg/kg was not achieved. In case 2, the sulfur content obtained in this study is the lowest as compared to that obtained by Shiraishi *et al*. (2003) and Fadhel (2010) despite its low surface area and non-uniform morphology.

The process parameters such as contact time, temperature, adsorbent amount and mixing speed have an effect on the adsorption process. Increasing the contact time increases the sulfur removal efficiency of the adsorbent until equilibrium is attained. For the adsorbent amount, the higher the adsorbent amount the higher the removal efficiency. Increasing the mixing speed increases the removal efficiency until a sharp decrease due to rigorous mixing environment. The process nature was found to be endothermic wherein increasing the temperature increases the removal efficiency until the adsorbent starts to decompose thus resulting in the rapid decrease in the removal efficiency. These findings were supported by both Case 1 and Case 2 results.

According to the calculated activation energies, 28.7 kJ/mol for PI and 37.7 kJ/mol for PI with CNTs, the process is classified as a physical process. Furthermore, the pseudo-second-order kinetic model was the best fit to the data which suggests that the overall adsorption rate was controlled by chemisorption. The equilibrium adsorption was best described by the Freundlich adsorption isotherm for both Cases. This indicated that the synthesized PI has heterogeneous surfaces and the adsorption process takes place at different sites with several adsorption energies.

As discussed in Chapter 2, various researchers are in favour of the adsorption process as an alternative desulfurization technique. This is due to its low operating conditions, less energy requirement and the regeneration of the spent adsorbents. It is postulated in the scientific community that the integration of this technique in the existing refinery will not be too expensive and complicated. Based on the obtained results from this study, it can be suggested that the adsorptive desulfurization unit can be placed in series with the traditional HDS unit. Further treatment of the fuel from an HDS reactor outlet (670.6 mg/kg) resulted in 26 mg/kg. In addition, another suggestion is not to place the adsorptive desulfurization unit before the traditional unit.

This is because this method could not achieve ultra-low sulfur level when treating the fuel with high sulfur content (i.e. 5200 mg/kg).

Recommendations

Future studies may focus on finding the optimum amount of CNTs that can lead to the highest removal since in this study the amount was kept constant. Furthermore, CNTs may be activated before use and/or functionalized to improve their activity. Another future method of improvement of the PI's adsorption capacity is to consider using different cross-linking methods of polystyrene as suggested by Cychosz *et al*. (2008) and Yang *et al*. (2011).

The three synthesized products were all found to have the capability of lowering the sulfur content especially in the fuel with low sulfur content. Since this study only focused on PI, there is a future opportunity to study the adsorption capacity of the first two products (PI_1 and PI_2) and to explore the potential of achieving ultra-clean fuel. Achieving ultra-clean fuel using the proposed adsorption process has been proven to be possible. Future studies may focus on ways of integrating this process in the existing refinery configuration.

Chapter 6 References

Abotsi, G.M. and Scaroni A. (1989) A review of carbon-supported hydrodesulfurization catalysts. *Fuel Processing Technology*. 22, 107–133.

Adinaya, K., Sivalingam, A. and Kannadasan ,T. (2013) Desulfurization of liquid fuels by selective extraction method: a Review. 2 (6), 2277–8179.

AFPM. (nd). *The refinery process*. [Online] Available at: http://www.afpm.org/The-Refinery-Process/ (accessed 30/07/14).

Ahmad, A.L., Bhatia, S., Ibrahim, N and Sumathi, S. (2005) Adsorption of residual oil from palm oil mill effluent using rubber powder. *Brazilian Journal of Chemical Engineering*. 22 (3), 371–379.

Ahmed, M., Malik, M.A., Pervez, S. and Raffiq, M. (2004) Effect of porosity on sulfonation of macroporous styrene-divinylbenzene beads. *European Polymer Journal*. 40 (8), 1609–1613.

Ali, M.F., Al-Malki, A. and Ahmed, S. (2009) Chemical desulfurization of petroleum fractions for ultra-low sulfur fuels. *Fuel Processing Technology*. 90 (4), 536–544.

Al-Sahlawi, M.A. (1992) *Petroleum Economics and Engineering, Second Edition*. CRC Press: New york.

Ania, C.O. and Bandosz, T.J. (2006) Metal-loaded polystyrene-based activated carbons as dibenzothiophene removal media via reactive adsorption. *Carbon*. 44 (12), 2404–2412.

Armor, J.N. (2005) Do you really have a better catalyst? *Applied Catalysis A: General*. 282 (1–2), 1–4.

Babich, I. and Moulijn, J. (2003) Science and technology of novel processes for deep desulfurization of oil refinery streams: a review. *Fuel*. 82 (6), 607–631.

Bacquet, M., Salunkhe, M. and Caze, C. (1991) Influence of chlorosulfonation on textural and chemical parameters of styrene-divinylbenzene porous copolymers. *Reactive Polymers*. 16 (1), 61–69.

Bogoczek, R. and Kociołek-Balawejder, E. (1986) Synthesis and main properties of uniformly chlorosulfonyl-substituted styrene-divinylbenzene resins. *Reactive Polymers, Ion Exchangers, Sorbents*. 4 (4), 311–316.

Bogoczek, R., Kociołek-Balawejder, E. and Stanisławska, E. (2006) A macromolecular oxidant, the N,N-dichlorosulfonamide for removal of residual nitrites from aqueous media. *Reactive and Functional Polymers*. 66 (6), 609–617.

Bogoczek, R., Kociołek-Balawejder, E. and Stanisławska, E. (2005) Macromolecular N-Chlorosulfonamide as an Oxidant for Residual Nitrites in Aqueous Media. *Industrial & Engineering Chemistry Research*. 44 (23), 8530–8534.

Bösmann, A., Datsevich, L., Jess, A., Lauter, A., Schmitz, C. and Wasserscheid P. (2001) Deep desulfurization of diesel fuel by extraction with ionic liquids. *Chemical Communications*. (23), 2494–2495.

Brevoord, E., Gerritsen, L., Mayo, S. and Plantenga, F. (2001) Process ultra-low sulfur diesel. 2 (84). Available at: http://www.hydrocarbonprocessing.com/Article/2600512/Process-ultra-low-sulfur-diesel.html (accessed 05/09/14).

Bu, J., Loh, G., Gwie, C.G., Dewiyanti, S., Tasrif, M. and Borgna, A. (2011a) Desulfurization of diesel fuels by selective adsorption on activated carbons: Competitive adsorption of polycyclic aromatic sulfur heterocycles and polycyclic aromatic hydrocarbons. *Chemical Engineering Journal*. 166 (1), 207–217.

Bu, J., Loh, G., Gwie, C.G., Dewiyanti, S., Tasrif, M. and Borgna, A. (2011b) Desulfurization of diesel fuels by selective adsorption on activated carbons: Competitive adsorption of polycyclic aromatic sulfur heterocycles and polycyclic aromatic hydrocarbons. *Chemical Engineering Journal*. 166 (1), 207–217.

Bulbul, Sonmez. H., Senkal, B.F., Sherrington, D.C. and Bıcak, N. (2003) Atom transfer radical graft polymerization of acrylamide from N-chlorosulfonamidated polystyrene resin, and use of the resin in selective mercury removal. *Reactive and Functional Polymers*. 55 (1), 1–8.

Buryakovsky, L., Eremenko, N.A., Gorfunkel, M.V. and Chilingarian, G.V. (2005) *Geology and Geochemistry of Oil and Gas*. Elsevier

Campos-Martin, J M., Capel-Sanchez, M. C., Perez-Presas, P. and Fierro, J.L. G. (2010) Oxidative processes of desulfurization of liquid fuels. *Journal of Chemical Technology & Biotechnology*. 85 (7), 879–890.

Carretta, N., Tricoli, V. and Picchioni, F. (2000) Ionomeric membranes based on partially sulfonated poly(styrene): synthesis, proton conduction and methanol permeation. *Journal of Membrane Science*. 166 (2), 189–197.

Chakrabarti, A. and Sharma, M. (1993) Cationic ion exchange resins as catalyst. *Reactive Polymers*. 20, 1.

Chang, J.H, Kim, Y.J., Lee, B.H., Cho, K. S., Ryu, H.W, Chang, Y.K. and Chang, H.N. (2001) Production of a Desulfurization Biocatalyst by Two-Stage Fermentation and Its Application for the Treatment of Model and Diesel Oils. *Biotechnology Progress*. 17 (5), 876–880.

Chiou, M.S. and Li, H.Y. (2002a) Equilibrium and kinetic modeling of adsorption of reactive dye on cross-linked chitosan beads. *Journal of Hazardous Materials*. 93 (2), 233–248.

Chiou, M.S. and Li, H.Y. (2002b) Equilibrium and kinetic modeling of adsorption of reactive dye on cross-linked chitosan beads. *Journal of Hazardous Materials*. 93 (2), 233–248.

Coutinho, F.M.B., Siqueira, M.I.N. and Barbosa, C.R. (1990) Synthesis and characterization of copolymers based on 2-vinylpyridine and divinylbenzene. *European Polymer Journal*. 26 (11), 1189–1193.

Cychosz, K.A., Wong-Foy, A.G. and Matzger, A.J. (2009) Enabling Cleaner Fuels: Desulfurization by Adsorption to Microporous Coordination Polymers. *Journal of the American Chemical Society*. 131 (40), 14538–14543.

Cychosz, K.A., Wong-Foy, A.G. and Matzger, A.J. (2008) Liquid Phase Adsorption by Microporous Coordination Polymers: Removal of Organosulfur Compounds. *Journal of the American Chemical Society*. 130 (22), 6938–6939.

Dan Liu, L.S. (2007) Adsorption structures of heterocyclic sulfur compounds on Cu(I)Y zeolite: a first principle study. *Studies in Surface Science and Catalysis*. 170, 1699–1704.

Eijsbouts, S., Plantenga, F., Leliveld, B., Inoue, Y. and Fujita, K. (2003) STARS and NEBULA - New Generations of Hydroprocessing Catalysts for the Production of Ultra Low Sulfur Diesel. *ACS Division of Fuel Chemistry*. 48 (2), 494.

Emerson, D. and Ifalade, S. (2005) Improved Preparation of Macroporous, Chlorosulfonated Poly(styrene-co-divinylbenzene) and Conversion to Sulfonamides and Sulfonylhydrazines. *Industrial and Engineering Chemistry Research*. 44, 7045–7048.

Emerson, D., Shea, D. and Sorensen, E. (1978) Functionally Modified Poly(styrene-divinylbenzene). Preparation, Characterization, and Bactericidal Action. *Industrial and Engineering Chemistry Product Research and Development*. 17 (3), 269–274.

Fadhel, S .Z (2010) *Desulfurization of Light Diesel Fuel Using Chloramine T and Polymer Supported Imidation Agent*. University of Technology. Available at: http://www.uotechnology.edu.iq/dep-chem-eng/thesis/Zainab%20Subhi%20Thesis.pdf.

Fahim, M.A., Al-Sahhaf, T.A. and Elkilani, A. (2009) *Fundamentals of Petroleum Refining*. Elsevier: United Kingdom

Farag, H., Mochida, I. and Sakanishi, K. (2000) Fundamental comparison studies on hydrodesulfurization of dibenzothiophenes over CoMo-based carbon and alumina catalysts. *Applied Catalysis A: General*. 194–195, 147–157.

Farag, H., Sakanishi, K., Mochida, I. and Whitehurst, D.D. (1999) Kinetic Analyses and Inhibition by Naphthalene and H2S in Hydrodesulfurization of 4,6-Dimethyldibenzothiophene (4,6-DMDBT) over CoMo-Based Carbon Catalyst. *Energy & Fuels*. 13 (2), 449–453.

Forte, P. (1996) Process for the removal of sulfur from petroleum fractions. Available at: http://www.google.com/patents/US5582714 (accessed 29/09/14).

Fritz, J. and Story, J. (1974) Selectivity behaviour of low capacity, partially sulfonated, macroporous resin beads. *Journal of Chromotography*. 90, 267–274.

Funakoshi, I. and Aida, T. (1998) Process for recovering organic sulfur compounds from fuel oil. Available at: http://www.google.com/patents/US5753102 (accessed 29/09/14).

Gilchrist, T. and Moody, C. (1977) The Chemistry of Sulfilimines. *Chemical Reviews*. 77 (3), 409–435.

Gong, Y., Dou, T., Kang, S., Li, Q. and Hu, Y. (2009) Deep desulfurization of gasoline using ion-exchange zeolites: Cu(I)- and Ag(I)-beta. *Fuel Processing Technology*. 90 (1), 122–129.

Gosling, C., Gatan, R. and Barger, P. (2007). *Process for producing hydroperoxides*. USPatent4202992.Available at:http://patft1.uspto.gov/netacgi/nph-Parser?Sect1=PTO1&Sect2=HITOFF&d=PALL&p=1&u=/netahtml/PTO/srchnum.htm&r=1&f=G&l=50&s1=%22+4202992+%22.PN.&OS=PN/%22+4202992+%22&RS=PN/%22+4202992 (accessed 28/11/15)

Grossman, M.J., Lee, M.K., Prince, R.C., Garrett, K.K., George, G.N. and Pickering, I.J. (1999) Microbial Desulfurization of a Crude Oil Middle-Distillate Fraction: Analysis of the Extent of Sulfur Removal and the Effect of Removal on Remaining Sulfur. *Applied and Environmental Microbiology*. 65 (1), 181–188.

Grossman, M.J., Lee, M.K., Prince, R.C., Minak-Bernero, V., George, G.N. and Pickering, I.J. (2001) Deep Desulfurization of Extensively Hydrodesulfurized Middle Distillate Oil by Rhodococcus sp. Strain ECRD-1. *Applied and Environmental Microbiology*. 67 (4), 1949–1952.

Gunnerman, R. (2003) Continuous process for oxidative desulfurization of fossil fuels with ultrasound and products thereof. Available at: http://www.freepatentsonline.com/y2003/0014911.html (accessed 29/09/14).

Guobin, S., Huaiying, Z., Jianmin, X., Guo, C., Wangliang, L. and Huizhou, L. (2006) Biodesulfurization of hydrodesulfurized diesel oil with Pseudomonas delafieldii R-8 from high density culture. *Biochemical Engineering Journal*. 27 (3), 305–309.

Gutch, P.K., Srivastava, R.K. and Sekhar, K. (2008) Polymeric decontaminant 2 (N,N-dichloropolystyrene sulfonamide): Synthesis, characterization, and efficacy against simulant of sulfur mustard. *Journal of Applied Polymer Science*. 107 (6), 4109–4115.

Hameed, B.H., Mahmoud, D.K. and Ahmad, A.L. (2008) Equilibrium modeling and kinetic studies on the adsorption of basic dye by a low-cost adsorbent: Coconut (Cocos nucifera) bunch waste. *Journal of Hazardous Materials*. 158 (1), 65–72.

Haupt, K. and Mosbach, K. (2000) Molecularly imprinted polymers and their use in biomimetic sensors. *Chemical Reviews*. 100 (7), 2495–2504.

Helferich, F. (1962) *Ion exchange*. New York: McGraw-Hill

Hernández-Maldonado, A.J. and Yang, R.T. (2004a) Desulfurization of Diesel Fuels by Adsorption via π-Complexation with Vapor-Phase Exchanged Cu(I)−Y Zeolites. *Journal of the American Chemical Society*. 126 (4), 992–993.

Hernández-Maldonado, A.J. and Yang, R.T. (2004b) New sorbents for desulfurization of diesel fuels via ?-complexation. *AIChE Journal*. 50 (4), 791–801.

Hernández-Maldonado, A., Yang, F., Qi, G. and Yang, R.T. (2005) Desulfurization of transportation fuels by π-complexation sorbents: Cu(I)-, Ni(II)-, and Zn(II)-zeolites. *Applied Catalysis B: Environmental*, 111–126.

Hernandez-Maldonado, A. and Yang, R. (2003) Desulfurization of Liquid Fuels by Selective Adsorption via π Complexation with Cu (I)-Y Zeolite. *Industrial and Engineering Chemistry Research*. 42, 3103–3110.

Hernández-Maldonado, A. and Yang, R.T. (2003) Desulfurization of Commercial Liquid Fuels by Selective Adsorption via π-Complexation with Cu(I)−Y Zeolite. *Industrial and Engineering Chemistry Research*. 42 (13), 3103 - 3110.

Hernandez, S.P., Fino, D. and Russo, N. (2010) High performance sorbents for diesel oil desulfurization. *Chemical Engineering Science*. 65 (1), 603–609.

Hernández, S., Solarino, L., Orsello, G., Russo, N., Fino, D., Saracco, G. and Specchia, V. (2008) Desulfurization processes for fuel cells systems. *2nd World Congress of Young Scientists on Hydrogen Energy Systems*. 33 (12), 3209–3214.

Holbrey, J., Lopez-Martin, I., Rothenberg, G., Seddon, K., Silvero, G. and Zheng, X. (2008) Desulfurisation of oils using ionic liquids: selection of cationic and anionic components to enhance extraction efficiency. *Green Chemistry*. 10, 87–92.

Horii, Y., Onuki, H., Doi, S., Mori, T., Takatori, T., Sato, H., Ookuro, T. and Sugawara, T. (1996) Desulfurization and denitration of light oil by extraction. Available at: http://www.google.com/patents/US5494572 (accessed 29/09/14).

Huang,D., Wang, Y. and Luo, G. (2006) A surfactant-enhanced oxidation-extraction process for desulfurization of oils. *The Chinese journal of process engineering*. 6 (3), 84–387.

IARC (1989) *IARC monographs on the evaluation of carcinogenic risks to humans*. France: World Health Organisation (WHO), UK Available at: http://monographs.iarc.fr/ENG/Monographs/vol45/mono45.pdf (accessed 16/10/14).

Iimura, S., Manabe, K. and Kobayashi, S. (2003) Hydrophobic, low-loading and alkylated polystyrene-supported sulfonic acid for several organic reactions in water: remarkable effects of both the polymer structures and loading levels of sulfonic acids. *Organic & amp; biomolecular chemistry*. 1 (14), 2416–8.

Irvine, R. (1998) Process for desulfurizing gasoline and hydrocarbon feedstocksUS 5730860 A. Available athttps://www.google.com/patents/US5730860 (accessed 28/11/2015)

Ito, E. and van Veen, J.A.R. (2006) On novel processes for removing sulphur from refinery streams. *Sulfur Removal to Produce Ultra Clean Fuel*. 116 (4), 446–460.

Jawad, Z. (2007) *Sulfur dioxide removal in coal slurry reactor*. University of Technology.

Jiwalak, N., Rattanaphani, S., Bremner, J.B. and Rattanaphani, V. (2010) Equilibrium and kinetic modeling of the adsorption of indigo carmine onto silk. *Fibers and Polymers*. 11 (4), 572–579.

Kale, A.A. (2013) Evaluation of sieved biomass of Cicer arientinum (horse bean) for removal of methylene blue : batch study. *International Journal of Recycling of Organic Waste in Agriculture*, 2 (18).

Karas,L.J., Grey, R.A. and Lynch, M.W. (2008) Desulfurization process.US Patent 047875. Available at: http://www.freepatentsonline.com/y2008/0047875.html (accessed 29/09/14).

Key, R.,Laurent, J., Ackerson, M. and Hallock, J. (2003) "Isotherming – a new technology for ultra low sulfur fuels". In NPRA Annual Meeting, San Antonio, 11 March. Available at: http://www.lppusa.com/International/Web/LE/US/likeleuslbpp30.nsf/repositorybyalias/am-03-11/$file/AM-03-11.pdf (accessed 25/09/14).

Kilbane II, J. and Borgne, S. (2004) Petroleum biorefining: the selective removal of sulfur, nitrogen, and metals. *Studies in Surface Science and Catalysis*. 151, 29–66.

Kim, J., Ma, X., Zhou, A. and Song, C. (2006) Ultra-deep desulfurization and denitrogenation of diesel fuel by selective adsorption over three different adsorbents: A study on adsorptive selectivity and mechanism. *Catalysis Today*. 111, 74–83.

Kitagawa, S., Kitaura, R. and Noro, S. (2004) Functional Porous Coordination Polymers. *Angewandte Chemie International Edition*. 43 (18), 2334–2375.

Ko, C.H., Park, J.G., Park, J.C., Song, H., Han, S.S. and Kim, J.N. (2007) Surface status and size influences of nickel nanoparticles on sulfur compound adsorption. *Sixth International*

Symposium on Effects of surface heterogeneity in adsorption and catalysis on solids ISSHAC-VI. 253 (13), 5864–5867.

Kociołek-Balawejder, E. (2002a) A copolymer with N-chlorosulfonamide pendant groups as oxidant for residual sulfides. *Reactive and Functional Polymers*. 52 (2), 89–97.

Kociołek-Balawejder, E. (2002b) A macromolecular N,N-dichlorosulfonamide as oxidant for residual sulfides. *European Polymer Journal*. 38 (5), 953–959.

Kotze, C. (2012) *Local refineries face many challenges*. [Online] Available at: http://www.engineeringnews.co.za/article/refineries-challenged-by-ageing-infrastructure-unreliability-trade-sanctions-and-legislation-2012-09-07 (accessed 22/08/14).

Kraus, R. (2011) *Petroleum Refining Process*. [Online] Available at: http://www.ilo.org/oshenc/part-xii/oil-and-natural-gas/item/384-petroleum-refining-process (accessed 30/07/14).

Krylova, A.V., Ustimenko, G.A. and Torocheshnikov, N.S. (1983) 'Preparation Of Non-Pyrophoric Metallic Catalysts'. In: P. G. and P. A. J. G. Poncelet (ed). *Studies in Surface Science and Catalysis*. Preparation of Catalysts III Scientific Bases for the Preparation of Heterogeneous Catalysts. Elsevier. 441–450. Available at: http://www.sciencedirect.com/science/article/pii/S0167299109600409 (accessed 11/04/15).

Kucera, F. and Jancar, J. (1996) Preliminary Study of Sulfonation of Polystyrene by Homogeneous and Heterogeneous Reaction. *Chemical Paper*. 50 (4), 224–227.

Kumar, P.S. and Kirthika, K. (2009) Equilibrium and kinetic study of adsorption of nickel from aqueous solution onto bael tree leaf powder. *Journal of Engineering Science and Technology*. 4 (4), 351–363.

Kumar, S. and Jain, S. (2013) History, Introduction, and Kinetics of Ion Exchange Materials. *Journal of Chemistry*. 2013, 1 - 13.

Lagergren, S. (1898) Zur theorie der sogenannten adsorption gelöster stoffe. *K. Sven. Vetenskapsakad. Handl.* 24, 1–39.

Lakshmi, U.R., Srivastava, V.C., Mall, I.D. and Lataye, D.H. (2009) Rice husk ash as an effective adsorbent: evaluation of adsorptive characteristics for Indigo Carmine dye. *Journal of Environmental Management*. 90 (2), 710–720.

Lee, E., Park, D.W., Lee, J.O., Kim, D.S., Lee, B.H. and Kim, B.S. (2008) Molecularly imprinted polymers immobilized on carbon nanotube. *Colloids and Surfaces A: Physicochemical and Engineering Aspects*. 313–314, 202–206.

Lee, H.Y. and Kim, B.S. (2009) Grafting of molecularly imprinted polymers on iniferter-modified carbon nanotube. *Biosensors & Bioelectronics*. 25 (3), 587–591.

Leffler, W.L. (2008) *Petroleum Refining in Nontechnical Language*. PennWell Books

Liew, C. (2007) *Public Environmental Report*. Australia Available at: http://www.bp.com/content/dam/bp/pdf/sustainability/country-reports/Kwinana_refinery_2006_V2.pdf (accessed 11/08/14).

Llewellyn, P.L., Bloch, E. and Bourrelly, S. (2012) Surface Area/Porosity, Adsorption, Diffusion. In: M. Che & J. C. Védrine eds. *Characterization of Solid Materials and Heterogeneous Catalysts*. 853–879.

Loeb, G.I. and Schrader, M.E. (1992) *Modern Approaches to Wettability: Theory and Applications.* 1992 edition. New York: Springer

Lofrano, G. (2012) *Emerging Compounds Removal from Wastewater: Natural and Solar Based Treatments*. Springer Science & Business Media

Lü, H., Gao, J., Jiang, Z., Yang, Y,, Song, B. and Li, C. (2006) Oxidative desulfurization of dibenzothiophene with molecular oxygen using emulsion catalysis. *Chemical Communications*. (2), 150–152.

Ma, C.Q., Feng, J.H., Zeng, Y.Y., Cai, X.F., Sun, B.P., Zhang, Z.B., Blankespoor, H.D. and Xu, P. (2006) Methods for the preparation of a biodesulfurization biocatalyst using Rhodococcus sp. *Chemosphere*. 65 (1), 165–169.

Mann, F. and Pope, W. (1922) The Sulphilimines, a New Class of Organic Compounds containing Quadrivalent Sulphur. *Journal of Chemical Society*. 121, 1052–1055.

Ma, X., Sakanishi, K, and Mochida, I. (1994) Hydrodesulfurization reactivities of various sulfur compounds in diesel fuel. *Industrial & Engineering Chemistry Research*. 33 (2), 218–222.

Ma, X., Sun, L. and Song, C. (2002) A new approach to deep desulfurization of gasoline, diesel fuel and jet fuel by selective adsorption for ultra-clean fuels and for fuel cell applications. *Catalysis Today*. 77 (1–2), 107–116.

Ma, X., Velu, S., Kim, J.. and Song, C. (2005) Deep desulfurization of gasoline by selective adsorption over solid adsorbents and impact of analytical methods on ppm-level sulfur quantification for fuel cell applications. *Applied Catalysis B: Environmental*, 137–147.

McFarland, B.L., Boron, D.J., Deever, W., Meyer, J.A., Johnson, A.R. and Atlas, R.M. (1998) Biocatalytic sulfur removal from fuels: applicability for producing low sulfur gasoline. *Critical Reviews in Microbiology*. 24 (2), 99–147.

McKinley, S.G. and Angelici, R.J. (2003) Deep desulfurization by selective adsorption of dibenzothiophenes on Ag^{+}/SBA-15 and Ag^{+}/SiO2. *Chemical Communications*. (20), 2620–2621.

Meille, V., Schulz, E., Meille, V., Vrinat, M. and Lemaire, M. (1998) A new route towards deep desulfurization: selective charge transfer complex formation. *Chemical Communications*. (3), 305–306.

Milenkovic, A., Schulz, E., Meille, V., Loffreda, D., Forissier, M., Vrinat, M., Sautet, P. and Lemaire, M. (1999) Selective Elimination of Alkyldibenzothiophenes from Gas Oil by Formation of Insoluble Charge-Transfer Complexes. *Energy & Fuels*. 13 (4), 881–887.

Mittal, A., Kurup, L. and Mittal, J. (2007) Freundlich and Langmuir adsorption isotherms and kinetics for the removal of Tartrazine from aqueous solutions using hen feathers. *Journal of Hazardous Materials*. 146 (1–2), 243–248.

Mochida, I. and Choi, K.H. (2004) An Overview of Hydrodesulfurization and Hydrodenitrogenation. *Journal of the Japan Petroleum Institute*. 47 (3), 145–163.

Mohebali, G. and Ball, A.S. (2008) Biocatalytic desulfurization (BDS) of petrodiesel fuels. *Microbiology*. 154 (8), 2169–2183.

Monticello, D.J. (2000) Biodesulfurization and the upgrading of petroleum distillates. *Current Opinion in Biotechnology*. 11 (6), 540–546.

Mužic, M., Sertić-bionda, K. and Adžamić, T. (2009) Kinetic , Equilibrium and Statistical Analysis of Diesel Fuel Adsorptive. *Adsorption Journal Of The International Adsorption Society*, 384–394.

Nehlsen, J. (2005) *Developing Clean Fuels: Novel Techniques for Desulfurization*. Princeton University. Available at: http://pemfc.princeton.edu/Documents/Theses/Nehlsen_thesis.pdf.

Nkosi, M. (2014) *Desulphurisation of petroleum distillates using adsorption method*. University of the Witwatersrand. Available at http://wiredspace.wits.ac.za/handle/10539/45/browse?type=author&value=Nkosi%2C+Melusi (accessed 29/11/2015)

Nollet, H., Roels, M., Lutgen, P., Van der Meeren, P. and Verstraete, W. (2003) Removal of PCBs from wastewater using fly ash. *Chemosphere*. 53 (6), 655–665.

Otsuki, S., Nonaka, T., Takashima, N., Qian, W., Ishihara, A., Imai, T. and Kabe, T. (2000) Oxidative Desulfurization of Light Gas Oil and Vacuum Gas Oil by Oxidation and Solvent Extraction. *Energy & Fuels*. 14 (6), 1232–1239.

Oxford Business Group (2012) *The Report: South Africa 2012*. Oxford Business Group. Available at

https://books.google.co.za/books?id=CqVSPEQvpvwC&printsec=frontcover&source=gbs_ge_summary_r&cad=0#v=onepage&q&f=false

Park, J.G., Ko, C.H., Yi, K.B., Park, J.H., Han, S.S., Cho, S.H. and Kim,.JN. (2008) Reactive adsorption of sulfur compounds in diesel on nickel supported on mesoporous silica. *Applied Catalysis B: Environmental*. 81 (3–4), 244–250.

Pawelec, B., Mariscal, R., Fierro, J.L.G., Greenwood, A. and Vasudevan, P.T. (2001) Carbon-supported tungsten and nickel catalysts for hydrodesulfurization and hydrogenation reactions. *Applied Catalysis A: General*. 206 (2), 295–307.

Piero, M. Adsorption. Available at: http://cpe.njit.edu/dlnotes/CHE685/Cls11-1.pdf (accessed 07/10/14).

Rabia, I., Bencheikh, Z., Guettaf, H., Iayadene, F., Saggou, A. and Zerouk, J. (1996) Scanning electron microscopy study of chlorosulfonated styrene-divinylbenzene macroporous resins. *Reactive and Functional Polymers*. 31 (2), 149–153.

Ramakrishna, B.K.R. (1996) Dye Removal Using Peat. *American Dyestuff Reporter*. (October). Available at http://citeseerx.ist.psu.edu/viewdoc/download?doi=10.1.1.551.2796&rep=rep1&type=pdf (accessed 29/11/2015)

Rodrigues, A.K.O., Ramos, J.E.T., Cavalcante, J.R.C.L, Rodríguez-Castellón, E. and Azevedo, D.C.S. (2014) Pd-loaded mesoporous silica as a robust adsorbent in adsorption/desorption desulfurization cycles. *Fuel*. 126 (0), 96–103.

Ruthven, D.M. (1984) *Principles of Adsorption and Adsorption Processes*. John Wiley & Sons

Saha, P. and Datta, S. (2009) Assessment on thermodynamics and kinetics parameters on reduction of methylene blue dye using flyash. *Desalination and Water Treatment*. 12 (1-3), 219–228.

Salem, A.S. and Hamid, H. (1997) Removal of Sulfur Compounds from Naphtha Solutions Using Solid Adsorbents. *Chemical Engineering Technology*. 20, 342.

Sarda, K.K., Bhandari, A., Pant, K.K. and Jain, S. (2012) Deep desulfurization of diesel fuel by selective adsorption over Ni/Al2O3 and Ni/ZSM-5 extrudates. *Fuel*. 93 (0), 86–91.

Senkal, B.F., Bildik, F., Yavuz, E. and Sarac, A. (2007) Preparation of poly(glycidyl methacrylate) grafted sulfonamide based polystyrene resin with tertiary amine for the removal of dye from water. *Reactive and Functional Polymers*. 67 (12), 1471–1477.

Senkal, B.F. and Yavuz, E. (2006) Preparation of poly(vinyl pyrrolidone) grafted sulfonamide based polystyrene resin and its use for the removal of dye from water. *Polymers for Advanced Technologies*. 17 (11-12), 928–931.

Seredych, M. and Bandosz, T. (2010) Adsorption of dibenzothiophenes on activated carbons with copper and iron deposited on their surfaces. *Fuel Processing Technology*. 91, 693–701.

Seredych, M. and Bandosz, T. (2011) Removal of dibenzothiophenes from model diesel fuel on sulfur rich activated carbons. *Applied Catalysis B: Environmental*. 106, 133–141.

Seredych, M., Khine, M. and Bandosz, T.J. (2011) Enhancement in dibenzothiophene reactive adsorption from liquid fuel via incorporation of sulfur heteroatoms into the nanoporous carbon matrix.*ChemSusChem*. 4 (1), 139–147.

Seredych, M., Lison, J., Jans, U. and Bandosz, T.J. (2009) Textural and chemical factors affecting adsorption capacity of activated carbon in highly efficient desulfurization of diesel fuel. *Carbon*. 47 (10), 2491–2500.

Seredych, M., Wu, C., Brender, P., Ania, C., Vix-Guterl, C. and Bandosz, T. (2012) Role of phosphorus in carbon matrix in desulfurization of diesel fuel using adsorption process. *Fuel*. 92 (1), 318–326.

Shen, W., Yang, X., Guo, Q., Liu, Y. and Song, Y. (2007) Adsorption desulfurization from gasoline by silver loaded on mesoporous aluminum oxide. *Studies in Surface Science and Catalysis*. 165, 811–815.

Shiraishi, Y., Naito, T., Hirai, T. and Komasawa, I. (2003) Desulfurization process for light oil based on chemical adsorption of sulfur compounds on polymer-supported imidation agent agent. *Journal of Chemical Engineering of Japan*. 36, 1528– 1531.

Shiraishi, Y., Naito, T., Hirai, T. and Komasawa, I. (2002) Novel Desulfurization Process for Light Oils Based on the Formation and Subsequent Adsorption of N-tosylsulfimides. *Fuel Chemistry Division Preprints*. 47 (2), 701– 702.

Shiraishi, Y., Taki, Y., Hirai, T. and Komasawa, I. (2001) A Novel Desulfurization Process for Fuel Oils Based on the Formation and Subsequent Precipitation of S-Alkylsulfonium Salts. 1. Light Oil Feedstocks. *Industrial & Engineering Chemistry Research*. 40 (4), 1213–1224.

Sie, S.T. (1999) Reaction order and role of hydrogen sulfide in deep hydrodesulfurization of gas oils: consequences for industrial reactor configuration.*Fuel Processing Technology*, 149–171.

Singh, R. and Zahra, F. (2014) Mixing kinetics in batch adsorption of chromium (vi) by emblica officinalis leaf powder. *International Journal of Advanced Technology in Engineering and Science*. 2 (1), 2348–7550.

Song, C. (2003) An overview of new approaches to deep desulfurization for ultra-clean gasoline, diesel fuel and jet fuel. *Catalysis Today*, 211–263.

Speight, J.G. (2011) *An Introduction to Petroleum Technology, Economics, and Politics*. John Wiley & Sons

Speight,J.G. and Ozum, B. (2001) *Petroleum Refining Processes*. CRC Press

Stanislaus, A., Marafi, A. and Rana, M. (2010) Recent advances in the science and technology of ultra low sulfur diesel (ULSD) production. *Catalysis Today*. 153 (1), 1–68.

Takahashi, A., Yang, F.H. and Yang, R.T. (2002) New Sorbents for Desulfurization by π-Complexation: Thiophene/Benzene Adsorption.*Industrial & Engineering Chemistry Research*. 41 (10), 2487–2496.

Toro, C.A., Rodrigo, R. and Cuellar, J. (2008) Sulfonation of macroporous poly(styrene-co-divinylbenzene) beads: Effect of the proportion of isomers on their cation exchange capacity. *Reactive and Functional Polymers*. 68 (9), 1325–1336.

Velu, S., Ma, X. and Song, C. (2002) Zeolite-based Adsorbents for Desulfurization of jet fuel by Selective Adsorption. *Fuel Chemistry Division Preprints*. 47 (2), 447–448.

Velu, S., Watanabe, S., Ma, X. and Song, C. (2003) Regenerable adsorbents for the adsorptive desulfurization of transportation fuels for fuel cell applications. *ACS Division of Fuel Chemistry, Preprints*. 48 (2), 526 – 528.

Vogel, A., Tatchel, A., Furnis, B. and Hannaford, A. (1996) *Practical Organic Chemistry: Aromatic Compounds* (5th edition). Prentice Hall

Wang, D., Qian, E.W., Amano, H., Okata, K., Ishihara, A. and Kabe, T. (2003) Oxidative desulfurization of fuel oil: Part I. Oxidation of dibenzothiophenes using tert-butyl hydroperoxide. *Applied Catalysis A: General*. 253 (1), 91–99.

Wang, J., Xu, F., Xie, W., Mei, Z., Zhang, Q., Cai, J. and Cai, W. (2009) The enhanced adsorption of dibenzothiophene onto cerium/nickel-exchanged zeolite *Y*. *Journal of hazardous materials*. 163 (2-3), 538 – 543

Wang, L., Sun, B., Yang, F.H. and Yang, R.T. (2012) Effects of aromatics on desulfurization of liquid fuel by π-complexation and carbon adsorbents. *Chemical Engineering Science*. 73 (0), 208–217.

Wang, L., Sun, Z., Ding, Y., Chen, Y., Li, Q., Xu, M., Li, H. and Song, L. (2011) A theoretical study of thiophenic compounds adsorption on cation-exchanged Y zeolites. *Applied Surface Science*. 257 (17), 7539–7544.

Weber, T.W. and Chakravorti, R.K. (1974) Pore and solid diffusion models for fixed-bed adsorbers. *AIChE Journal*. 20 (2), 228–238.

Weitkamp, J., Schwark, M. and Ernest, S. (1991) Removal of Thiophene Impurities from Benzene by Selective Adsorption in Zeolite ZSM-5. *Journal of the Chemical Society, Chemical Communications*, 16, 1133–1134.

Wu, Z., Li, C., Wei, Z., Ying, P. and Xin, Q. (2002) FT-IR Spectroscopic Studies of Thiophene Adsorption and Reactions on Mo2N/γ-Al2O3 Catalysts. *Journal of Physical Chemistry B*. 106 (5).

Yang, R.T. (2003) *Adsorbents: fundamentals and applications*. Hoboken, N.J. Wiley-Interscience

Yang, R.T., Hernández-Maldonado, A.J. and Yang, F.H. (2003) Desulfurization of transportation fuels with zeolites under ambient conditions. *Science (New York, N.Y.)*. 301 (5629), 79–81.

Yang, R.T., Takahashi , A. and Yang, F.H. (2001) New Sorbents for Desulfurization of Liquid Fuels by π-Complexation. *Industrial and Engineering Chemistry Research*. 40 (26), 6236–6239.

Yang, Y., Liu, X., Guo, M., Li, S., Liu, W. and Xu, B. (2011) Molecularly imprinted polymer on carbon microsphere surfaces for adsorbing dibenzothiophene. *Colloids and Surfaces A: Physicochemical and Engineering Aspects*. 377 (1-3), 379–385.

Yazu, K., Yamamoto, Y., Furuya, T., Miki, K. and Ukegawa, K. (2001) Oxidation of dibenzothiophenes in an organic biphasic system and its application to oxidative desulfurization of light oil. *Energy and Fuels.* 15 (6), 1535 - 1536.

Appendix A: Sulfur analysis data for Case 1

The batch adsorption experiment was carried out according to the procedure described in Chapter 3. The experiment was conducted on the commercial diesel taken from the HDS inlet stream with a sulfur content of 5200 mg/kg. The parameters investigated are contact time, adsorbent amount, temperature and mixing speed. All the parameters except contact time were investigated at a fixed methanol, acetic and fuel volume of 15ml, 0.6ml and 15 ml respectively. Other parameters were kept constant at 625 rpm, 50 ºC, 0.3 g and 0.01 g of CNTs. However, the difference with contact time is that 50 ml of fuel, 50 ml methanol, 2 ml acetic acid and 1 g were used.

The effect of contact time on adsorption process

Table A 1: Effect of contact time at C_o of 5200 mg/kg

PI			PI with CNTs	
Contact time (hrs)	**Sulfur content (mg/kg)**	**% η**	**Sulfur content (mg/kg)**	**% η**
0	5200		5200	
10	4467.81	14.08	4424.85	14.91
20	4304.59	17.22	4207.44	19.09
30	4275.00	17.79	4193.40	19.36
40	4274.25	17.80	4060.76	21.91

The effect the adsorbent amount on adsorption process

Table A 2: Effect of adsorbent amount at C_o of 5200 mg/kg

PI			PI with CNTs	
Amount of adsorbent (g)	**Sulfur content (mg/kg)**	**% η**	**Sulfur content (mg/kg)**	**% η**
0	5200		5200	
0.1	4291.56	17.47	4320.17	16.92
0.3	4403.49	15.32	3981.36	23.44
0.6	3766.33	27.57	4244.66	18.37
1	4352.58	16.30	4200.32	19.22

The effect the temperature on adsorption process

Table A 3: Effect of temperature at C_o of 5200 mg/kg

PI			PI with CNTs	
Temperature (°C)	**Sulfur content (mg/kg)**	**% η**	**Sulfur content (mg/kg)**	**% η**
0	5200		5200	
30	4209.09	19.06	3754.54	27.80
50	4120.21	20.77	3981.36	23.44
70	4345.29	16.44	4453.50	14.36
80	4403.49	15.32	4636.78	10.83

The effect the mixing speed on adsorption process

Table A 4: Effect of mixing at C_o of 5200 mg/kg

PI			PI with CNTs	
Mixing speed (rpm)	**Sulfur content (mg/kg)**	**% η**	**Sulfur content (mg/kg)**	**% η**
0	5200		5200	
150	4184.67	19.53	4112.11	20.92
300	4048.13	22.15	3462.64	33.41
450	4340.89	16.52	3981.36	23.44
625	4403.49	15.32	4273.09	17.83

Optimum operating conditions

Based on the investigation of the above parameters, an optimum operating condition was chosen for each adsorbent. This was done based on the parameter that gave the lowest sulfur content (the highest sulfur removal efficiency) as highlighted in the previous tables. The results are shown below.

Table A 5: Optimum operating conditions at C_0 of 5200 mg/kg

Parameter	PI	PI with CNTs
Amount of adsorbent (g)	0.6	0.3
Temperature (°C)	70	30
Stirring speed (rpm)	300	300
Contact time (hrs)	30	40

Appendix B: Sulfur analysis data for Case 2

The batch adsorption experiment was conducted on the commercial hydrotreated diesel fuel with a sulfur content of 670.6 mg/kg. The same parameters as in Appendix A were investigated and the experimental variables were kept constant.

The effect of contact time on adsorption process

Table B 1: Effect of mixing speed as a function of contact time at C_o of 670.6 mg/kg

Mixing speed of 300 rpm					**Mixing speed of 625 rpm**			
PI			**PI/CNTs**		**PI**		**PI/CNs**	
Time (hrs)	**Sulfur (mg/kg)**	**% η**	**Sulfur (mg/kg)**	**% η**	**Sulfur (mg/kg)**	**% η**	**Sulfur (mg/kg)**	**% η**
0	670.61	0	670.61	0	670.61	0	670.61	0
10	106.65	84.10	85.61	87.23	38.78	94.22	42.37	93.68
20	82.87	87.64	83.16	87.60	30.51	95.45	38.63	94.24
30	78.29	88.33	55.13	91.78	30.66	95.43	36.29	94.59
40	40.32	93.99	48.84	92.72	26.01	96.12	31.32	95.33

Table B 2: Effect of adsorbent amount as a function of contact time at C_o of 670.6 mg/kg

Adsorbent amount of 0.5 g					**Adsorbent amount of 1 g**			
PI			**PI/CNTs**		**PI**		**PI/CNs**	
Time (hrs)	**Sulfur (mg/kg)**	**% η**	**Sulfur (mg/kg)**	**% η**	**Sulfur (mg/kg)**	**% η**	**Sulfur (mg/kg)**	**% η**
0	670.61	0	670.61	0	670.61	0	670.61	0
10	104.82	84.37	144.33	78.48	38.78	94.22	42.37	93.68
20	72.99	89.12	105.91	84.21	30.51	95.45	38.63	94.24
30	68.93	89.72	68.38	89.80	30.66	95.43	36.29	94.59
40	61.76	90.79	41.27	93.85	26.01	96.12	31.32	95.33

The effect the adsorbent amount on adsorption process

Table B 3: Effect of adsorbent amount as a function of contact time at C_o of 670.6 mg/kg

PI			PI with CNTs	
Amount of adsorbent (g)	**Sulfur content (mg/kg)**	**% η**	**Sulfur content (mg/kg)**	**% η**
0	670.61	0	670.61	0
0.15	61.76	90.79	41.27	93.85
0.3	45.70	93.19	35.12	94.76
0.6	44.49	93.37	31.32	95.33
1	26.01	96.12	27.62	95.88

The effect the temperature on adsorption process

Table B 4: Effect of temperature as a function of time for PI

Sulfur content (mg/kg)					% removal efficiency			
Contact time (hrs)	**25 °C**	**50 °C**	**70 °C**	**80 °C**	**25 °C**	**50 °C**	**70 °C**	**80 °C**
10	86.96	38.78	38.74	40.94	87.03	94.22	94.22	93.90
20	69.88	30.51	35.98	37.46	89.58	95.45	94.64	94.41
30	63.62	30.66	34.21	36.62	90.51	95.43	94.90	94.54
40	39.15	26.01	31.10	33.48	94.16	96.12	95.36	95.01

Table B 5: Effect of temperature as a function of time for PI with CNTs

Sulfur content (mg/kg)					% removal efficiency			
Contact time (hrs)	**25 °C**	**50 °C**	**70 °C**	**80 °C**	**25 °C**	**50 °C**	**70 °C**	**80 °C**
10	63.18	42.37	42.80	35.63	90.58	93.68	93.62	94.69
20	51.07	38.63	40.24	34.87	92.38	94.24	94.00	94.80
30	46.39	36.29	36.84	34.68	93.08	94.59	94.51	94.83
40	45.11	36.29	31.32	30.37	93.27	94.59	95.33	95.47

Table B 6: Effect of temperature at Co of 670.6 mk/kg

PI			PI with CNTs	
Temperature	**Sulfur content (mg/kg)**	**% η**	**Sulfur content (mg/kg)**	**% η**
0	670.6	0	670.6	0
25	39.15	94.16	45.11	93.27
50	26.01	96.12	36.29	94.59
70	31.10	95.36	31.32	95.33
80	33.48	95.01	30.37	95.47

The effect the mixing speed on adsorption process

Table B 7: Effect of mixing at Co of 670.6 mg/kg

PI			PI with CNTs	
Mixing speed (rpm)	**Sulfur content (mg/kg)**	**% η**	**Sulfur content (mg/kg)**	**% η**
0	670.61	0	670.61	0
150	400.98	40.21	48.84	92.72
300	26.01	96.12	31.32	95.33
450	40.46	93.97	36.84	94.51
625	40.32	93.99	41.67	93.79

Optimum operating conditions

Table B 8: Optimum operating conditions at C_0 of 670.6 mg/kg

Parameter	PI	PI with CNTs
Amount of adsorbent (g)	1	1
Temperature (ºC)	50	70
Stirring speed (rpm)	300	150
Contact time (hrs)	30	30

Appendix C: Adsorption isotherm data

The data for the adsorption isotherm for both the inlet and outlet HDS streams are shown in this section.

The equilibrium concentration was converted into the desired units according to the following equation. The density of the used fuel is 820kg/m^3.

$$C_e\ (mg/l) = C_e\ (mg/kg)\ x\ \rho\ (kg/l)$$

The adsorption capacity was calculated using the following equation:

$$q_e(mg/g) = (C_o - C_e)(mg/l)\ x\ \frac{V\ (l)}{W\ (g)}$$

For the Langmuir model, C_e/q_e was plotted against C_e. The Langmuir constants, Q and b, were determined from the slope and the intercept of the plot respectively.

For the Freundlich model, log q_e was plotted against log C_e. The Freundlich constants, Q_f and n, were determined from the intercept and the slope of the plot respectively.

HDS inlet reactor stream (Case 1)

Langmuir isotherm data

Table C 1: Langmuir isotherm for Case 1

PI		**PI/CNTs**	
Ce (mg/g)	**Ce/qe**	**Ce (mg/g)**	**Ce/qe**
4.2091	0.10360	3.7545	0.06335
4.1202	0.09307	3.9814	0.07968
4.3453	0.12400	4.4535	0.14551
4.4035	0.13484	4.6368	0.20080

Freundlich isotherm data

Table C 2: Freundlich isotherm for Case 1

PI		PI/CNTs	
log Ce	**log qe**	**log Ce**	**log qe**
0.62419	1.6088	0.57456	1.7728
0.61492	1.6461	0.60003	1.6987
0.63802	1.5446	0.64870	1.4858
0.64380	1.5140	0.66622	1.3635

HDS outlet reactor stream (Case 2)

Langmuir isotherm data

Table C 3: Langmuir isotherm for Case 2

PI		PI/CNTs	
$1/C_e$ (g/mg)	**$1/q_e$(g/mg)**	**$1/C_e$ (g/mg)**	**$1/q_e$(g/mg)**
16.193	0.02003	24.232	0.01938
21.884	0.03903	28.472	0.03838
22.478	0.07791	31.931	0.07630
38.444	0.12613	36.203	0.12644

Freundlich isotherm data

Table C 4: Freundlich isotherm for Case 2

PI		PI/CNTs	
log Ce	**log qe**	**log Ce**	**log qe**
-1.2093	1.6983	-1.3844	1.7127
-1.3401	1.4086	-1.4544	1.4159
-1.3518	1.1084	-1.5042	1.1175
-1.5848	0.8992	-1.5587	0.8981

Appendix D: Adsorption kinetics data

The data for the adsorption kinetics for both the inlet and outlet HDS streams are shown in this section.

For the pseudo-first-order kinetics, log ($q_e - q_t$) versus time was plotted. The pseudo-first-order constants, k_1 and q_e, were determined from the slope and the intercept of the plot respectively.

For the pseudo-second-order kinetics, t/q_t versus time was plotted. The slope and intercept of the graph were used to obtain the pseudo-second-order constants, q_e and k_1 respectively.

HDS inlet reactor stream (Case 1)

Pseudo-first-order kinetics

Table D 1: Pseudo-first-order kinetic model for Case 1

PI		**PI/CNTs**	
time (min)	**log (q_e-q_t)**	**time (min)**	**log (q_e-q_t)**
600	0.89959	600	3.2553
1200	0.09485	1200	3.0792
1800	-1.5102	1800	2.7782

Pseudo-second-order kinetics

Table D 2: Pseudo-second-order kinetic model for Case 1

PI		**PI/CNTs**	
time (min)	**t/q_t**	**time (min)**	**t/q_t**
600	19.9867	600	18.8791
1200	32.6871	1200	29.4877
1800	47.4623	1800	43.6148

HDS outlet reactor stream (Case 2)

Pseudo-first-order kinetics for PI

Table D 3: Pseudo-first-order kinetic model for PI (Case 2)

Temperature	25 °C	50 °C	70 °C	80 °C
time (min)	log (q_e-q_t)	log (q_e-q_t)	log (q_e-q_t)	log (q_e-q_t)
600	0.29237	-0.28108	-0.50376	-0.51428
1200	0.10037	-0.73400	-0.69897	-0.78648
1800	0.00152	-0.72011	-0.89449	-0.88941

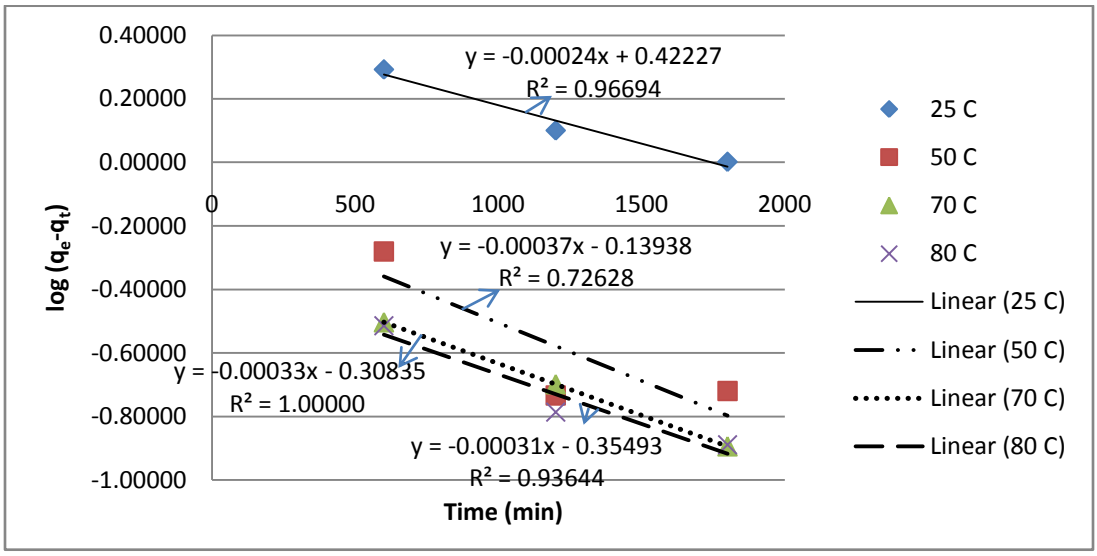

Figure D 1: Pseudo-first-order kinetic model for PI (Case 2)

Pseudo-first-order kinetics for PI/CNTs

Table D 4: Pseudo-first-order kinetic model for PI/CNTs (Case 2)

Temperature	25 °C	50 °C	70 °C	80 °C
time (min)	log (q_e-q_t)	log (q_e-q_t)	log (q_e-q_t)	log (q_e-q_t)
600	-0.13018	-0.60380	-0.32698	-0.66555
1200	-0.61172	-1.01773	-0.43652	-0.73400
1800	-1.27984		-0.64493	-0.75203

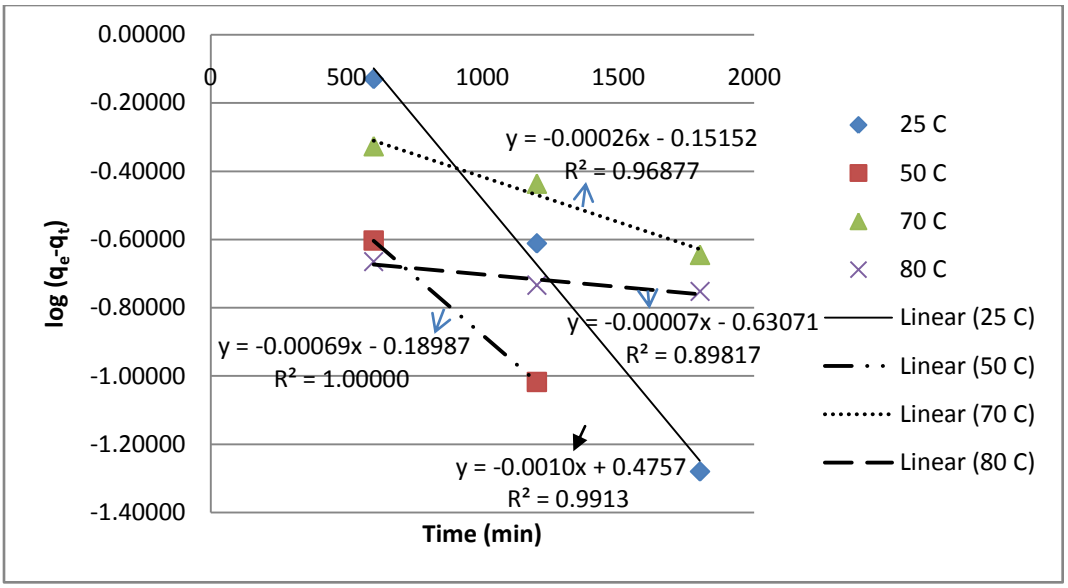

Figure D 2: Pseudo-first-order kinetic model for PI/CNTs (Case 2)

Pseudo-second-order kinetics

Table D 5: Pseudo-second-order kinetic data for Case 2

	PI				PI/CNTs			
Temperature	**25 °C**	**50 °C**	**70 °C**	**80 °C**	**25 °C**	**50 °C**	**70 °C**	**80 °C**
time (min)	**t/q_t**	**t/q_t**	**t/q_t**	**t/q_t**	**t/q_t**	**t/q_t**	**t/q_t**	**t/q_t**
600	25.074	23.162	23.160	23.241	24.092	23.294	23.310	23.047
1200	48.721	45.725	46.118	46.227	47.242	46.312	46.431	46.038
1800	72.328	68.603	68.985	69.248	70.332	69.212	69.272	69.037

Appendix E: Activation and thermodynamic parameters

Activation parameters

The data for the Arrhenius plot for Case 2

Table E 1: Data for the Arrhenius plot

	PI	PI/CNTs
1/T	ln k	ln k
0.003354	-6.8620	-6.5222
0.003095	-5.6469	-5.5019
0.002914	-5.2009	-5.5595
0.002832	-5.0750	-3.5446

Thermodynamic parameters

Sample calculation: From the Van't Hoff plot (Figure 4.29), ΔH^o was calculated from the slope and ΔS^o was calculated from the y-intercept. ΔG^o was obtained from Equation 2.20.

ΔH^o = (slope) x R = 304 x 8.314 = 2527.456 kJ/mol

ΔS^o = (y-intercept) x R = 3.917 x 8.314 = 32.57 kJ/mol.K

$\Delta G^o = \Delta H^o - T\Delta S^o$ = 2527.456 – (298.15) (32.57) = -7182.08 kJ/mol

Table E 2: Thermodynamic parameters for PI

Temp (K)	1/T	Kc	ln Kc	ΔG° (kJ/mol)	ΔH° (kJ/mol)	ΔS° (kJ/mol.K)	R^2
298.15	0.003354	16.13	2.781	-7182.08	2527.456	32.57	0.155
323.15	0.003095	24.78	3.210	-7996.23			
343.15	0.002914	20.56	3.024	-8647.55			
353.15	0.002832	19.03	2.946	-8973.21			

Table E 3: Thermodynamic parameters for PI/CNTs

Temp (K)	1/T	Kc	ln Kc	ΔG° (kJ/mol)	ΔH° (kJ/mol)	ΔS° (kJ/mol.K)	R^2
298.15	0.003354	13.87	2.629	-6535.72	6849.905	44.90	0.992
323.15	0.003095	17.48	2.861	-7658.11			
343.15	0.002914	20.41	3.016	-8556.02			
353.15	0.002832	21.08	3.049	-9004.98			